Institute of Molecular Virology
Prof. Frank Kirchhoff

Characterization of 90K/LGALS3BP

as antiviral factor

Dissertation

to obtain the Doctoral Degree of Human Biology (Dr. biol. hum.)

at the Faculty of Medicine, University of Ulm

presented by

Veronika Lodermeyer

Eichstätt

2014

Present Dean: Prof. Dr. Thomas Wirth

1st reviewer: Prof. Dr. Frank Kirchhoff
2nd reviewer: Jun.-Prof. Dr. Christine Goffinet

Date of graduation: 23.01.2015

To my mother

Contents

List of abbreviations II
1 Introduction 1
1.1 HIV-1 and AIDS 1
1.2 The HIV-1 envelope (Env) protein 1
1.3 HIV-1 restriction factors 3
1.4 The cellular glycoprotein 90K 6
1.5 Scientific aim 8
2 Material and Methods 9
2.1 Material 9
2.2 Methods 20
3 Results 28
3.1 90K expression reduces the particle infectivity of HIV-1 progeny by interfering with the maturation and incorporation of the Env proteins 28
3.2 90K inhibits multiple HIV-1 strains 31
3.3 90K expression reduces the amount of Env at the cell surface 32
3.4 90K is not a specific inhibitor of furin-mediated cleavage 34
3.5 90K and Env co-localize but do not seem to interact 35
3.6 90K does not retain HIV-1 Env in the ER 37
3.7 The two central domains of 90K are required and sufficient for its anti-HIV-1 activity 39
3.8 Antiviral activity of the 90K orthologs from seven non-human primates and the 90K mouse homolog CypCAP against HIV-1 41
3.9 Antiviral activity of the 90K orthologs from seven non-human primates and the 90K mouse homolog CypCAP against SIV and HIV-2 43
3.10 Antiviral activity of 90K chimeras against HIV-1 44
3.11 90K is expressed and interferon inducible in selected primary HIV-1 target cells 46
3.12 Cell-type specific expression of 90K protein 48
3.13 Depletion of 90K expression in primary HIV-1 target cells improves Env incorporation into HIV-1 progeny and accelerates HIV-1 spread 49
4 Discussion 53
5 Summary 61
6 References 62
Acknowledgements 76
Curriculum Vitae 77

List of abbreviations

A	adenine
Ab	antibody
agm	african green monkey
AIDS	Acquired Immunodeficiency Syndrome
Amp	ampicillin
APC	allophycocyanin
APOBEC3	apolipoprotein B mRNA-editing enzyme catalytic polypeptide-like 3
APS	ammonium persulfate
A.U.	arbitrary unit
b	base
bab	baboon
BSA	bovine serum albumin
BTB/POZ	broad-complex, tramtrack and bric á brac/ poxvirus and zinc finger
C	cytosine
C	control
°C	degree Celsius
$CaCl_2$	calcium chloride
CCR5	C-C chemokine receptor type 5
CO_2	carbon dioxide
CD	cluster designation
cDNA	complementary deoxyribonucleic acid
CMV	Cytomegalovirus
CNP	2´, 3´-Cyclic-Nucleotide 3´-Phosphodiesterase
Co-IP	co-immunoprecipitation
cpz	chimpanzee
CU	cytoplasmic unit
CXCR4	C-X-C chemokine receptor type 4
CypCAP	cyclophilin C-associated protein
Da	dalton
DMEM	Dulbecco´s modified Eagle Medium

DNA	deoxyribonucleic acid
dNTP	deoxynucleotide acid
DRK	Deutsches Rotes Kreuz
DTT	dithiothreitol
EDTA	ethylenediaminetetraacetic acid
eGFP	enhanced green fluorescent protein
ELISA	enzyme-linked immunosorbent assay
EndoH	endoglycosidase H
Env	envelope
ER	endolplasmatic reticulm
FACS	fluorescence activated cell sorting
FAM	fluorescein amidite
FCS	fetal calf serum
Fig.	figure
fwd	forward
g	gram
g	force of gravity
G	guanine
Gag	group specific antigen
gibb	gibbon
GM-CSF	granulocyte macrophage colony-stimulating factor
gor	gorilla
gp	glycoprotein
h	hour
h	human
HA	hemagglutinin
HBS	HEPES buffered saline
HCl	hydrochloric acid
HCV	Hepatitis C Virus
HIV	Human Immunodeficiency Virus
HRP	horse radish peroxidase
hum	human
IFITM 2/3	interferon- induced transmembrane proteins 2/3
IFN	interferon

IL	interleukin
IP	immunoprecipitation
IRES	internal ribosomal entry site
IVR	intervening region
k	kilo (10^3)
Kan	kanamycin
l	liter
LB	Luria Broth
LGALS3BP	lectin, galactoside-binding soluble 3 binding protein
LTR	long terminal repeat
m	meter
m	milli (10^{-3})
M	molarity (mol/l)
mac	rhesus macaque
Mac-2BP	mac-2 binding protein
MAPK	mitogen-activated protein kinase
MFI	mean fluorescence intensity
min	minute
mo	mouse
mRNA	messenger ribonucleic acid
Mx2	myxovirus resistance 2
MΦ	macrophages
µ	micro (10^{-6})
n	nano (10^{-9})
NaCl	sodium chloride
NaN_3	sodium azide
Nef	negative factor
NP-40	Nonidet P-40
n.s.	not significant
nt	nucleotide
ora	orangutan
owl	owl monkey
P	population
PBMC	peripheral blood mononuclear cell

PBS	phosphate-buffered saline
PCR	polymerase chain reaction
PFA	paraformaldehyde
PHA	phytohaemagglutinin
PNGaseF	peptide-N-Glycosidase F
PUUV	Puumala Virus
p24CA	p24 capsid antigen
qPCR	quantitative PCR
RER	rough endoplasmic reticulum
rev	reverse
rh	rhesus macaque
rhes	rhesus macaque
RNA	ribonucleic acid
RLU	relative light unit
rpm	rounds per minute
RPMI	Roswell Park Memorial Institute
RT	room temperature
R5	CCR5
sec	second
SAMHD1	SAM domain- and HD domain- containing protein 1
S.D.	standard deviation
SDS	sodium dodecyl sulfate
PAGE	polyacrylamide gel electrophoresis
S.E.M.	standard error of the mean
siRNA	small interfering RNA
SIV	Simian Immunodeficiency Virus
SLFN11	schlafen 11
smm	sooty mangabey
SOE	splicing by overlapping extension
SP	signal peptide
SRCR	scavenger receptor cysteine-rich
SU	surface unit
SV40	Simian Virus 40
T	thymidine

Tab.	table
TAE	Tris base, acetic acid, EDTA
TAMRA	tetramethylrhodamine
Tat	trans-activator of transcription
TEMED	tetramethylethylenediamine
TFV	transmitted founder virus
TNF-α	tumor necrosis factor alpha
TRIM5α	tripartite motif- containing protein alpha
Tris	trishydroxymethylaminomethane
tRNA	transfer ribonucleic acid
TU	transmembrane unit
U	unit
UNAIDS	United Nations Programme on HIV/AIDS
Vif	viral infectivity factor
Vpu	viral protein unknown
Vpx	viral protein X
VSV-G	Vesicular stomatitis Virus glycoprotein
v/v	volume/volume
WB	Western Blot
wt	wild type
w/v	weight/volume
X4	CXCR4

1 Introduction

1.1 HIV-1 and AIDS

The Joint United Nations Programme on HIV/AIDS (UNAIDS) reported that in 2013 approximately 35 million people were living with HIV/AIDS (Human Immunodeficiency Virus /Acquired Immunodeficiency Syndrome) worldwide. In the same year 2.1 million were newly infected and 1.5 million people died of AIDS. Thus this pathogen remains one of the most important threats to human health [164]. HIV-1 is a zoonotic infectious agent and arose from at least four independent cross species-transmissions of Simian Immunodeficiency Viruses (SIV) from non-human primates to humans, resulting in the four different HIV-1 subgroups M (major), O (outlier), N (non-M, non-O) and P. More than 40 African non-human primate species are naturally infected with different SIV strains, though most of them do not develop AIDS [63, 147]. SIVcpz can induce AIDS-like symptoms in wild chimpanzees [82]. Transmissions of SIVcpz naturally infecting chimpanzees (*Pan troglodytes troglodytes*) gave rise to HIV-1 subgroups M and N [83] whereas transmissions of SIVgor infecting gorillas (*Gorilla gorilla gorilla*) resulted in HIV-1 subgroups P and most likely O [125, 156, 165]. Only HIV-1 M accounts for the global AIDS pandemic. For the pandemic spread of HIV-1 M not only viral genetic factors seem to have played a role but also socio-historical circumstances like transport networks and sexual behaviour [43]. On the contrary, all HIV-1 non-M variants are rarely distributed [146]. HIV-2, a second type of HIV originating from SIVsmm infecting sooty mangabeys (*Cercocebus atys*) [30] shows clearly reduced abundance and virulence, compared to HIV-1 [84, 107, 130].

1.2 The HIV-1 envelope (Env) protein

HIV-1 particles are in average about 100 nm in size [19, 158]. These particles bear a cone-shaped core (capsid) containing two copies of the viral RNA genome [138]. The core is surrounded by the matrix and a host cell-derived lipid bilayer in which the Env glycoproteins are inserted [4, 133, 167] (Fig. 1 A). Env is present as trimeric complexes [124] both on virions and on productively infected cells and plays a key role in HIV-1 infection. Env binds to its primary receptor CD4 on CD4+ T-cells, macrophages and dendritic cells [85, 110]. CD4 binding induces conformational

changes within Env, facilitating the binding to the co-receptors CCR5 or/and CXCR4. Depending on the co-receptor used, the virus is classified as R5-, X4- or dual-tropic [28, 39, 44, 91]. Co-receptor binding induces exposure and insertion of the Env fusion peptide into the host membrane and initiates fusion of viral and cellular membranes [172]. For this purpose, each Env monomer consists of a dimer of the glycoprotein (gp) gp120, mediating attachment, and gp41, anchoring the Env complex in membranes [62] and promoting fusion [22] (Fig. 1 B).

The highly *N*- and *O*-glycosylated Env subunits gp120 and gp41 [10, 96, 175] are co-translationally directed to the rough endoplasmic reticulum (ER) as gp160 precursor proteins (Fig. 1 C, step 1) followed by their trimerization (Fig. 1 C, step 2). Subsequently, the gp160 trimers are transported into the Golgi complex (Fig. 1 C, step 3) [41]. In order to become fusion competent, the gp160 precursors are cleaved into the Env subunits gp120 and gp41 by cellular furin or furin like proteases (Fig. 1 C, step 4) [64, 109]. The mature gp120 and gp41 subunits remain non-covalently associated and are directed to the cellular plasma membrane (Fig. 1 C, step 5), where the trimeric complex is incorporated into the budding virus particles (Fig. 1 C, step 6) [24].

Indeed, a variety of Env-targeting antibodies have been identified in HIV-1 infected patients. After 2-3 years, about 20% of infected individuals develop broadly neutralizing antibodies which are capable to neutralize different HIV-1 strains [59, 86, 104, 169]. Env-targeting broadly neutralizing antibodies have been successfully used to protect rhesus macaques from infection or to block virus acquisition and control plasma viraemia in already infected animals [120, 151]. Despite these promising animal studies, vaccine development remains challenging. The virus changes Env surface structures by rapid mutations and masks vulnerable epitopes with glycan shields [178]. Immune escape might also be one reason why Env, which is present at the cell surface, is rapidly internalized by endocytosis [137]. Concomitant with this rapid turnover a nascent HIV-1 particle is decorated with only 7-14 Env trimers randomly distributed on the virus surface [26, 177]. To mediate efficient fusion with a target cell the few Env trimers have to cluster during virus maturation [29, 153] (Fig. 1 A).

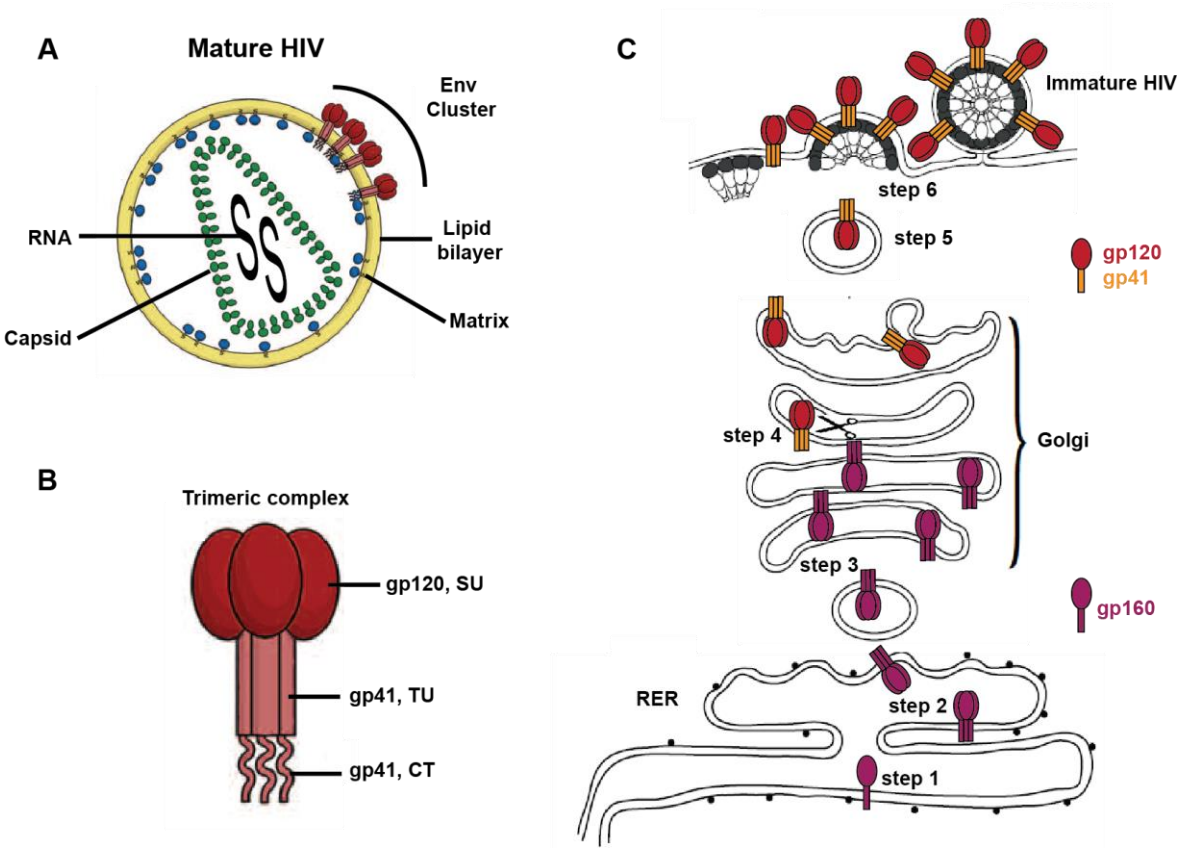


Fig. 1: Organisation and biosynthesis of HIV-1 Env. (A) Scheme of a mature HIV-1 particle and (B) the trimeric Env complex. Figures adapted from [29], p.525. (C) Overview of the Env synthesis. The Env precursor gp160 is synthesized into the RER (step 1) followed by its trimerization (step 2) and trafficking into the Golgi network (step 3). There, the gp160 precursors are cleaved into gp120 and gp41 (step 4) and transported to the plasma membrane (step 5). The fusion competent, trimeric Env complexes are incorporated into the budding virions (step 6). Figure adapted from [24], p.585. gp= glycoprotein, SU= surface unit, TU= transmembrane unit, CT= cytoplasmic unit, RER= rough endoplasmic reticulum.

1.3 HIV-1 restriction factors

Mammalian cells are equipped with a variety of proteins, so-called restriction factors, which are part of the intrinsic immunity. The intrinsic immunity constitutes a first line of defence against different viruses. In contrast to factors of the adaptive and innate immunity, restriction factors are constitutively expressed allowing the fast blockage of different steps of the viral replication cycle. The expression of restriction factors varies between cell types and can be induced or increased after interferon treatment [11]. Early stages of HIV-1 replication are inhibited by TRIM5α (tripartite motif-containing protein 5α) from old world monkeys, members of the APOBEC3 (apolipoprotein B mRNA-editing enzyme catalytic polypeptide-like 3) family, SAMHD1 (SAM domain- and HD domain-containing protein 1) and Mx2 (myxovirus

resistance 2) whereas SLFN11 (schlafen 11), CNP (2´, 3´-cyclic-nucleotide 3´-phosphodiesterase) and tetherin exert their antiviral function in the late phase of HIV-1 replication (Fig. 2). Immediately after fusion of the virion with the target cell, incoming capsid is bound by TRIM5α leading to disturbed uncoating of the capsid [154, 155]. Together with the viral capsid, diverse APOBEC3 proteins are delivered into the newly infected cell since they are incorporated into the virus. During reverse transcription, APOBEC3G proteins cause lethal G-to-A hypermutations in the viral genome [66, 105, 148], which has later on also been observed for APOBEC3D, APOBEC3F and APOBEC3H [74, 131]. For some APOBEC3 proteins additional deaminase-independent antiviral activities have been demonstrated [7]. In macrophages, dendritic cells and resting CD4+ T-cells reverse transcription is inhibited by SAMHD1 [8, 36, 73, 93]. SAMHD1, a deoxynucleoside triphosphate triphosphohydrolase, may act antiviral by reducing the cellular pool of dNTPs, thus limiting the reverse transcriptase [53, 94], however the ribonuclease activity accounts for the direct degradation of HIV-1 RNA [139]. Integration of proviral DNA into the host genome is diminished by Mx2 which is reported to abrogate uncoating and the capsid-dependent nuclear import or integration of the proviral DNA [46, 56, 80, 100]. At a later step of the HIV-1 replication cycle, the viral protein synthesis seems to be specifically impaired by SLFN11 which modulates the composition of the cellular tRNA pool and thereby hinders translation of HIV-1 mRNAs due to their specific codon bias [97]. Assembly of HIV-1 at the cellular plasma membrane is impeded by CNP that interacts with the viral structural polyprotein precursor Gag [173]. The relevance of these two factors awaits further confirmation and studies. Tetherin, as its name already indicates, tethers budding virions to the cell surface and thereby reduces virus release into the supernatant [117, 166] (Fig. 2).

Besides their potency to directly inhibit virus replication, tetherin and TRIM5α play an emerging role as sensors of viral infection. Tetherin or TRIM5α expression leads to NFκB signalling and proinflammatory cytokine expression, which is further increased after virus-tetherin association or capsid lattice recognition by TRIM5α [49, 122, 160].

HIV-1 is a successful pathogen and has evolved strategies to circumvent these cellular barriers by the expression of accessory genes or developing resistance. The HIV-1 accessory protein Vif targets APOBEC proteins to proteasomal degradation [148, 149] and the HIV-1 accessory protein Vpu as well as the HIV-1 O Nef disables

tetherin by sequestering it away from the viral budding sites [88, 117, 142, 166]. Surprisingly, the accessory protein Vpx that leads to degradation of SAMHD1 is not encoded by HIV-1 and is only expressed in HIV-2 and some SIV lineages [73, 93]. No HIV-1 encoded antagonist of Mx2 and CNP has been identified yet, but the virus can achieve escape mutations within their respective targets, capsid and matrix within Gag [56, 80, 100, 173]. In case of TRIM5α, HIV-1 capsid has adapted to this barrier and is not susceptible to inhibition. In striking contrast, TRIM5α from Old World monkeys is still highly active against HIV-1 [154]. Thus these restriction factors act in a species-specific manner [69].

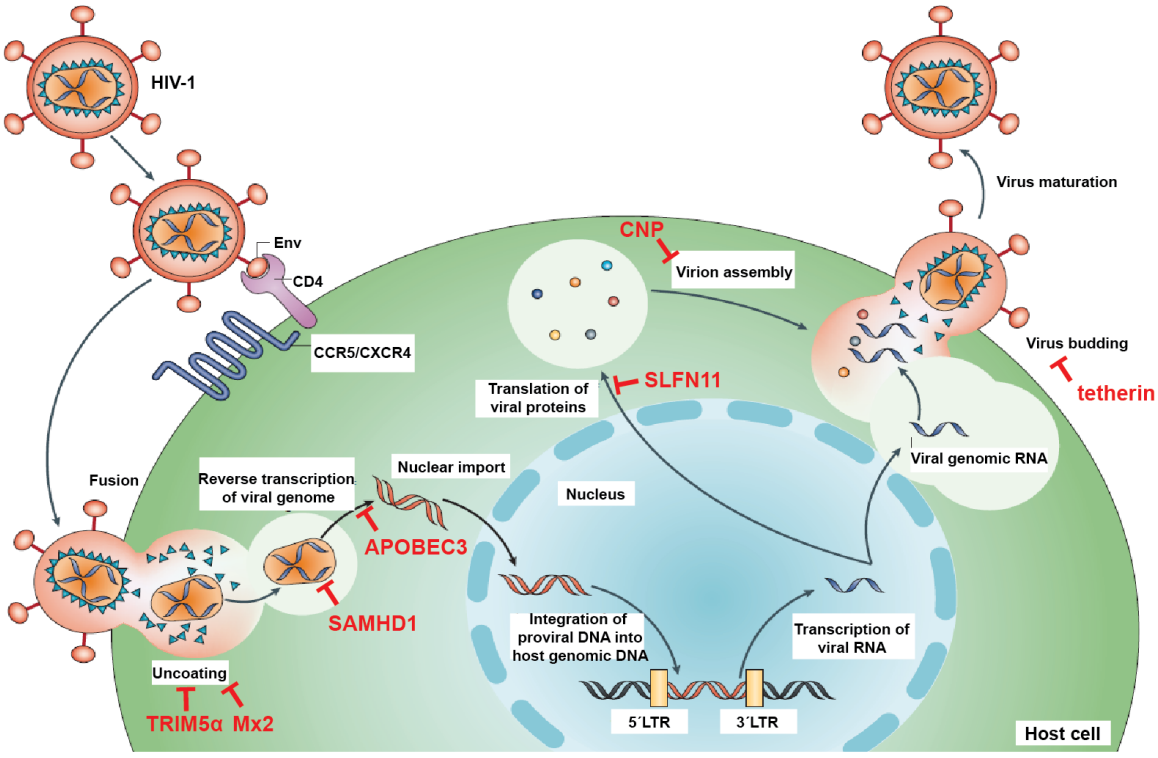


Fig. 2: Restriction factors of HIV-1. Scheme of the HIV-1 replication cycle. HIV-1 attaches to the host cell by binding the primary receptor CD4 and a co-receptor. After fusion, the capsid is delivered into the cytoplasm followed by uncoating and reverse transcription of the viral RNA into DNA. Proviral DNA is imported into the nucleus where it integrates into the host genome. After protein and genomic RNA synthesis the components assemble at the plasma membrane to virus particles. Following budding and virus release, the virus matures and can infect new target cells. Host restriction factors are indicated in red and their targets during the viral replication are marked with a red T. LTR= Long terminal repeat. Figure adapted from [127], p.53.

The evolution of cellular restriction factors as well as their viral counteractors illustrates the molecular arm race between virus and host, and implicates an

evolutionary selection pressure on genes encoding restriction factors. Thereby, each single positive selected mutation within a restriction factor could have been the result from another independent ancient pathogen-host conflict. This might explain the broad antiviral activity of some present day restriction factors, because they most likely emerged from multiple host-pathogen conflicts irrespective of HIV-1 [67]. Conclusively, the hallmarks of restriction factors are interferon responsiveness, antiviral activity in overexpression assays, evolution under positive selection and counteraction by viral encoded antagonists, but not all points may apply [67].

1.4 The cellular glycoprotein 90K

90K is so called because of its molecular mass of 90 kDa (kilodalton) in SDS-PAGE (sodium dodecyl sulphate polyacrylamide gel electrophoresis). It is also known as LGALS3BP (lectin, galactoside-binding soluble 3 binding protein) and Mac-2BP (Mac-2 binding protein) and is 585 amino acids in size. 90K is a cellular secreted glycoprotein [176] and is present in several body fluids including tears, urine, breast milk, semen and, most importantly, also in blood at concentrations in the µg/ml range [90].

To reach the extracellular milieu, 90K enters the secretory pathway via its N-terminal signal peptide (SP). In the endoplasmic reticulum and Golgi network 90K is modified on its seven *N*-glycosylation sites [25, 71, 141]. C-terminal of the signal peptide, 90K can be divided into four domains, first a scavenger receptor cysteine-rich (SRCR) domain, counting it to the SRCR domain-containing protein superfamily, second a BTB/POZ (broad-complex, tramtrack and bric à brac/ poxvirus and zinc finger) domain followed by thirdly an intervening region (IVR) and fourthly a C-terminal domain with no homology to any known protein [113] (Fig. 3 A). A characteristic feature of BTB domains is their ability to self-oligomerize to dimers or tetramers [3, 5]. Indeed, extracellular 90K has been reported to dimerize through its BTB/POZ domain [71] and to further self-oligomerize to huge ring structures consistent of five to eight 90K dimers, with a molecular mass of 1000-1500 kDa and a diameter of 30-40 nm [113, 141] (Fig. 3 A). Whether dimerization and/or oligomerization already occurs within the cell was not investigated and cannot be excluded so far.

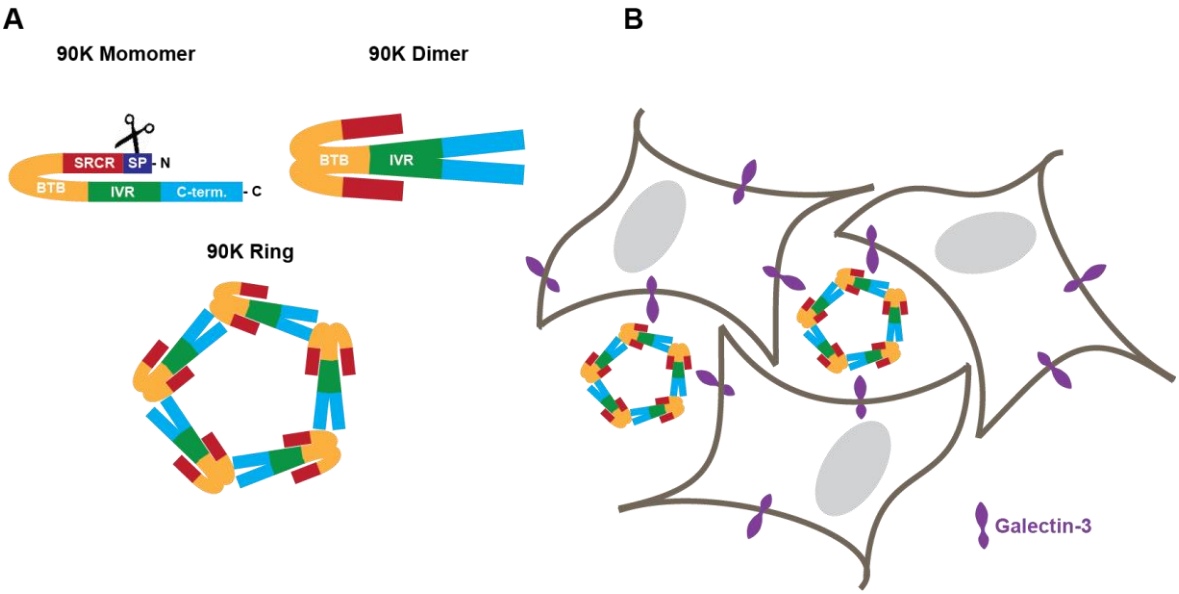


Fig. 3: 90K. (A) Schematic overview of the monomeric, dimeric and oligomeric organisation of 90K. 90K dimers probably interact via their domains two and four, but interaction has not experimentally proven. Scheme was created according a model from [113]. (B) Scheme of the 90K mode of action as cell adhesion factor. SP = signal peptide, SRCR = scavenger receptor cysteine-rich, BTB/POZ = broad-complex, tramtrack and bric à brac / poxvirus and zinc finger, IVR = intervening region, C-term. = C-terminal domain.

In addition to body fluids, a wide range of epithelial tissues harbour 90K [75, 90, 99]. The ring structure of 90K oligomers is thought to be important for its natural function as a cell adhesion factor. Secreted 90K binds to several ligands in the extracellular matrix, *in vivo* mainly Galectin-3, also known as Mac-2, but *in vitro* also different collagens and fibronectin [71, 90, 135, 141]. Hence, the 90K oligomers and rings may offer a perfect structure to mediate cell-cell and cell-extracellular matrix linkage through multiple binding capabilities (Fig. 3 B). This feature may contribute to 90K´s association to tumor growth [58]. Indeed, 90K was originally identified as a tumor associated antigen [75, 99, 115] in patients with various types of cancer like breast cancer [76], lung cancer [106], colon cancer [60, 163] as well as lymphoma [45] and high 90K levels are often associated with lower survival rates [159]. Likewise, 90K levels are upregulated and linked to more severe disease progression in Hantavirus PUUV (Puumala virus) [72], HCV (Hepatitis C virus) [6] and HIV-1 [18, 102, 116] infected patients. The secreted glycoprotein 90K may serve as a predictive marker for disease progression in HIV-1 infected patients as the amount of 90K protein correlates with the HIV-1 RNA levels [61, 116].

In light of 90K´s association with cancer and virus infections it may display additional functions besides cell adhesion. 90K has been proposed to serve as an immune

stimulator by inducing cytokine production including IL-2, IL-6, GM-CSF and TNF-α and thereby activating natural killer cell activity [126, 162]. A role of 90K in the immune response is further supported by *lgals3bp* being an interferon stimulated gene [16, 76, 108].

1.5 Scientific aim

There is still no vaccine against HIV-1 available and long term therapy of AIDS is difficult by reason of the high variability of this virus. A better understanding of the cellular intrinsic immunity against HIV-1 infection could enable alternative strategies in controlling the infection and thereby contribute to therapy improvement.

The gene encoding the cellular glycoprotein 90K/LGALS3BP shares two important characteristics with genes encoding other known HIV-1 restriction factors. They are interferon-inducible and their expression is upregulated in CD4+ T-cells of HIV-1 infected patients. Thus, the aim of the present study was to test a potential anti-HIV activity of 90K. Specifically, it was of interest to reveal an anti-HIV-1 effect of 90K in overexpression assays, to examine its antiviral mode of action and to determine its species specificity. Importantly, *90K* expression and interferon-inducibility in HIV-1 target cells as well as the relevance of a 90K-induced anti-HIV-1 effect within these cells was investigated.

2 Material and Methods

2.1 Material

Eukaryotic cells

293T	Human cell line originally derived from embryonic kidney. Transformed by adenovirus type 5 expressing SV40 (simian virus 40) large T-antigen [57]. Obtained from ATCC.
TZM-bl	HeLa derived cell line expressing CD4, CCR5 and CXCR4, encoding *luciferase* and *β-galctosidase* genes under the control of the HIV-LTR promoter [170]. Obtained from the NIH AIDS Reagent Program.
SupT1	Non Hodgkin´s T-cell lymphoma [152]. Obtained from the NIH AIDS Reagent Program.
J-Tag	Simian virus 40 T antigen-transfected human leukemic Jurkat T-cells.
Jurkat	Human T-cell leukemia cell line [171]. Obtained from the NIH AIDS Reagent Program.
CEMx174	Human T lymphoblastoid cell line, encoding *luciferase* and *gfp* genes under the control of the HIV-LTR promoter [17]. Obtained from the NIH AIDS Reagent Program.
Chessie 8	Balb/c mouse splenocyte x P3X63 Ag8.X653 myeloma, which produces monoclonal antibody of isotype IgG1 reacting with HIV-1 LAI gp41 [1]. Provided by Valerie Bosch, (DKFZ, Heidelberg).

PM1	Clonal derivative of HUT 87 [103]. Obtained from the NIH AIDS Reagent Program.
PBMCs	Peripheral blood mononuclear cells were isolated from human Buffy Coat (DRK, Ulm).
Macrophages	PBMCs were isolated from human Buffy Coat (DRK, Ulm) and differentiated to macrophages for 10-15 days in the presence of 10% human AB serum (Sigma).
CD4+ T-cells	CD4+ T-cells were isolated from Buffy Coat (DRK, Ulm) by negative selection with the RosetteSep Human CD4+ T Cells Enrichment Cocktail (StemCell Technologies, Grenoble).

Bacteria

Escherichia coli XL2-Blue™	*recA1 endA1 gyrA96 thi-1 hsdR17 supE44 relA1 lac* [F´proAB lacqZΔM15 Tn10 (Tetr) Amy Camr] [20] (Stratagene, Agilent Technologies, Waldbronn)

Media

Adherent cells	DMEM (Dulbecco´s modified Eagle Medium) (Gibco) supplemented with 350 µg/ml L-glutamine, 120 µg/ml Streptomycinsulfate, 120 µg/ml Penicillin and 10% (v/v) heat inactivated FCS.
Suspension cells	RPMI-1640 (Gibco) supplemented with 350 µg/ml L-glutamine, 120 µg/ml Streptomycinsulfate, 120 µg/ml Penicillin and 10% (v/v) heat inactivated FCS.

LB medium for bacteria culture	10 g/l Bacto-trypton, 5 g/l Yeast extract, 8 g/l NaCl, 1 g/l Glucose and 100 mg/l Ampicillin or Kanamycin, respectively.
LB agar for bacteria plates	15 g/l agar in LB Medium
S.O.C. medium for bacteria	Life Technologies (Carlsbad, USA)

Buffers and Solutions

Cell fixation for FACS	2 % PFA (w/v) in PBS
FACS buffer	1 % (v/v) FBS in PBS
Lysis buffer for ELISA samples	1 % (v/v) Triton X-100 in H_2O
NP-40 lysis buffer	150 mM NaCl, 10 mM TrisHCl pH 7.4, 1 mM EDTA, 0.5 % NP-40
NP-40 wash buffer	150 mM NaCl, 10 mM TrisHCl pH 7.4, 1 mM EDTA, 0.1 % NP-40
PBS-Tween	0.05 % (v/v) Tween in PBS
Resolving gel (7.5 %)	for one Gel: 1.5 ml Rotiphorese® Gel 30, 1.2 ml 1.88 M TrisHCl pH 8.8, 1.2 ml 0.5 % (w/v) SDS, 2.1 H_2O, 10 µl TEMED, 60 µl 10 % (w/v) APS
SDS Sample Buffer (2x)	200 mM TrisHCl pH 6.8, 6 % SDS, 20% Glycerol, 2 % DTT, 0.1 mg Bromphenol blue
Stacking gel	for one Gel: 0.33 ml Rotiphorese® Gel 30, 0.4 ml 0.625 M TrisHCl pH 6.8, 0.4 ml 0.5 % (w/v) SDS, 0.87 ml H_2O, 4 µl TEMED, 20 µl 10 % (w/v) APS
Sucrose for virus purification	20 % (w/v) in PBS, sterile filtered
Transfer buffer	6 g Tris, 28.8 g Glycin, 2 g SDS, 400 ml Methanol, add to 2 l with H_2O
Western Blot first antibodies	1 % (v/v) BSA, 0.05 % (w/v) NaN_3 in PBS
Western Blot second antibodies	0.5 % (w/v) Powdered milk in PBS
Western Blot blocking buffer	1 % (w/v) Powdered milk in PBS

Oligonucleotides (Biomers, Ulm)

90K 3´untr fwd	5´-GCTTCCTTCCTCTCTGCAATGA-3´
90K 3´untr rev	5´-TCAGGTGAGTAGGGCGACATC-3´
90K 3´untr probe	5´FAM-CTTCAACAACCGGCCAC-TAMRA3´
SP-BTB/POZ fwd	5´-CGAAGCTTATGACCCCTCCGAGGCTCTTCT GGGTGTGGCTGCTGGTTGCAGGAACCCAAGG CGTGAACGATGGATGACACCAGGAGCACCCA CACCCTGGACCTC-3´
BTB/POZ rev	5´-CGTCTAGAGGGGAGGAGGATGGCAAAGAG GCTTGC-3´
SP-IVR fwd	5´-CGAAGCTTAGACCCCTCCGAGGCTCTTCTG GGTGTGGCTGCTGGTTGCAGGAACCCAAGGC GTGAACGATGGTCTCCTCCCCCAGGACCCCT CGTTCCAGATG-3´
IVR rev	5´-CGTCTAGAAATCCGGGGCTTGTAGGTATCC T-3´
SP fwd	5´-GCAAGCTTGGATGACCCCTCCG-3´
Domain four rev	5´-CCTCTAGAGTCCACACCTGAGGAGTTGGTC AGG-3´
hI fwd	5´-CTCGGATCCACCATGACCCCTCCGAGGC-3´
rhI fwd	5´-CTCGGATCCACCATGGCCCCTCCGAGGC-3´
hIrhII rev	5´-GGGTGCTCCTGGTTTCATTGGTG-3´
hIrhII fwd	5´-CACCAATGAAACCAGGAGCACCC-3´
rhIV rev	5´-CGAAGGGCCCTCTAGAGTCCACACC-3´
hIIrhIII rev	5´-GGTCCTGGGGGAGGAGGATGGCAAAGAG-3´
hIIrhIII fwd	5´-CTCTTTGCCATCCTCCTCCCCCAGGACC-3´
rhIIIhIV rev	5´-CCAGGTGGGCGAGGTGTAAATCCGG-3´
rhIIIhIV fwd	5´-CCGGATTTACACCTCGCCCACCTGG-3´
hImoII rev	5´-GAAGCCCCGTGGTTTCATTGGTGCAG-3´
hImoII fwd	5´-CTGCACCAATGAAACCACGGGGCTTC-3´
moIV rev	5´-GGGCCCTCTAGACACCATGTCAGTGG-3´
hIImoIII rev	5´-GGGTCTTGGGGGAGGAGGATGGCAAAG-3´
hIImoIII fwd	5´-CTTTGCCATCCTCCTCCCCCAAGACCC-3´

moIIhIII rev	5´-GGTCCTGGGGGAGGAGGGTGGCAAAAAG-3´
moIIhIII fwd	5´-CTTTTTGCCACCCTCCTCCCCCAGGACC-3´
moIIIhIV rev	5´-CAGGTGGGCGAGGTGTAAAGGCGGGGC-3´
moIIIhIV fwd	5´-GCCCCGCCTTTACACCTCGCCCACCTG-3´
moI fwd	5´-CTCGGATCCACCATGGCTCTCCTGTGGC-3´
moIhII rev	5´-GGGTGCTCCTGGTATCGTTGGAGCAG-3´
moIhII fwd	5´-CTGCTCCAACGATACCAGGAGCACCC-3´
hIIImoIV rev	5´-CAGGTGGAAGAGGTGTAAATCCGGGG-3´
hIIImoIV fwd	5´-CCCCGGATTTACACCTCTTCCACCTG-3´

Plasmids

For selection in bacteria, plasmids encode a gene for ampicillin or kanamycin resistance.

pcDNA6/myc-His	Eukaryotic vector designed for overexpression in mammalian cell lines. Provided by Ji Hee Lee (South Korea) [95]. (Amp.)
pcDNA6.90K-myc	CMV promoter driven expression of C-terminally myc-tagged human 90K, in the pcDNA6/myc-His vector backobone. Provided by Ji Hee Lee (South Korea) [95]. Truncation mutants thereof, containing the authentic signal peptide and the C-terminal myc-tag, were generated by Nicola Schrott using *Hind*III/*Xba*I sites. (Amp.)
pcDNA6.90K-orthologs-myc	CMV promoter driven expression of C-terminally myc-tagged 90K orthologs. cDNAs provided by Amalio Telenti (Lausanne, Switzerland), cloned in the pcDNA6/myc-His vector backbone by Christina Stürzel using *Bam*HI/*Xba*I sites. (Amp.)
pcDNA6.CypCAP-myc	CMV promoter driven expression of C-terminally myc-tagged mouse CypCAP. Mouse cDNA was obtained from Sino Biological Incorporation, cloned in the pcDNA6/myc-His vector backobone by Christian Kolbe using *Hind*III/*Xba*I sites. (Amp.)

pcDNA6.90K-chimeras-myc	Chimeras were generated by SOE (splicing by overlapping extension) PCR and inserted in the pcDNA6/myc-His backbone using *Bam*HI/*Xba*I sites. For SOE PCR, first, domains of each species were amplified using primers with overlaps for the proximate domains of the various species, respectively. In a following PCR, products with overlaps were amplified to one chimeric product. (Amp.)
pIRES2-EGFP vector	Expression of the gene of interest and AcGFP1 from the same transcript (Clontech). (Kan.)
pIRES2.-EGFP.90K-myc	Expression plasmid for 90K-myc with an IRES-GFP was generated by amplification of *90K-myc* and insertion into pIRES2-EGFP (Clontech), using *Nhe*I/*Bam*HI sites. (Kan.)
pREP4.Glypican-3-HA	Expression plasmid for HA-tagged Glypican-3 provided by Guido David (Leuven, Belgium) [168]. (Amp.)
pA11SVL3.Influenza Virus HA	Expression plasmid for Hemagglutinin of Influenza A/chicken/Rostock/8/1934(H7N1) provided by Wolfgang Garten (Marburg) [52]. (Amp.)
pCMV4neo.Ebola GP	Expression plasmid for the Ebola glycoprotein provided by Mark Goldsmith [23]. (Amp.)
pCMVhygro.CD4	Expression plasmid for CD4 provided by Oliver Keppler (Frankfurt). (Amp.)
pcG-nef IRES GFP	Expression plasmid encoding *nef* under the control of a CMV promoter and *eGFP* via an IRES [157]. (Amp.)
pcG-nef*****IRES GFP	pcG-nef IRES GFP with a stop codon in *nef*, serving as empty vector control, provided by Daniel Sauter. (Amp.)
pcG-HIV-1 NL4.3 Vpu IRES GFP	CMV promoter driven expression of NL4.3 Vpu provided by Daniel Sauter. (Amp.)

pVSV-G	Expression plasmid for VSV-G provided by Oliver Keppler (Frankfurt). (Amp.)
pBR-NL4.3 eGFP	Modified pBR322 vector expressing NL4.3 provirus. Nef and eGFP are expressed from a bicistronic mRNA via an IRES [143]. (Amp.)
pNL4.3	Expression plasmid for proviral HIV-1 NL4.3 [2] provided by Oliver Keppler (Frankfurt). (Amp.)
pLAI.2	Expression plasmid for proviral LAI provided by Oliver Keppler (Frankfurt). (Amp.)
pYU-2	Expression plasmid for proviral YU-2 provided by Oliver Keppler (Frankfurt). (Amp.)
pCR-XL-TOPO-CH058.c	Expression plasmid for proviral CHO58 [118] provided by Beatrice Hahn. (Kan.)
pCR-XL-TOPO-THRO.c	Expression plasmid for proviral THRO (Ochsenbauer et al., 2012) provided by Beatrice Hahn. (Kan.)
pCR-XL-TOPO-CH077.t	Expression plasmid for proviral CHO77 [118] provided by Beatrice Hahn. (Kan.)
pblueskript HIV-2 7312A	Expression plasmid for proviral HIV-2 7312A provided by Beatrice Hahn [50, 51]. (Amp.)
pBR-SIVmac239	Modified pBR322 vector expressing SIVmac239 provirus, provided by Jan Münch. (Amp.)

siRNAs

non-targeting control siRNA (Dharmacon)

human 90K targeting (MWG)	5´-GAAGCUCUGCCUACAGUUC-3´
Mac-2BP siRNA (Santa Cruz)	pool of 3 target-specific 19-25 nt siRNAs

Antibodies

goat polyclonal anti-90K	R&D Systems (Minneapolis, USA); (WB: 1:1000, IP: 1:100)
mouse monoclonal anti-myc	Hybridoma supernatant, provided by Jens von Einem (University of Ulm); (WB: 1:2.5, IP: 1:10)
goat polyclonal anti-myc	Novus Biologicals (Littleton, USA); (IF: 1:1000)
rabbit polyclonal anti-HIV-1 gp120	Provided by Valerie Bosch (DKFZ, Heidelberg); (WB: 1:1000, IP: 1:100)
mouse monoclonal anti-HIV-1 gp41	Chessie 8 Hybridoma supernatant [1], provided by Valerie Bosch (DKFZ, Heidelberg); (WB: 1:2.5; IF: pure)
human monoclonal anti-HIV-1 gp120 2G12	Obtained from the NIH AIDS Reagent Program [161]. (FACS: 1:300)
mouse monoclonal anti-p24 MAK183	Exbio (Vestec, Czech Republic) (WB: 1:1000; ELISA: 1:6200)
rabbit polyclonal anti-p24	Eurogentec (Seraing, Belgium) (ELISA: 1:7700)
rabbit anti-ERK2 (MAPK)	Santa Cruz (Dallas, USA); (WB: 1:1000)
mouse anti-HA	abcam (Cambridge, UK); (WB: 1:1000)
mouse anti-Ebola GP	Provided by Stephan Becker (University of Marburg); (WB: 1:1000)
rabbit anti-H7 serum	Provided by Wolfgang Garten (University of Marburg); (WB: 1:6000-8000)

rabbit anti-Vpu serum	Provided by Ulrich Schubert (University of Erlangen); (WB: 1:10000)
rabbit anti-HIV-2 gp105	Obtained from the EVA Centre for AIDS Reagents (NIBSC); (WB: 1:200)
SIVmac251 serum	Obtained from the DPZ (Göttingen); (WB: 1:100)
mouse anti-CD4	abcam (Cambridge, UK); (WB: 1:1000, IP: 1:100-160)
anti-CD4-APC	BD Pharmingen (San Diego, USA); (FACS: 1:100)
anti-goat Alexa 488	Invitrogen (Oregon, USA); (IF: 1:1000)
anti-mouse Alexa 647	Invitrogen (Oregon, USA); (IF: 1:1000)
anti-human Alexa 633	Invitrogen (Oregon, USA); (FACS: 1:100)
anti-mouse Alexa 800	LI-COR Biosciences (Lincoln, USA); (WB: 1:2000)
anti-rabbit Alexa 800	LI-COR Biosciences (Lincoln, USA); (WB: 1:2000)
goat anti-human IgG, FC-IRDye800	Genway (San Diego, USA); (WB: 1:1000)
goat anti-rabbit IgG, Fc-HRP	Dianova (Hamburg); (ELISA: 1:2000)

Kits

Amaxa nucleofection	Lonza (Basel, Switzerland)
Anti-90K ELISA	eBioscience (San Diego, USA)
CalPhos^{TM} Mammalian Transfection Kit	Clontech (Mountain View, USA)
DNA Ligation Kit Ver.2.1	Takara Bio Inc. (Shiga, Japan)
EndoH	NEB BioLabs (Frankfurt)
Lipofectamine® RNAiMAX	Life Technologies (Carlsbad, USA)

Lipofectamine® 2000	Life Technologies (Carlsbad, USA)
Luciferase Assay System	Promega (Madison, USA)
Miniprep Kit	Qiagen (Hilden)
Phire® Hot Start DNA polymerase Kit	Thermo Scientific (Waltham, USA)
PNGase	NEB BioLabs (Frankfurt)
ProtoScript® First Strand cDNA Synthesis Kit	NEB BioLabs (Frankfurt)
RNeasy® Protect Midi Kit	Qiagen (Hilden)
RosetteSep™ Human CD4+ T Cell Enrichment Cocktail	Stemcell Technologies (Köln)
SIV p27 Antigen Capture Assay	ABLinc. (Rockville, USA)
Turbo DNA-*free*™ Kit	Life Technologies (Carlsbad, USA)
Ultra Clean™ 15 Purification Kit	MoBio Laboratories (Carlsbad, USA)
Wizard® Plus Midipreps Kit	Promega (Madison, USA)

Reagents

Agarose Standard	Roth (Karlsruhe)
Ammonium persulfate (APS)	Roth (Karlsruhe)
Ampicillin	Bayer (Leverkusen)
Bacto-Agar	BD/Difco (Heidelberg)
Bacto-Tryptone	BD/Difco (Heidelberg)
Bacto-Yeast Extract	BD/Difco (Heidelberg)
Bromphenol blue	Biomol (Hamburg)
BSA Diluent/Blocking Solution	KPL (Gaithesburg)
Cell culture flasks	Sarstedt (Nümbrecht)
Cell culture plates	Greiner Bio-one (Frickenhausen)
DNA Ladder 1kb Plus	Life Technologies (Carlsbad, USA)
dNTP	Invitrogen/Gibco (Karlsruhe)
Dulbecco´s modified eagle medium (DMEM)	Invitrogen/Gibco (Karlsruhe)
EDTA-Trypsin	Invitrogen/Gibco (Karlsruhe)
Ethanol	Sigma (München)
Ethidiumbromide (EtBr)	AppliChem (Darmstadt)
Ethylenediaminetetraacetic acid (EDTA)	Biochrom (Berlin)
Falcon Tubes (15/50ml)	Sarstedt (Nümbrecht)

Fetal calf serum (FCS)	Invitrogen/Gibco (Karlsruhe)
Ficoll separation solution	Biochrom (Berlin)
Filter tips	Greiner Bio-one (Frickenhausen)
Glycerin	Merck (Darmstadt)
G-Sepharose Beads	GE Healthcare (Buckinghamshire, GB)
HiPerSolv Chromanorm Water	VWR (Fontenay-sous-Bois, France)
Humanes AB serum	Sigma (München)
Interferon-α (Roferon)	Roche (Basel, Switzerland)
Interferon-γ	Sigma (München)
Interleukin-2 (IL-2)	Sigma-Ark (München)
Isopropanol	Merck (Darmstadt)
Kanamycin	Bayer (Leverkusen)
L-Glutamine	Invitrogen/Gibco (Karlsruhe)
Lipofectamin RNAiMax	Invitrogen/Gibco (Karlsruhe)
Lipofectamin2000	Invitrogen/Gibco (Karlsruhe)
Mounting medium with DAPI	Vectashield (Burlingame, USA)
M-PER® Mammalian Protein Extraction Reagent	Thermo Scientific (Rockford, USA)
NP-40	Sigma (München)
Nunc-Immuno™ MicroWell™ 96 well solid plates MaxiSorp™	Sigma (München)
Nunclon-delta white microwell plate	Sigma (München)
NuPAGE® MES SDS Running Buffer	Invitrogen (Karlsruhe)
Opti-MEM	Invitrogen/Gibco (Karlsruhe)
Paraformaldehyd (PFA)	Merck (Darmstadt)
Penicillin-Streptomycin	Invitrogen/Gibco (Karlsruhe)
Phosphate-Buffered Saline (PBS)	Invitrogen/Gibco (Karlsruhe)
Phytohemagglutinin (PHA)	Murex (Burgwedel)
Powdered milk	Roth (Karlsruhe)
Precision Plus Protein™ Kaleidoscope™	BioRad (München)
Reaction tubes (1.5/2ml)	Sarstedt (Nümbrecht)

RNase P Primer-Probe (VIC^{TM}) Mix	Applied Biosystems (Branchburg, USA)
Roswell Park Memorial Institute medium (RPMI-1640)	Invitrogen/Gibco (Karlsruhe)
Rotiphorese® Gel	Roth (Karlsruhe)
Serological pipette	Sarsted (Nümbrecht)
Sodiumchloride	Sigma (München)
Sodiumdodecylsulfate (SDS)	Sigma (München)
Sucrose	Sigma (München)
TAE buffer 50x	5Prime GmbH (Hamburg)
TaqMan Universal PCR Master Mix	Applied Biosystems (Branchburg, USA)
Tetramethylethylenediamine (TEMED)	Sigma (München)
Tris	AppliChem (Darmstadt)
Triton X-100	Sigma (München)
Trypsin	Life Technologies (Carlsbad, USA)
Tween 20	Roth (Karlsruhe)
Whatman paper	Whatman (Maidstone, Kent, UK)
Whatman® Protran® nitrocellulose membrane	GE Healthcare (Buckinghamshire, GB)

2.2 Methods

Bacteria transformation and culture

To introduce DNA into bacteria, plasmid DNA or ligated vectors were incubated with 5 µl or 15 µl *E.coli XL2-Blue*™, respectively, on ice for 20 min. After a heat shock at 42 °C for 30 sec to permeabilize the bacterial membrane, bacteria were chilled on ice for 2 min. To initiate bacterial growth, 200 µl S.O.C. medium was added and bacteria were incubated at 300 rpm and 37 °C for 30 min. Bacteria were plated onto LB agar plates containing 100 mg/l Ampicillin or Kanamycin for selection. Plates were incubated at 37 °C over night. In case of proviral DNA, growth of transformed bacteria was initiated for 2 h at 30 °C and agar plates were incubated for 24 h at 30 °C, in order to minimize recombination.

Bacteria were cultured in LB containing 100 mg/l Ampicillin or Kanamycin for selection at 37 °C over night or 30 °C for 24 h.

Plasmid DNA preparation

Plasmid DNA for cloning was isolated with the Miniprep Kit, plasmid DNA for transfection with the Wizard™ Plus Midiprep Kit, according to the manufacturer´s instructions. DNA concentration and purity was determined with the Nano Drop spectrophotometer (peqlab, Erlangen). DNA sequencing was performed by MWG-Biotec/Operon (Ebersberg).

Polymerase Chain Reaction (PCR)

PCR reactions were performed with the Phire™ Hot Start DNA polymerase Kit under following conditions:

(1) Initial denaturation: 98 °C, 2 min
(2) Denaturation: 98 °C, 5 sec
(3) Annealing: 58 °C, 5 sec
(4) Extension: 72 °C, 20 sec/kb, 35 cycles
(5) Final Extension: 72 °C, 7 min

Restriction digest and agarose gel electrophoresis

Restriction endonucleases (New England BioLabs, Frankfurt) were used with appropriate buffers according to the manufacturer´s instructions. Loading buffer was added to DNA and electrophoretically separated with a 1 % agarose gel, which was prepared with 1x TAE and three drops/100 ml ethidiumbromide.

DNA gel elution

Electrophoretically separated DNA fragments were visualized by ethidiumbromide incorporation on an UV (366 nm) screen (Syngene, USA). DNA from the isolated bands was purified with the UltraClean 15 DNA purification kit according to the manufacturer´s instructions.

DNA Ligation

Vector and insert DNA were mixed in a ratio 1:3 and ligated using the DNA Ligation Kit Ver.2.1 according to the manufacturer´s instructions.

Cell culture

Adherent and suspension cells were passaged in 25 cm^2 or 75 cm^2 cell culture flasks (Sarstedt, Nümbrecht) with supplemented DMEM or RPMI-1640, respectively, in a 37 °C incubator with 90 % relative humidity and 5 % CO_2. The cells were splitted 1:10 twice a week.

Isolation of primary blood cells

Buffy Coat (lymphocyte concentrate from 500 ml whole blood) from healthy blood donors (DRK, Ulm) was diluted 1:2 with PBS. Ficoll separation solution was overlaid with the same volume of diluted Buffy Coat and centrifuged for 30 min at 700 *g* without brakes, afterwards the white interphase layer constituting the peripheral blood mononuclear cells (PBMCs) was transferred into a new tube. In order to remove remaining erythrocytes, cells were resuspended in 1 % EDTA and washed twice in PBS by centrifugation for 7 min at 275 *g*. Two million PBMCs/ml were cultured in supplemented RPMI-1640 and stimulated with 1 µg/ml PHA and 10 ng/ml IL-2 for three days.

For differentiation to primary macrophages via adhesion, two million PBMCs/ml were cultured in supplemented RPMI-1640 with 10 % (v/v) heat inactivated human AB serum (Sigma) for 10-15 days. Before use, macrophages were thoroughly washed with warm RPMI-1640.

For preparation of CD4+ T-cells from Buffy Coat by negative selection, 1.5 ml Rosette RosetteSep™ Human CD4+ T Cell Enrichment Cocktail were added to 11 ml Buffy Coat diluted with 19 ml PBS and the mixture was incubated for 20 min at RT prior to centrifugation through Ficoll cushion. The resulting white interphase layer contains CD4+ T-cells. Following EDTA treatment and washing, CD4+ T-cells were cultured in supplemented RPMI-1640 and stimulated with 1 µg/ml PHA and 10 ng/ml IL-2 for three days prior to infection or siRNA nucleofection.

DNA transfection of 293T cells

293T cells were transiently transfected with the CalPhos™ Mammalian Transfection Kit according to the manufacturer´s instructions. One day before transfection $1.8x10^5$ cells/ml were seeded in 6-well or 12-well plates and transfected at a confluence of 60-80 %. For one 6-well 12.4 µl 2 M $CaCl_2$, 100 µl HBS and 5 µg DNA,

for triplicates of 12-wells 18.6 µl 2 M $CaCl_2$, 150 µl HBS and 8 µg DNA were used. After 6-16 h medium was exchanged.

siRNA transfection of primary macrophages

For siRNA transfection of primary macrophages, Lipofectamine® RNAiMAX Transfection Reagent was used according to the manufacturer´s instructions. The macrophages were transfected twice, on day one with 15 nM siRNA and day four with 5 nM siRNA. Transfections were performed over night, followed by medium exchange the next day. Human 90K targeting siRNA (MWG) was used.

siRNA nucleofection of PBMCs

For siRNA nucleofection of PBMCs, the Amaxa nucleofection system with the program U14 was used. One- five million PBMCs were nucleofected with 2.5 µM siRNA per transfection. Transfection was performed twice, on day three and day five after stimulation. Nucleofected cells were cultured in supplemented RPMI-1640 with 10 ng/ml IL-2 prior to infection.

Generation of high-titer HIV-1

293T cells were transfected in 6-wells with the calcium-phosphate precipitation method using 5 µg proviral DNA. For generation of HIV-1 pseudotypes, 4 µg proviral DNA in combination with 1 µg VSV-G expression plasmid was used. 48 hours post transfection, supernatant was collected and centrifuged for 3 min at 453 *g*. Ba-L was passaged on PM-1 cells. The infectious titers and virus stock concentrations were determined by a TZM-bl-based luciferase assay and an anti-p24 capsid antigen ELISA, respectively. Virus stocks were stored at -80 °C.

Infection of primary cells

Infection of one 6-well primary macrophages was performed using 1 µg p24 equivalent for 24 h. 0.5 million PBMCs in 100 µl RPMI-1640 with 10 ng/ml IL-2 were infected in a V-bottom-96-well plate with 5 ng p24 equivalent for 6-8 h. Following infection, cells were thoroughly washed three times with warm RPMI-1640 to remove excess virus. For verification of the removal of excess virus a post wash control, in form of an aliquot of the cell culture supernatant after washing, was taken and subjected to anti-p24 capsid antigen ELISA.

Infectivity Assay

TZM-bl cells are genetically modified HeLa cells that were engineered to stably express *CD4* and *CCR5* as well as *luciferase* under the control of a Tat dependent promoter [170]. 10.000 TZM-bl cells/well were seeded in flat-bottom-96-well plates, followed by infection with appropriate volume of virus containing supernatant the day after. 48-65 h after infection, firefly luciferase activity was measured with the Luciferase Assay System (Promega). For this purpose, supernatant was removed, cells were lysed in 40 µl lysis buffer and 10 µl of the lysate was transferred into a 96-well Nunclon-delta white microwell plate (Nunc™). Following addition of substrate, light emission was detected with the Orion Microplate Luminometer (Berthold Detection systems) and the enzyme activity was quantified as RLU (relative light units) using the software Simplicity 4.02 (Berthold Detection systems).

RNA isolation and cDNA synthesis

Total cellular RNA was isolated with the RNeasy® Protect Midi Kit (Qiagen) according to the manufacturer´s instructions. In order to remove contaminating traces of DNA, DNase digestion was performed with the Turbo DNA-*free*™ Kit (Life Technologies) according to the manufacturer´s instructions. For reverse transcription the ProtoScript® First Strand cDNA Synthesis Kit (NEB) was used according to the manufacturer´s instructions. The Kit contains poly-A binding primers and allows specific cDNA synthesis of the mRNA within the DNase treated RNA extract. For every sample one additional approach without M-MuLV reverse transcriptase was used as a control for the specific detection of cDNA to exclude genomic DNA contaminations.

Quantitative Real-Time PCR

Quantification of relative 90K mRNA levels was performed with the Step One Plus Real Time PCR System (Applied Biosystems) using Taq-Man Universal PCR Master Mix (Applied Biosystems) with a FAM and TAMRA labeled 90K specific probe. As an internal control, mRNA of the housekeeping gene *RNaseP* was quantified using the RNase P Primer-Probe (VIC™) Mix (Applied Biosystems). PCR reaction was performed under following conditions:

Holding State:
(1) 50 °C, 2 min
(2) 95 °C, 10 min
Cycling State (40 cycles):
(1) 95 °C, 15 sec
(2) 60 °C, 1 min
Data analysis was performed with the Applied Biosystems Step One Software v2.1 and relative 90K mRNA levels were determined using the ΔΔCt method [145].

anti-HIV-1 p24 capsid antigen ELISA

For detection of p24 capsid antigen a homemade sandwich ELISA was used. Virus in cell culture supernatant was lysed in 1 % Triton X-100 for 1 h at 37 °C, to inactivate the virus and get access to the capsid antigen p24. Nunc-Immuno™ MicroWell™ 96 well solid plates MaxiSorp™ (Sigma) were coated over night with monoclonal mouse anti-p24 antibody MAK 138 (Exbio) (stock: 3.1 mg/ml, diluted 1:6200). After blocking with 1 % FCS in PBS for 2 h at 37 °C, virus lysate as well as duplicates of p24 capsid standard (abcam) diluted in 0.05 % Triton X-100 in PBS-Tween was loaded on the plates. The standard was diluted in 1:2 steps and ranged from 12.5 ng/ml to 0.098 ng/ml, 0.05 % Triton X-100 was added as blank. Following incubation over night, unbound p24 capsid antigen was removed by washing with PBS-Tween. For detection of bound p24 capsid antigen the plates were incubated first with polyclonal rabbit anti p24 serum (Eurogentec) (diluted 1:7700) and second with goat anti rabbit IgG-Fc-HRP (Dianova) (stock: 0.8 mg/ml, diluted 1:2000), diluted in blocking solution for 1 h at 37 °C each. To reduce background, plates were always washed with PBS-Tween between the individual antibody additions. Horse radish peroxidase (HRP) enzyme activity was started by adding TMB (KPL) substrate and stopped with 0.5 M HCl. Chemiluminescence was measured at 450 nm and 659 nm with the Thermomax microplate reader (Molecular devices).

anti-SIV p27 capsid antigen ELISA

For detection of SIV p27 capsid antigen a commercial ELISA was used (ABLinc.). Samples were processed according to the manufacturer´s instructions.

anti-90K ELISA

For quantification of intracellular 90K protein, one million primary cells were lysed in 25 µl 1 % Triton X-100, diluted 1:5 in 1x sample diluent (included in the Kit) and subjected to the 90K ELISA (eBioscience) according to the manufacturer´s instructions with 90K standard dilutions ranging from 100-0.78 ng/ml.

FACS

Two days post transfection, 293T cells were pelleted and stained in FACS tubes (BD). For staining of CD4 a direct APC-conjugated antibody was used, for Env surface stain the human monoclonal anti HIV-1 gp120 2G12 was used as first antibody, followed by secondary antibody anti-human Alexa 633. Cells were incubated with antibodies in FACS-buffer for 30 min at 4 °C and subsequently washed with PBS. Following staining, cells were fixed with 2 % PFA for 1 h at 4 °C. Flow cytometry was performed using the FACS Canto II (BD) and the BD FACSDiva™ software.

Virus purification

20 % (w/v) sucrose was overlayed with virus containing supernatant using 200 µl sucrose cushion per 1 ml supernatant. Small virus samples were purified by centrifugation at 20817 *g*, 4 °C for 90 min, virus samples more than 2 ml were purified via ultracentrifugation (Beckman coulter) at 41.000 rpm (SW60Ti rotor), 4 °C for 1 h or 28.000 rpm (SW41Ti rotor), 4 °C for 2 h. Pelleted virus was dissolved in appropriate volume of PBS.

SDS-PAGE and Western Blot

Cells were lysed in appropriate volume of M-PER Mammalian Protein Extraction Reagent followed by 20 min centrifugation at 20817 *g* at 4 °C. Cell lysates and purified virus, respectively, were mixed with 2x SDS sample buffer and heated for 5 min at 95 °C. Proteins and protein standard, a mixture of 10 multicolor recombinant proteins (Precision Plus Protein™ Kaleidoscope™, BioRad), were run on a 7.5 % SDS-PAGE and transferred onto nitrocellulose. Blocked membranes were incubated with primary antibody over night at 4 °C on a rotating scatter. Secondary antibodies conjugated with Alexa 800 fluorescent dye were used for detection by

Odyssey Infrared Imaging System (LI-COR Biosciences). Membranes were analyzed with the Odyssey software.

Co-immunoprecipitation

Cells were lysed in 100 µl 0.5 % NP-40 lysis buffer and a 10 µl aliquot was used for control of protein expression (Input). Residual lysate was filled up to final volume of 500 µl with 0.5 % NP-40 and incubated with antibody for 1 h on ice. 30 µl G-Sepharose Beads (GE Healthcare) were added and precipitated 90 min at 4 °C on a rotating scatter. Beads were washed three times by centrifugation at 106 *g* for 30 sec at 4 °C with 1 ml 0.1 % NP-40 wash buffer, treated with 2x SDS sample buffer and heated for 5 min at 95 °C. Supernatants contained the precipitated proteins.

Digestion with PNGase or EndoH

Cell lysates were treated with PNGase (NEB) and EndoH (NEB) according to the manufacturer´s instructions. Digestion was performed with 625 Units PNGase for 20 min or with 100 Units EndoH for 5 min at 37 °C in 15 µl cell lysate. Enzymes were inactivated by adding 2x SDS sample buffer and heating for 5 min at 95 °C.

Confocal immunofluorescence microscopy

Cells grown on coverslips were transfected with Lipofectamine2000 and fixed with 4 % PFA. They were permeabilized with 0.1 % Triton X-100, blocked with 1 % BSA and immune stained with first antibody in one step for 1 h at 37 °C. Following, goat anti-myc or Chessie 8 hybridoma supernatant anti-gp41 stained cells were treated with their respective secondary antibodies anti-goat Alexa 488 and anti-mouse Alexa 647, diluted in 1 % BSA, for 30 min at 37 °C. Coverslips were mounted with mounting medium containing DAPI and analyzed with a Zeiss LSM confocal microscope. Images were recorded and processed with the ZEN (2010) software.

3 Results

Parts of these results have been published in [101].

3.1 90K expression reduces the particle infectivity of HIV-1 progeny by interfering with the maturation and incorporation of the Env proteins

A putative antiviral effect of 90K on HIV-1 was first determined in a heterologous assay based on 90K expression in 293T cells, which do not endogenously express 90K (Fig. 4 A). Thus, a full length proviral DNA, encoding IRES *gfp* after the *nef* open reading frame, was co-transfected with decreasing amounts of a C-terminally myc-tagged 90K (90K-myc) expression plasmid. Dose-dependent expression of 90K-myc was monitored by Western Blot (Fig. 4 A). Equal transfection efficiency was verified by flow cytometry of GFP expression (data not shown). The infectivity of secreted virus in culture supernatants was quantified using a TZM-bl cell based luminometric infectivity assay. Upon co-expression of 90K-myc in the producer cells, supernatants displayed decreased amounts of infectious virus (Fig. 4 B). To investigate if 90K affects virus release, the amount of secreted viral antigen in the very same supernatants was analyzed using a p24 capsid antigen ELISA. Released p24 in supernatants was not altered grossly by 90K co-expression (Fig. 4 C). These results suggest that 90K expression does not interfere with virus release but rather lowers the infectivity of newly produced virus particles. Concordantly, particle infectivity, defined as infectivity normalized to the amount of released p24, was reduced by 90K expression in a dose dependent manner (Fig. 4 D).

To determine how 90K expression interferes with the infectiousness of HIV-1 progeny, immunoblotting of 293T producer cell lysates was performed. Interestingly, a marked difference in the Env expression pattern was observed within 90K transfected cells (Fig. 5 A). In the context of 90K expression, the amounts of mature Env subunits gp120 and gp41 were diminished compared to control cells. Reduction of gp120 and gp41 levels was accompanied by a relative accumulation of the Env precursor protein. The band intensities were quantified by Infrared-based imaging with the LICOR system allowing a calculation of the processing efficiency of the gp160 precursor to mature gp120 and gp41. Mirroring the particle infectivity (Fig. 4

D), the processing efficiency of gp160 was dose dependently reduced upon 90K expression (Fig. 5 A).

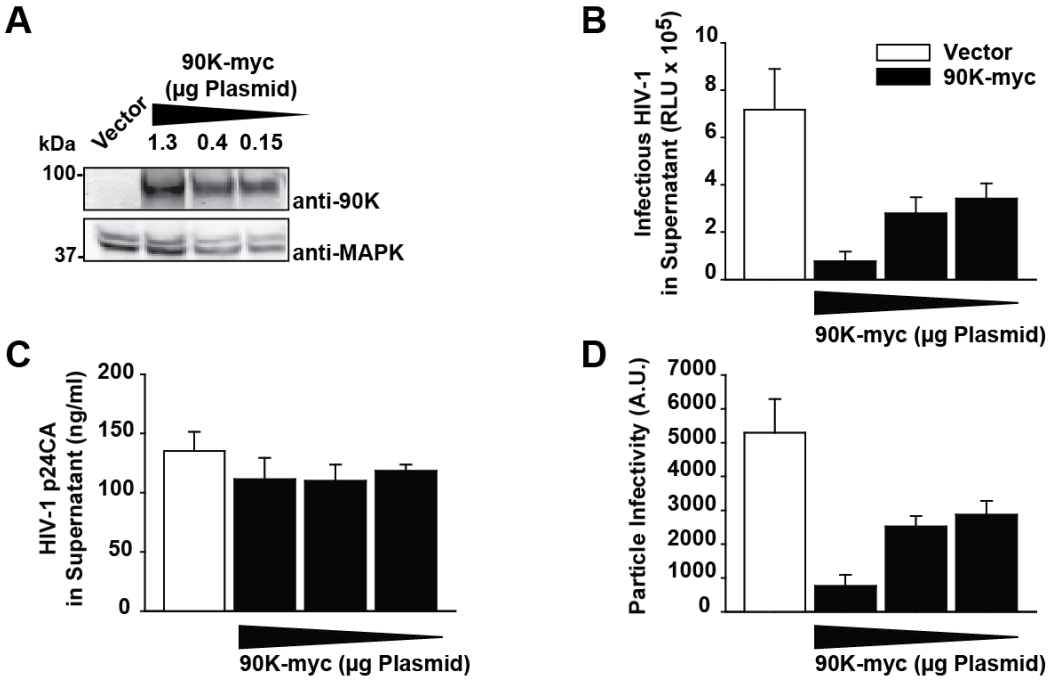


Fig. 4: 90K expression reduces the particle infectivity of HIV-1 progeny. (A) 293T cells were transfected with decreasing amounts of 90K-myc expression plasmid. DNA content was kept constant by filling up with empty vector. Immunoblot of the cell lysates was processed with indicated antibodies. (B) 293T cells were co-transfected with 1.3 µg proviral HIV-1 NL4.3 IRES-eGFP plasmid and decreasing amounts (1.3, 0.4, 0.15 µg) of 90K-myc expression plasmid. DNA content was kept constant by filling up with empty vector. 48 h post transfection, infectivity of newly produced virus in supernatant was analyzed by a TZM-bl cell based infectivity assay. (C) The very same supernatants were analyzed for virus release by measuring the secreted p24 capsid antigen by ELISA. (D) Particle infectivity was determined by normalizing the infectivity values from B to the secreted p24 capsid concentration from C. Shown are arithmetic means ± S.D. of triplicates. MAPK= MAP kinase, p24CA= p24 capsid antigen, RLU= relative light units, A.U.= arbitrary units. Figure adapted from [101], p.3.

In contrast to Env processing, the cleavage of the capsid precursor Pr55 to mature capsid p24 was not impaired by 90K. Additionally, equal expression of the viral proteins Nef and Vpu within all samples ruled out a general influence of 90K on the biosynthesis of viral proteins (Fig. 5 A) supporting a specific effect of 90K on HIV-1 Env biosynthesis.

Further, the protein composition of virions, generated in presence or absence of 90K expression, was analyzed by immunoblotting. This analysis revealed a reduction of gp120 and gp41 incorporation into HIV-1 virions by 90K (Fig. 5 B). In accordance

with the release data obtained by ELISA (Fig. 4 C), Western Blot of p24 capsid did not reveal 90K- dependent changes of virus release.

Particle infectivities of multiple experiments were plotted in relation to their respective relative gp120 incorporations as a function of 90K expression (Fig. 5 C small dots). Statistical analysis indicates a positive correlation between particle infectivity and gp120 incorporation.

Conclusively, these results strongly suggest that 90K interferes with the processing of the Env precursor gp160 to gp120 and gp41, diminishes the gp120 and gp41 incorporation into the virus and thereby reduces the infectivity of newly synthesized HIV-1 particles.

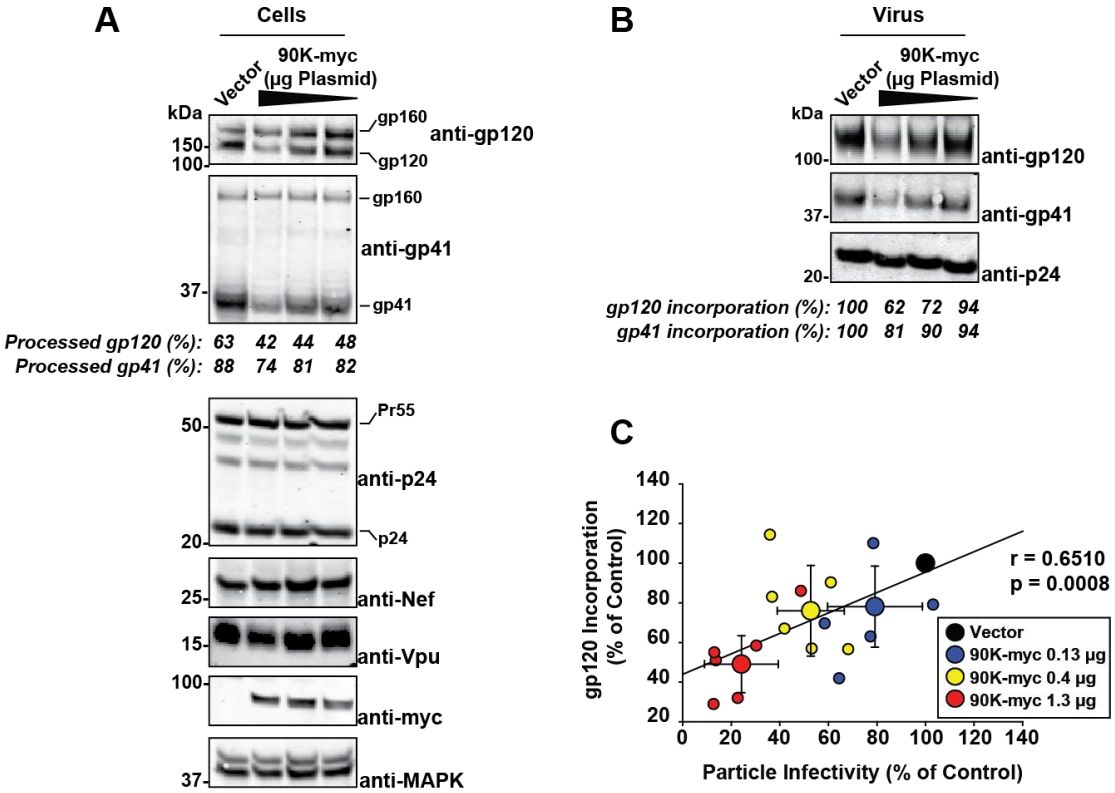


Fig. 5: 90K expression interferes with the maturation and incorporation of Env into HIV-1 progeny. (A) Cell lysates of transfected 293T cells shown in Fig. 4 and (B) sucrose cushion purified virus particles in supernatants thereof were analyzed by immunoblotting using the indicated antibodies. Band intensities were quantified by Infrared-based imaging with the LICOR system. Numbers indicate the Env processing efficiency as percentage of gp120 or gp41 from total Env and the relative gp120 and gp41 incorporation as amount of gp120 and gp41 per p24, respectively. (C) Correlation plot of particle infectivity and gp120 incorporation as a function of 90K-myc amount from multiple experiments. Small dots represent the values of five to six individual experiments, large dots the arithmetic means ± S.E.M. thereof. The Pearson´s correlation coefficient r and the corresponding p value were calculated with GraphPad Prism. MAPK = MAP kinase. Figure adapted from [101], p.3.

3.2 90K inhibits multiple HIV-1 strains

The initial evidence that 90K has an inhibitory effect on HIV-1 (Fig. 4-5) was obtained with the X4-tropic laboratory adapted strain NL4.3. Since Env is not only important for viral infectiousness but also determines the viral tropism, the ability of 90K to inhibit R5-tropic strains was investigated. In addition to the strains LAI and YU-2, three transmitted founder viruses (TFV) CH058, THRO and CH077 were included. TFVs are viruses obtained from patients early after transmission and are considered to represent the single transmitted variant [118]. Therefore, the TFVs are useful to elucidate 90K´s inhibitory effect on HIV-1 particles occurring during transmission and very early in HIV-1 infection.

As observed for HIV-1 NL4.3, co-transfection of proviral DNA encoding the various HIV-1 strains and 90K-myc expression plasmid led to a marked reduction of infectious virus in supernatant for all R5-tropic viruses including the TFVs (Fig. 6 A). Calculation of the particle infectivity further confirmed 90K´s antiviral efficacy against all HIV-1 strains tested, with particularly strong effects against the TFVs CH058 as well as THRO and, interestingly, with the highest inhibition of the TFV CH077 (Fig. 6 B). Additionally, immunoblotting of sucrose cushion purified virus in supernatants revealed an incorporation defect of gp120 into particles from all tested HIV-1 strains when 90K was expressed (Fig. 6 C). Concomitant with the paucity of mature gp120 in the newly produced virus, the processing efficiency from the gp160 precursor to mature gp120 in the producer cells was impaired in presence of 90K, ranging from 26 % for NL4.3 to 46 % for LAI (Fig. 6 D).

Since 90K reduces the particle infectivity, gp120 incorporation and Env processing of not only the laboratory adapted X4-tropic strain NL4.3 but also of several R5-tropic strains, including LAI, YU-2 and the TFVs CH058, THRO and CH077, 90K constitutes a general inhibitor of HIV-1. Interestingly, TFVs are even more potently inhibited, suggesting that 90K could represent a bottleneck to virus seeding following transmission.

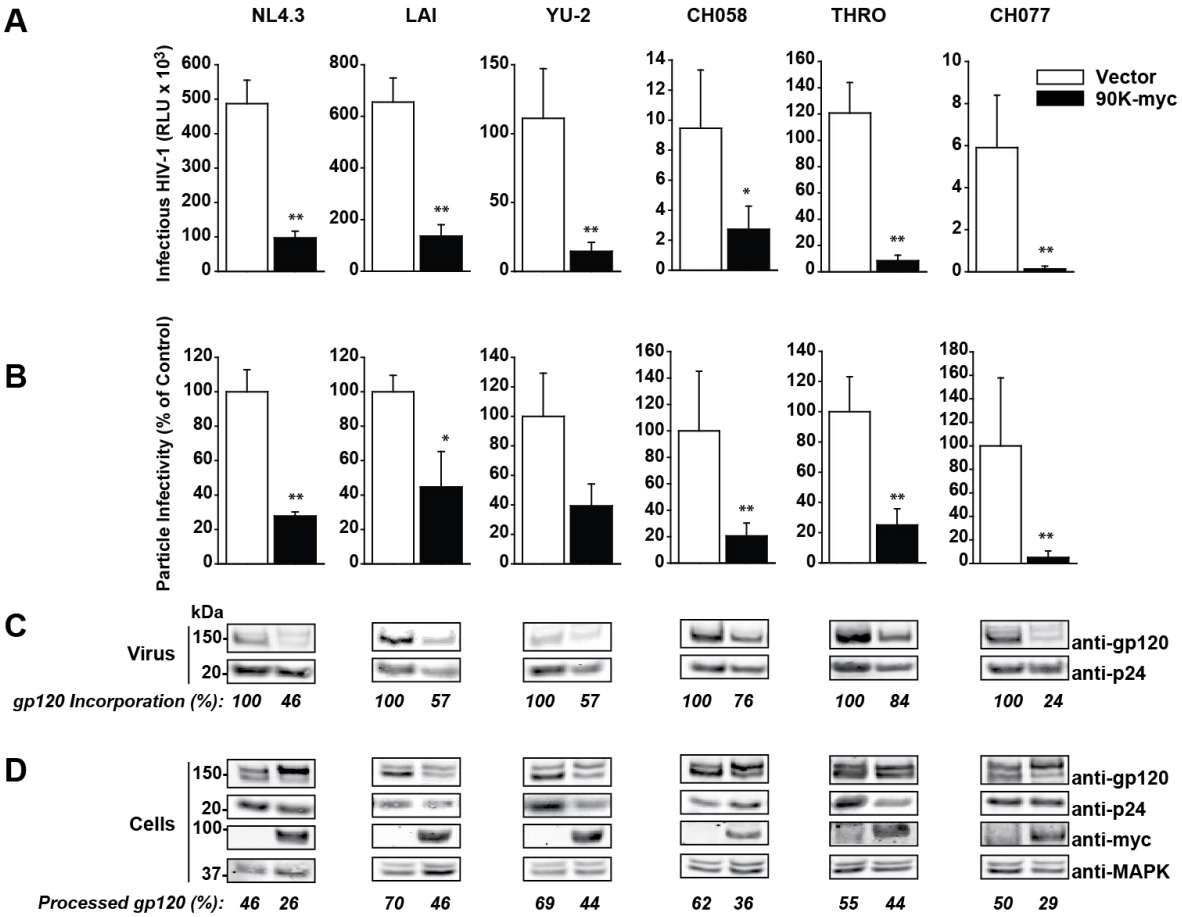


Fig. 6: 90K inhibits multiple HIV-1 strains. (A) 293T cells were co-transfected with 1.3 µg of indicated proviral DNA and 1.3 µg 90K-myc expression vector or empty vector. 48 h post transfection, infectivity of newly produced virus in the supernatant was measured by a TZM-bl cell based infectivity assay. (B) The corresponding particle infectivity was determined by normalizing the infectivity to the amount of released p24 capsid antigen and particle infectivity for vector transfected cells was set to 100 %. (C) Sucrose cushion purified virus and (D) cell lysates of producer cells were analyzed by immunoblotting using the indicated antibodies. Band intensities were quantified by Infrared-based imaging with the LICOR system. Numbers indicate (C) the relative gp120 incorporation as amount of gp120 per p24 and (D) the Env processing efficiency as percentage of gp120 from total Env. *: $p<0.05$; **:$p<0.02$ (Student´s T-Test). MAPK= MAP kinase, RLU= relative light units. Figure adapted from [101], supplement.

3.3 90K expression reduces the amount of Env at the cell surface

During its synthesis, Env is directed to HIV-1 budding sites at the cellular plasma membrane where it is eventually incorporated into the newly produced virus. In order to analyze if the 90K-mediated reduction of virally incorporated Env is accompanied by low Env levels exposed at the cell surface, Env expression was determined by flow cytometry of non-permeabilized cells. 293T cells were co-transfected with HIV-1 wt IRES eGFP proviral DNA and empty vector or a 90K-myc expression

plasmid, respectively. Env exposed at the cell surface was immunostained with the neutralizing 2G12 antibody which binds to a conformational- and carbohydrate-dependent epitope of gp120, followed by an appropriate Alexa 633 conjugated secondary antibody, and measured by flow cytometry. As expected, the 2G12 antibody specifically detected Env since the *env* deficient HIV-1Δ*env* control displayed only background signals (Fig. 7 A). Env surface expression on HIV-1wt transfected cells was determined as APC-MFI (mean fluorescence intensity) of GFP-positive cells (P3) normalized to APC-MFI of GFP-negative cells (P2) (Fig. 7 A). Comparing the Env surface levels of 90K expressing cells to control cells, the amount of Env at the cellular plasma membrane was reduced about three fold in presence of 90K (Fig. 7 B).

To rule out any unspecific effect on protein surface levels due to 90K overexpression, the amount of the CD4 receptor on the plasma membrane likewise was analyzed in vector or 90K-myc transfected cells. 90K did not alter the CD4 cell surface levels (data not shown).

All together, these findings revealed a specific reduction of the Env surface levels by 90K, which could contribute to the paucity of Env incorporation into budding virions.

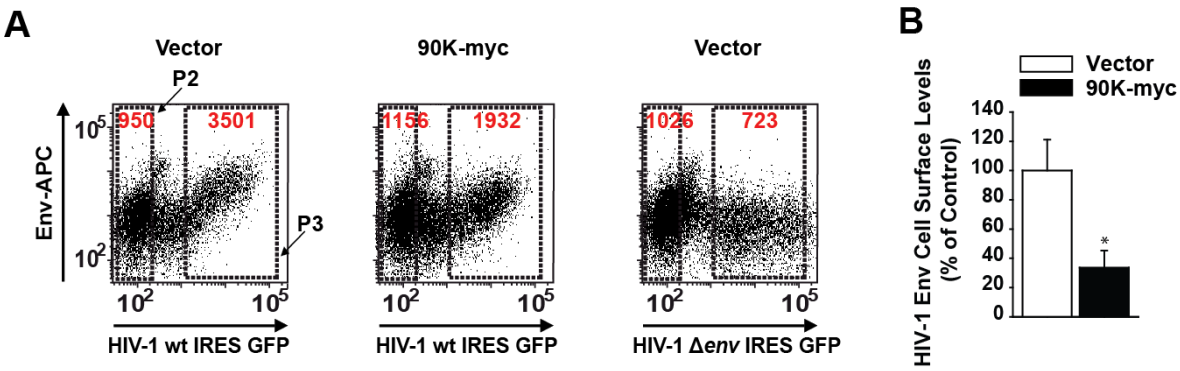


Fig. 7: 90K expression reduces the amount of Env at the cell surface. (A) 293T cells were co-transfected with equal amounts of wt or *env* deficient HIV-1 NL4.3 IRES eGFP proviral constructs and empty vector or a 90K-myc expression plasmid. 48h post transfection, Env levels at the cell surface were stained with the primary antibody 2G12, followed by the secondary antibody anti-human AlexaFluor 633 and cells were analyzed by flow cytometry. Shown are representative dot plots from one experiment out of three. (B) Env cell surface levels were calculated as ratio of APC-MFI (red numbers) of GFP positive cells (P3) normalized to GFP negative cells (P2).The ratio for vector transfected cells was set to 100 %. Shown are arithmetic means ± S.E.M. of three independent experiments. P = population, APC = Allophycocyanin, GFP = green fluorescent protein. Figure adapted from [101], p.5.

3.4 90K is not a specific inhibitor of furin-mediated cleavage

90K expression reduces the processing of the Env precursor gp160 to mature gp120 (Fig. 5 A) and lowers Env cell surface amounts (Fig. 7). 90K-mediated inhibition of the cellular protease causing Env cleavage might be one explanation for the impaired processing efficiency of Env. gp160 is processed in the Golgi complex by furin and/or furin-like proteases, thus an incomplete processing of Env could simultaneously lead to reduced trafficking of the mature Env subunits to the plasma membrane. To investigate a possible influence of 90K on furin activity, proteolytic processing of various furin substrates was analyzed. For this purpose, 293T cells were co-transfected with expression plasmids for different furin substrates as well as 90K-myc or empty vector. Noteworthy, the 90K-imposed processing defect for over-expressed HIV-1 Env with 64 % to 35 % (Fig. 8 A) was similar in magnitude compared to HIV-1 Env expressed in the proviral context with 63 % to 42 % (Fig. 5 A) suggesting an exclusive role of 90K on Env without requiring the presence of additional HIV-1 proteins.

In contrast, the processing pattern of HA-tagged Glypican 3, a cellular protein that is cleaved by furin, was not markedly altered in 90K-myc expressing cells compared to 90K negative control cells (Fig. 8 B). To test whether 90K specifically exerts its function on viral proteins, processing of the Ebola and Influenza glycoproteins, two known furin substrates, was investigated. 90K expression strikingly reduced the processing efficiency of the Ebola virus precursor GP to mature GP1 from 23 % to 8 % (Fig. 8 C). Conversely, the fold difference of Influenza virus Hemagglutinin (HA) processing efficiency constituted just 1.1 between control and 90K-myc expressing cells (Fig. 8 D).

Since 90K did neither interfere with the furin-dependent processing of cell encoded Glypican 3 nor Influenza virus protein HA, 90K does not seem to generally interfere with furin cleavage activity. Interestingly, 90K expression interfered not only with the processing of HIV-1 Env but also Ebola virus GP, providing a first hint for a broader antiviral spectrum of 90K activity.

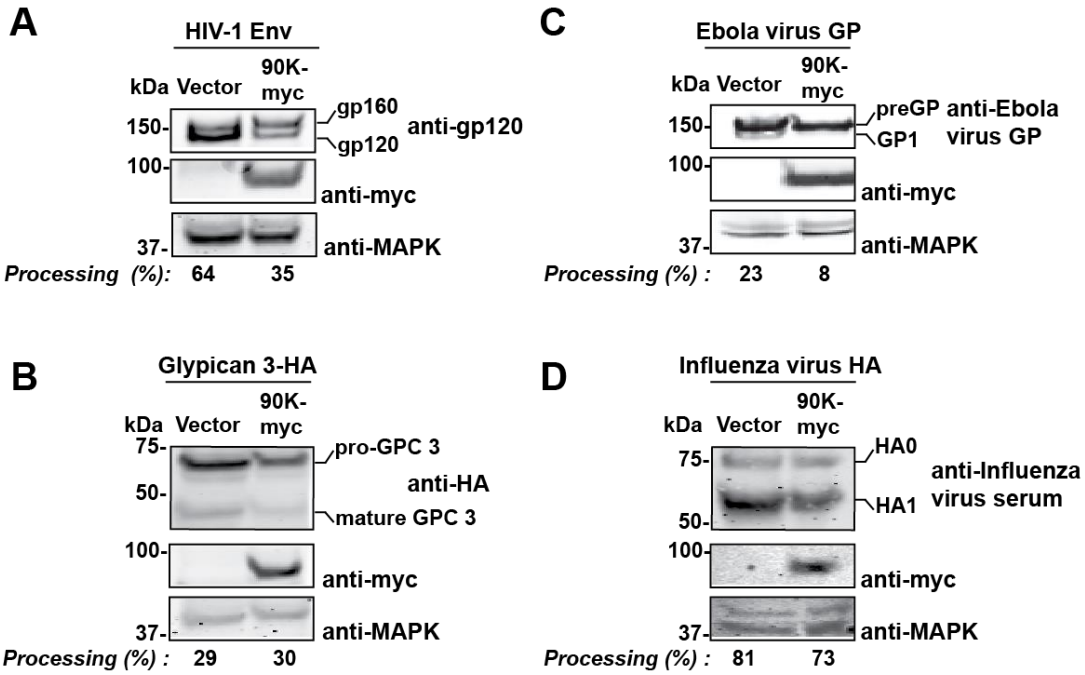


Fig. 8: 90K is not a specific inhibitor of furin mediated cleavage. (A-D) 293T cells were co-transfected with expression plasmids for the indicated furin-dependent proteins and the same amount of 90K-myc or empty vector. Two days post transfection, cell lysates were analyzed by immunoblotting using the indicated antibodies. Band intensities were quantified by Infrared-based imaging with the LICOR system. Numbers indicate the processing efficiency as percentage of cleavage product from total protein. MAPK = MAP kinase, pro-GPC 3 = Glypican 3 precursor, preGP = Ebola glycoprotein precursor, GP1 = mature Ebola glycoprotein, HA0 = Influenza HA precursor, HA1 = mature Influenza HA. Figure adapted from [101], p.5.

3.5 90K and Env co-localize but do not seem to interact

To exert their antiviral function, restriction factors often interact directly or indirectly with their target molecule, for example TRIM5α binds to incoming capsid [154] and tetherin is anchored in viral membranes [117, 121, 166]. Hence, it was first analyzed by confocal immunofluorescence microscopy whether 90K and its viral target Env get into close proximity within the cellular environment. To this end, 293T cells were co-transfected with plasmids encoding HIV-1 Env and 90K-myc and newly synthesized proteins were immunostained with fluorophore conjugated antibodies. The cellular distribution of 90K (green) and Env (red) revealed a high degree of co-localization of both proteins in the merged picture (Fig. 9 A). Determining the co-localization coefficient of 90K with Env and *vice versa* in 105 cells revealed a significant co-localization of both proteins (Fig. 9 B).

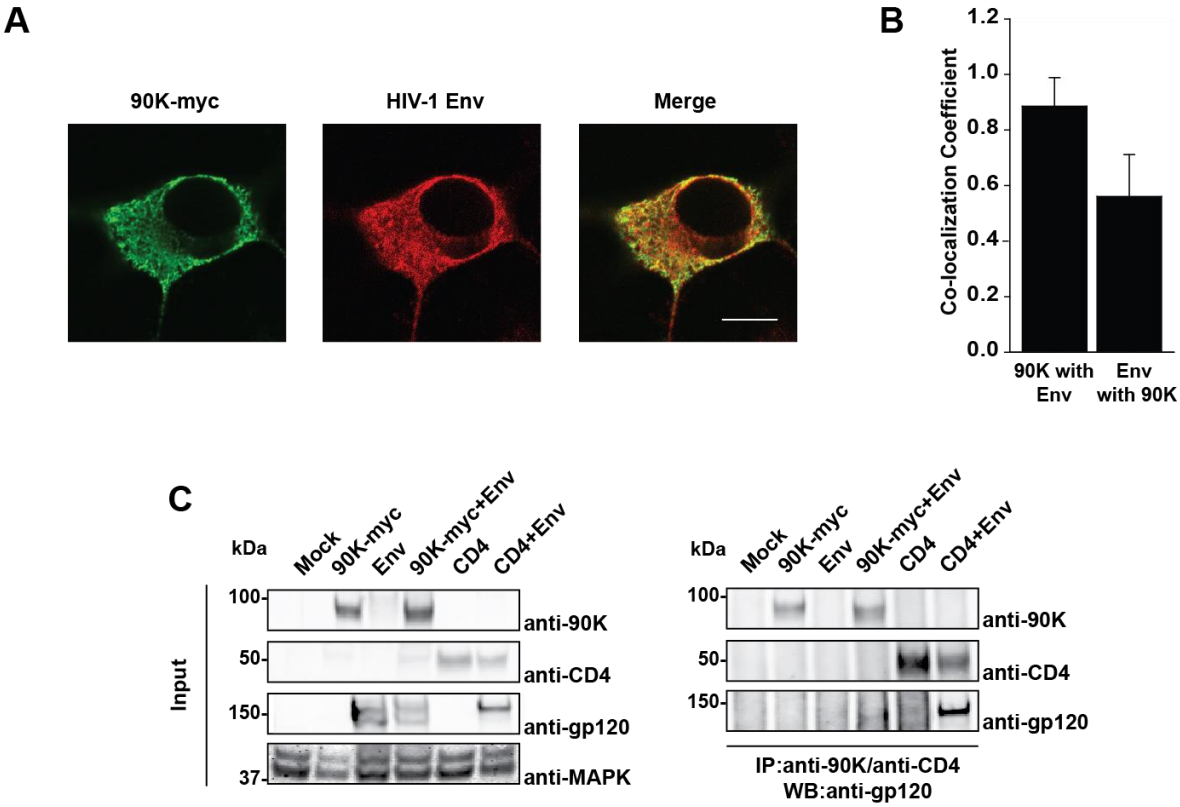


Fig. 9: 90K and Env co-localize but do not seem to interact. (A) 293T cells were co-transfected with 90K-myc and Env expression plasmids, and stained with specific primary antibodies followed by appropriate fluorophore conjugated secondary antibodies. 90K was immunostained using AlexaFluor 488 (green) and Env using AlexaFluor 647 (red). Scale bar: 10 µm. (B) The classic co-localization coefficient was calculated using ZEN2010 software. The data represent the arithmetic mean ± S.D. of 105 analyzed cells. (C) For the Co-IP 293T cells were co-transfected with pcDNA6, pcDNA6.90K-myc, an HIV-1 Env expression plasmid, pCMVhygro.CD4 or a combination thereof. An aliquot of whole cell lysate was used for expression control (Input) (left). 90K, CD4 and bound proteins were precipitated from cell lysates by using anti-90K or anti-CD4 antibody, respectively. Immunoblotting of whole cell lysates and precipitates was performed with indicated antibodies. MAPK = MAP kinase, IP = immunoprecipitation, WB = Western Blot. Figure adapted from [101], supplement.

Principally, a strong co-localization could allow a physical interaction of the two proteins. This possibility was addressed by a co-immunoprecipitation (Co-IP). 293T cells were co-transfected with plasmids encoding Env, 90K, CD4 and combinations thereof. Env combined with CD4 served as a positive control due to the documented interaction of Env and CD4 in the ER [15, 32, 78]. Immunoblotting of an aliquot of the cell lysates confirmed equal protein expression in the IP Input (Fig. 9 C, left panel). For the IP, 90K or CD4 were precipitated with specific antibodies and the co-precipitated proteins were detected by immunoblotting (Fig. 9 C, right panel). Env clearly precipitated with CD4 (Fig. 9 C, right panel, lane 6), and the lack of bands in

Env- or CD4-only transfected cells demonstrated the specificity of the CD4-Env association (Fig. 9 C, right panel, lanes 3 and 5). In contrast, no Env precipitation was observed in the 90K and Env co-expressing cells (Fig. 9 C, right panel, lane 4). Co-IP was repeated with anti-myc precipitation as well as *vice versa* with anti-gp120 precipitation, confirming the initial result (data not shown). Negative results in Co-IP do not prove the lack of interaction of two proteins, and weak interactions might not be detectable. However, these experiments do not provide evidence for interaction of 90K and Env.

Conclusively, the immunofluorescence microscopy affirmed strong co-localization between 90K and Env, which is not entirely surprising since both proteins posttranslationally mature in the secretory pathway. The Co-IP studies argue against a direct interaction of 90K with its viral target Env.

3.6 90K does not retain HIV-1 Env in the ER

The secretory protein 90K becomes highly glycosylated during its trafficking through the ER and the Golgi, a characteristic which 90K shares with Env. Hence an outcompetition of Env for glycosylation moieties or a disturbance of Env glycosylation by the presence of 90K could occur. Therefore, in order to detect any influence of 90K on the glycosylation pattern of Env, a Peptide-*N*-Glycosidase F (PNGaseF) digestion was performed, removing *N*-linked glycans from glycoproteins. 293T cells were co-transfected with an Env expression plasmid and a plasmid encoding 90K-myc or empty vector. Cell lysates were divided and one half of each condition was treated with the amidase PNGase while the other half served as untreated control. Both, 90K and the Env subunits, showed lower molecular weights after PNGaseF treatment confirming the modification of both proteins with *N*-glycans (Fig. 10 A). No difference in the pattern of deglycosylated gp160 and gp41 was observed after PNGaseF digestion regardless of 90K expression (Fig. 10 A), indicating that 90K does not alter the gylcosylation composition of Env.

Since 90K and Env both use the secretory pathway and co-localize to a high extent in the same cellular compartments (Fig. 9 A-B), 90K possibly traps Env in the ER. To investigate the trafficking of Env from the ER to the Golgi, Endoglycosidase H (EndoH) treatment was used. EndoH cleaves within the chitobiose core of high

mannose and some hybrid oligosacchrides and thereby specifically removes the glycan moieties added in the medial Golgi region. As expected, the glycans attached to the ER residing gp160 were removed by EndoH digestion whereas the gp41 glycans that have already been modified within the Golgi, were not sensitive to EndoH treatment (Fig. 10 B, vector cells). In comparison to the control cells, the glycosylation pattern was not altered by 90K expression. Although the Env processing defect in the untreated cells was clearly visible (Fig. 10 B, left panel), no EndoH resistant gp160 accumulated in the 90K expressing cells (Fig. 10 B, right panel), arguing against a 90K induced block in trafficking from the ER to the Golgi.

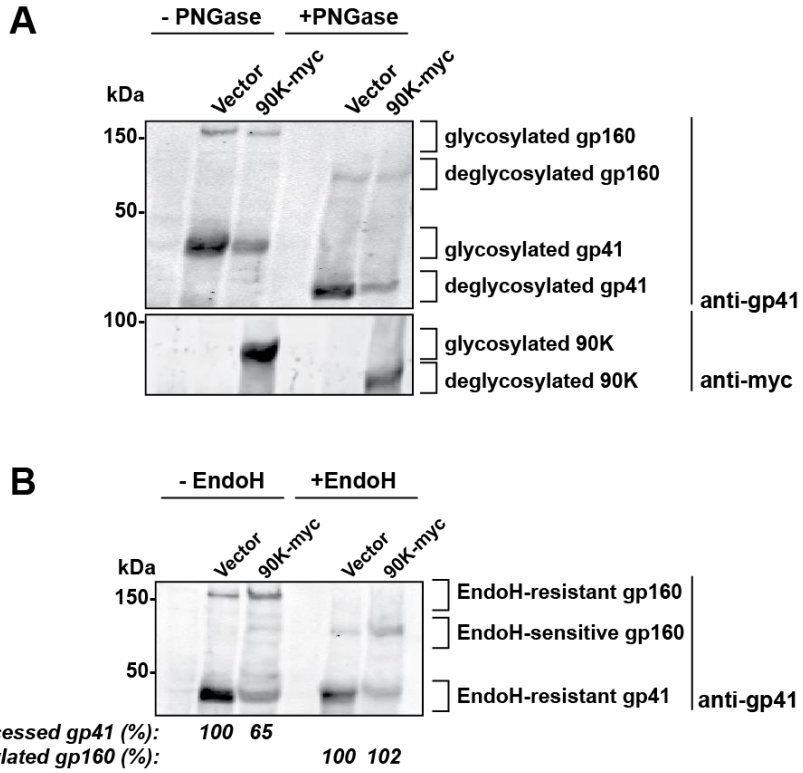


Fig. 10: 90K does not retain HIV-1 Env in the ER. (A-B) 293T cells were co-transfected with plasmids encoding HIV-1 IRES-eGFP proviral DNA and 90K-myc or empty vector. Cell lysates were digested with (A) PNGaseF or (B) EndoH, respectively. Untreated lysates served as controls. Proteins were analyzed by immunoblotting using the indicated antibodies. Numbers indicate the Env processing efficiency as percentage of gp41 from total Env or the percentage of deglycosylated gp160 from total gp160 signal. Figure adapted from [101], supplement.

3.7 The two central domains of 90K are required and sufficient for its anti-HIV-1 activity

Based on sequence homologies, 90K can be divided into four domains, a scavenger receptor cysteine-rich (SRCR) domain, a BTB/POZ domain followed by the intervening region (IVR) and lastly a C-terminus without homology to any known protein (Fig.11 A). In order to determine which regions within 90K exert the antiviral function, 90K truncation mutants were generated, each expressing two domains in their natural configuration. Like wt 90K, the shortened 90K mutants are targeted to the secretory pathway by preservation of the authentic signal peptide at the N-terminus of all truncation mutants and a C-terminal myc-tag enables detection of all 90K variants by immunoblotting (Fig. 11 A). The similar expression rate of 90K and its mutants after transfection in 293T cells was verified by immunoblotting and all 90K constructs showed the expected molecular weight (Fig. 11 B).

Co-transfection of HIV-1 with the various 90K mutants revealed that expression of the two intermediate domains of 90K was even more potent in reducing the HIV-1 particle infectivity than full length 90K. In contrast, the 90K mutant consisting of the two first domains 90K-(1-2)-myc reduced the particle infectivity less efficiently than wt 90K and 90K-(3-4)-myc bearing only domains three and four totally failed to inhibit HIV-1 (Fig. 11 C). Going along with the particle infectivity, 90K-(2-3)-myc strongly reduced the gp120 incorporation into HIV-1 progeny as well as the Env processing efficiency (Fig. 11 D-E). Viral Env incorporation was less impaired by 90K-(1-2)-myc compared to wt 90K and unaffected by 90K-(3-4)-myc (Fig. 11 D). Both mutants altered the gp160 processing not significantly (Fig. 11 E). The strong antiviral potential observed for 90K-(2-3)-myc suggests that the determinants for 90K´s antiviral activity lay within its second and third domains. Therefore, the single domain mutants SP-90K-(2)-myc and SP-90K-(3)-myc were constructed, and their expression was verified by immunoblotting (Fig. 11 B, right panel). Co-transfection with HIV-1 proviral DNA revealed that domain two had very low antiviral potential in reducing HIV-1 particle infectivity and Env processing, but no effect on Env incorporation. Domain three alone had no antiviral potential at all (Fig. 11 C-E, right panel each).

These analyses indicate that a variant of 90K that is devoid of the N-terminal SRCR domain and the C-terminal domain, efficiently diminishes HIV-1 particle infectivity, gp120 incorporation and gp160 processing. Hence the two central protein binding

domains BTB/POZ and IVR are sufficient and required for the anti-HIV-1 function imposed by 90K. However, the individual presence of either domain two or three failed to restrict HIV-1.

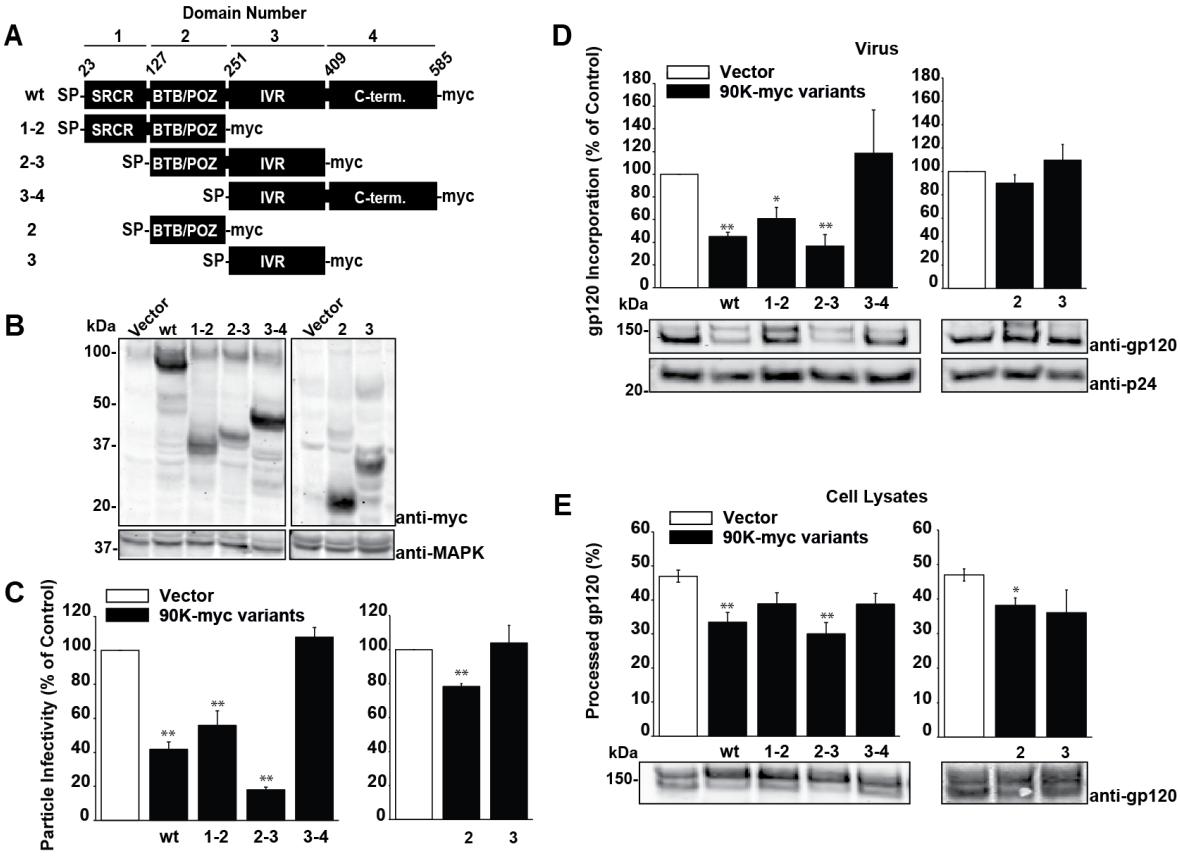


Fig. 11: The two central domains of 90K are required and sufficient for its anti-HIV-1 activity. (A) Scheme of the 90K protein domain organization and the analysed truncated mutants. Numbers indicate amino acid positions. Scheme adapted from [101], p.9. (B) 293T cells were transfected with the indicated constructs and equal protein expression was verified by immunoblotting using anti-myc antibody. (C) 293T cells were co-transfected with HIV-1 NL4.3 proviral DNA and the various 90K constructs. 48 hours post transfection the particle infectivity in the supernatant was measured as infectivity per ng p24. Values for vector control cells were set to 100 %. Shown are arithmetic means ± S.E.M. from 3-5 independent experiments. (D) Sucrose cushion purified progeny virions were analyzed by Western Blot and band intensities were quantified by Infrared based imaging. gp120 incorporation defined as gp120 per p24 was calculated from 3-5 independent experiments and the condition without 90K was set to 100 %. Shown is one representative blot. (E) Cells were lysed and proteins were detected by immunoblotting using the indicated antibodies. Band intensities were quantified by Infrared-based imaging and the percentage of mature gp120 from total Env protein is depicted. The bar diagrams show the arithmetic means ± S.E.M. of 3-5 independent experiments with one representative immunoblot. **: $p<0.01$, *: $p<0.05$, no *: not significant (Student´s T-Test). SP = signal peptide, SRCR = scavenger receptor cysteine-rich, BTB/POZ = broad-complex, tramtrack and bric à brac / poxvirus and zinc finger, IVR = intervening region, C-term. = C-terminal domain, MAPK = MAP kinase.

3.8 Antiviral activity of the 90K orthologs from seven non-human primates and the 90K mouse homolog CypCAP against HIV-1

The 90K protein is not unique to humans and 90K orthologs from seven non-human primates share even high sequence homology on the protein level to human 90K ranging from 90 % up to 98 % (Tab.1). To figure out whether the antiviral potential of 90K is evolutionary conserved, these 90K orthologs from seven non-human primates were compared in their ability to restrict HIV-1. For this purpose, expression plasmids encoding myc-tagged 90K orthologs were co-transfected with HIV-1 proviral DNA. Expression of 90K orthologs from chimpanzee (cpz), orangutan (ora), african green monkey (agm), owl monkey (owl), gibbon (gibb) and baboon (bab) reduced the HIV-1 particle infectivity to similar degrees as human 90K. Interestingly, in multiple experiments the 90K ortholog from rhesus macaque (rhes) was unable to impair HIV-1 particle infectivity (Fig. 12 A).

Tab. 1: Homology of 90K orhologs and the mouse homolog CypCAP in percentage.

Human 90K	100 %
Chimpanzee 90K	98 %
Orangutan 90K	97 %
Gibbon 90K	96 %
Baboon 90K	94 %
Rhesus Monkey 90K	94 %
African Green Monkey 90K	94 %
Owl Monkey 90K	90 %
Mouse CypCAP	69 %

Mice encode for a 90K homolog protein which shares 69 % homology to human 90K (Tab.1) and is referred to as cyclophylin C-associated protein (CypCAP) because of its binding to cyclophilin C [27, 47]. It was interesting to examine if the antiviral activity of 90K is even conserved in a less related mammalian species, and therefore the potential of the heterolog CypCAP to inhibit HIV-1 was investigated. To this end an expression plasmid encoding myc-tagged CypCAP was co-transfected with HIV-1 proviral DNA. In contrast to human and most non-human primate 90Ks, mouse CypCAP was not able to reduce the particle infectivity of newly produced HIV-1 (Fig. 12 A, gray bar). Sucrose cushion purified HIV-1 produced from 90K and

CypCAP expressing cells was analyzed by immunoblotting (Fig. 12 B). Concomitant with the particle infectivity, the gp120 incorporation into newly produced virus was lowered by all 90K orthologs with the exception of rhesus 90K and the mouse homolog CypCAP (Fig. 12 C). Surprisingly, immunoblotting of lysates of producer cells (Fig. 12 B) revealed that all tested proteins, including the inactive 90K from rhesus macaque and mouse CypCAP, induced a processing defect (Fig. 12 D).

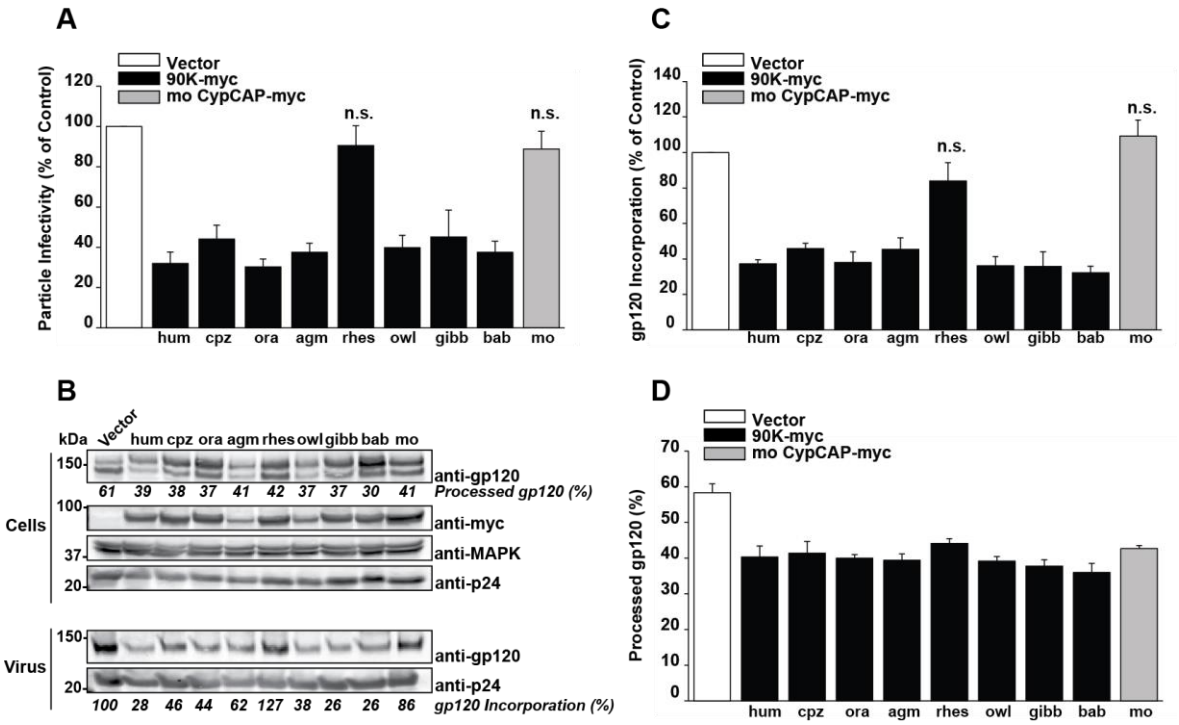


Fig. 12: Antiviral activity of the 90K orthologs from seven non-human primates and the mouse homolog CypCAP against HIV-1. (A) 293T cells were co-transfected with 1.3 µg HIV-1 NL4.3 proviral DNA and 1.3 µg of the indicated 90K constructs. 48 h post transfection, particle infectivity was calculated as infectivity per p24 capsid antigen in the supernatant. Particle infectivity in the absence of 90K was set to 100 %. Shown are mean values of 3-4 independent experiments ± S.E.M.. (B-D) Cell lysates and sucrose cushion purified virus from 3-7 independent experiments were analyzed by immunoblotting. (B) Shown is one representative blot. (C-D) Band intensities were quantified by Infrared-based imaging and gp120 incorporation was calculated as the ratio of gp120 signal intensity to p24 signal intensity. Value for vector transfected cells was set to 100 %. Relative gp160 processing was determined as mature gp120 per whole Env (gp120+gp160) signal. Bar diagrams show the arithmetic means ± S.E.M. of 3-7 independent experiments for (C) the gp120 incorporation into virus progeny and (D) the processed gp120 within the cell lysates. n.s. = not significant, bars not marked with n.s. = $p<0.05$ (Student´s T-Test). hum = human, cpz = chimpanzee, ora = orangutan, agm = african green monkey, rhes = rhesus macaque, owl = owl monkey, gibb = gibbon, bab = baboon, mo = mouse, MAPK = MAP kinase.

Comparison of human and non-human primate 90Ks indicated that the antiviral activity against HIV-1 is highly conserved between these orthologs with the exception of 90K from rhesus macaques. In contrast, the 90K homolog CypCAP from mice failed to reduce HIV-1 particle infectivity. The impaired HIV-1 particle infectivity induced by active 90K proteins went along with reduced gp120 incorporation into newly synthesized virus particles. The discrepancy between normal gp120 incorporation but visible gp160 processing defect for the inactive rhesus 90K ortholog and the mouse CypCAP could point toward a potential uncoupling of these two events.

3.9 Antiviral activity of the 90K orthologs from seven non-human primates and the 90K mouse homolog CypCAP against SIV and HIV-2

HIV originated from SIV and several independent cross species transmissions from SIVcpz/gor and SIVsmm to humans gave rise to HIV-1 and HIV-2, respectively. It is assumed that restriction factors act in a species specific manner and might constitute a barrier to cross-species transmission of viruses, which have not properly adapted [54, 68, 69]. Hence it was of interest to compare the antiviral activity of human 90K, the 90K orthologs from seven non-human primates and the mouse homolog CypCAP against SIV and HIV-2 with the degree of HIV-1 inhibition. To this end, 293T cells were co-transfected with constant amounts of proviral DNA encoding HIV-1, SIVmac239 or HIV-2 7312A with decreasing amounts of the various 90K constructs and particle infectivity of the respective virus progeny were calculated. Human 90K and the six 90K orthologs with anti-HIV-1 activity, dose dependently decreased the particle infectivity of SIVmac239 in a similar range to HIV-1. Rhesus macaque derived 90K again failed to reduce the particle infectivity of SIVmac239 potently. Surprisingly, mouse CypCAP lowered the particle infectivity of SIVmac239 to an extent similar to the antiviral 90Ks (Fig. 13). Furthermore, mouse CypCAP as well as all tested 90K orthologs including rhesus macaque-derived 90K, negatively affected the HIV-2 particle infectivity (Fig. 13). Noteworthy the inhibition for HIV-2 was lower than for HIV-1 and SIVmac239.

These observations show that most tested 90K orthologs act antivirally against HIV-1, HIV-2 and SIVmac239 in a highly conserved mode of action, indicating that 90K might also constitute a hurdle to cross-species-transmissions. On the other

hand, the different antiviral strength of rhesus derived 90K and mouse CypCAP against HIV-1, HIV-2 and SIVmac239 implicates a species specific mode of action.

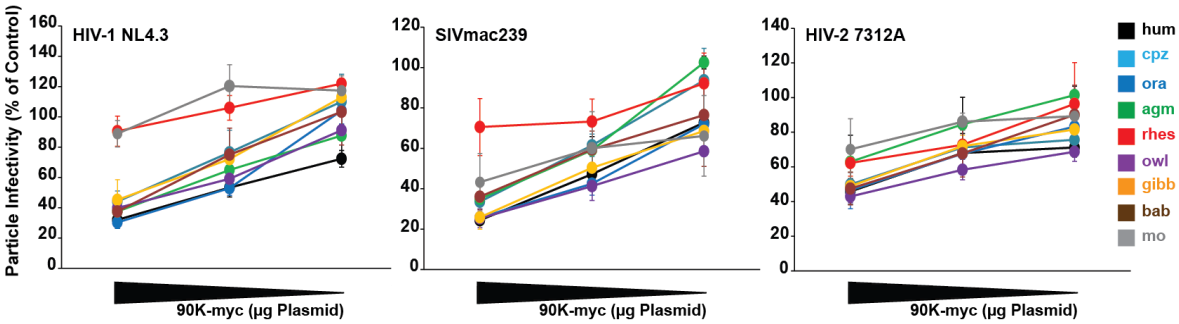


Fig. 13: Antiviral activity of the 90K orthologs from seven non-human primates and the mouse homolog CypCAP against SIV and HIV-2. 293T cells were co-transfected with 1.3 µg NL4.3, SIVmac239 or HIV-2 7312A proviral DNA and decreasing amounts (1.3, 0.4, 0.15 µg) of indicated expression plasmids. DNA content was kept constant by filling up with empty vector. 48 hours post transfection, particle infectivity of retroviral progeny was calculated as infectivity per capsid antigen in the supernatant. Particle infectivity in absence of 90K was set to 100 %. Shown are mean values ± S.E.M. of 3-7 independent experiments. hum = human, cpz = chimpanzee, ora = orangutan, agm = african green monkey, rhes = rhesus macaque, owl = owl monkey, gibb = gibbon, bab = baboon, mo = mouse.

3.10 Antiviral activity of 90K chimeras against HIV-1

The determinants for 90K´s antiviral potential have been mapped to domain two and three (Fig. 11). To elucidate, whether solely these two intermediate domains within rhesus macaque-derived 90K and mouse CypCAP account for their failure to inhibit HIV-1 (Fig. 12), chimeras are a useful tool. For this purpose, chimeras of active human 90K with domains two, three or a combination of both domains from inactive rhesus 90K or mouse CypCAP were created and cloned by SOE-PCR. *Vice versa* the active domains from human 90K were introduced into rhesus macaque 90K and mouse CypCAP (Fig. 14). 293T cells were co-transfected with HIV-1 proviral DNA and expression plasmids encoding these chimeras in order to test their antiviral potential. Immunoblot of cell lysates verified chimeras expression (Fig. 15 A).

Individually replacing domain two or three in human 90K with the respective rhesus or mouse derived domains did not impede the anti-HIV-1 activity. Exchange of both intermediate domains, however, rendered human 90K considerably less active (Fig. 15 B) confirming the observations with the truncation mutants (Fig. 11).

In striking contrast, the introduction of the antivirally active domains two and three from human 90K into rhesus 90K or mouse CypCAP did not lead to a gain of antiviral

activity (Fig. 15 B). This could indicate that the domains one and four from rhesus 90K and mouse CypCAP supress the antiviral capacity of the central protein binding domains. Noteworthy, CypCAP containing human domain three (mo3h) seemed to gain some antiviral potential although expressed less efficiently than the other chimeric constructs.

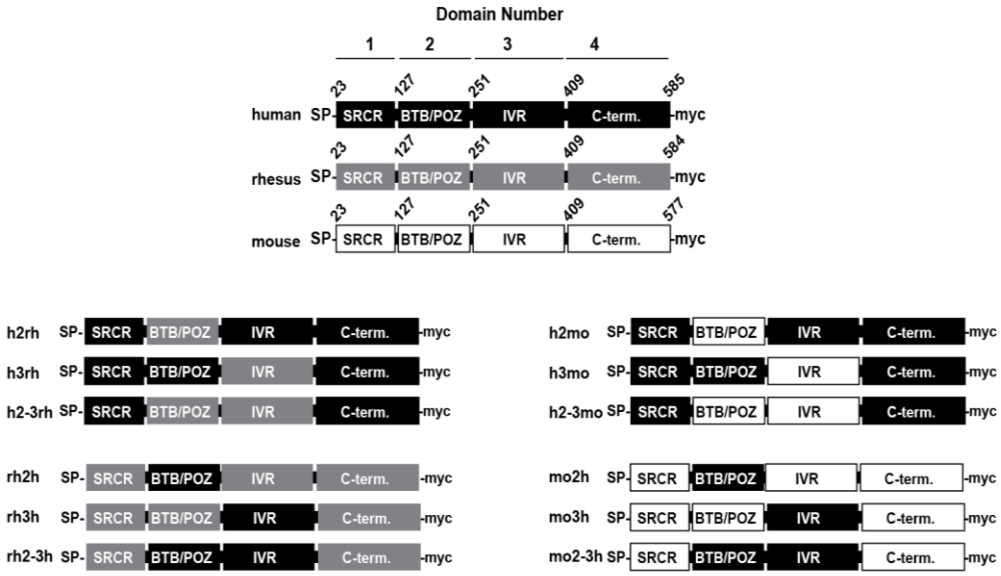


Fig. 14: Scheme of the different human 90K, rhesus 90K and mouse CypCAP chimeras. Numbers indicate amino acid positions. SP = signal peptide, SRCR = scavenger receptor cysteine-rich, BTB/POZ = broad-complex, tramtrack and bric à brac / poxvirus and zinc finger, IVR = intervening region, C-term. = C-terminal domain, h = human, rh = rhesus macaque, mo = mouse.

Going along with the observations for the particle infectivity, exclusively the antivirally active chimeras led to a paucity in incorporated gp120 in HIV-1 progeny as shown in the immunoblots of sucrose cushion purified virus (Fig. 15 C). The gp120 incorporation defect and the reduced gp160 processing again seemed to be uncoupled events since all tested chimeras, including the non-active variants, elicited a reduction of processed gp120 within the cell lysates. In particular for the rhesus and mouse chimeras containing human domains the effect was low but reproducible (Fig. 15 D).

Taken together, the two central protein binding domains of human 90K exert the antiviral effect of particle infectivity reduction by less efficient gp120 incorporation into virus progeny, whereas the corresponding domains of the inactive rhesus 90K and mouse CypCAP do not share these properties. Moreover, the flanking domains

one and four of the inactive rhesus 90K and mouse CypCAP seem to additionally inhibit the antiviral efficiency of the two central protein binding domains.

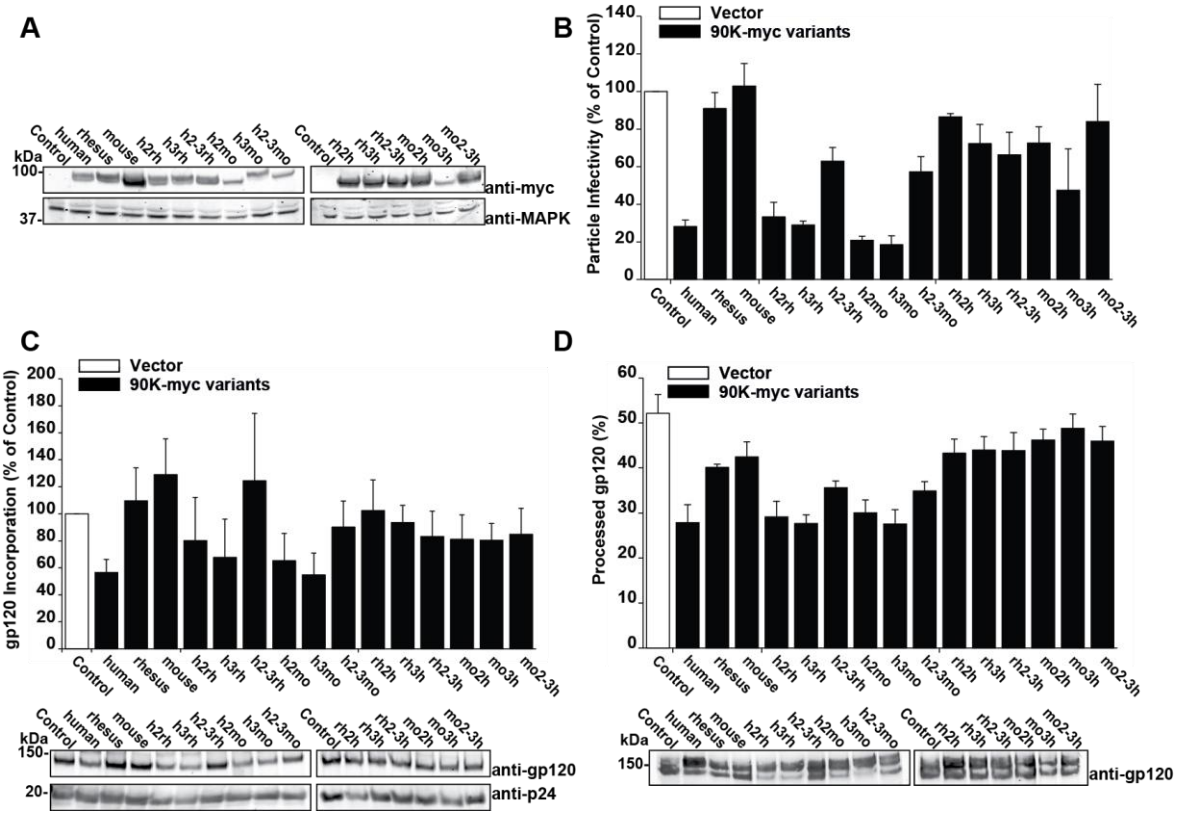


Fig. 15: Antiviral activity of 90K chimeras against HIV-1. (A) 293T cells were co-transfected with 1.3 µg HIV-1 NL4.3 proviral DNA and 1.3 µg of indicated expression plasmids. 48 hours post transfection, cell lysates were analyzed by immunoblotting using the indicated antibodies to verify chimeras expression. (B) Particle infectivity of HIV-1 progeny in the supernatants thereof was calculated as infectivity per secreted p24 capsid antigen. Particle infectivity in absence of 90K was set to 100 %. Shown are arithmetic means ± S.E.M. from 4-7 independent experiments. (C) gp120 incorporation was calculated as ratio of gp120 signal intensity to p24 signal intensity and value for vector transfected cells was set to 100 %. Bar diagrams show the arithmetic means ± S.E.M. of 4-7 independent experiments. Depicted is one representative blot of sucrose cushion purified virus used for the calculation. (D) Relative gp160 processing was determined as mature gp120 per whole Env (gp120+gp160) signal. Bar diagrams indicate the arithmetic means ± S.E.M. of 3-6 independent experiments. Shown is one representative blot used for the calculation. h = human, rh = rhesus macaque, mo = mouse, MAPK = MAP kinase.

3.11 90K is expressed and interferon inducible in selected primary HIV-1 target cells

From the 90K overexpression studies in 293T cells there was clear evidence for an antiviral effect of 90K in the late phase of the HIV-1 replication cycle. To prove the relevance of this potential new antiviral factor in case of a natural infection, different

HIV-1 target cells were screened for their endogenous 90K expression by qPCR. 90K mRNA levels in 293T cells were arbitrarily set to 1 (Fig. 16 A). In T-cell lines, variable 90K mRNA levels were detected with the highest relative amount in Jurkat cells. Importantly, HIV-1 relevant CD4+ T-cells and macrophages harboured about 10-fold more 90K mRNA than 293T cells. Noteworthy, the 90K mRNA levels increased after IL-2 and PHA stimulation in PBMCs and to a lower degree in CD4+ T-cells compared to untreated cells, suggesting that 90K mRNA expression is inducible by this immunogenic stimulus (Fig. 16 A).

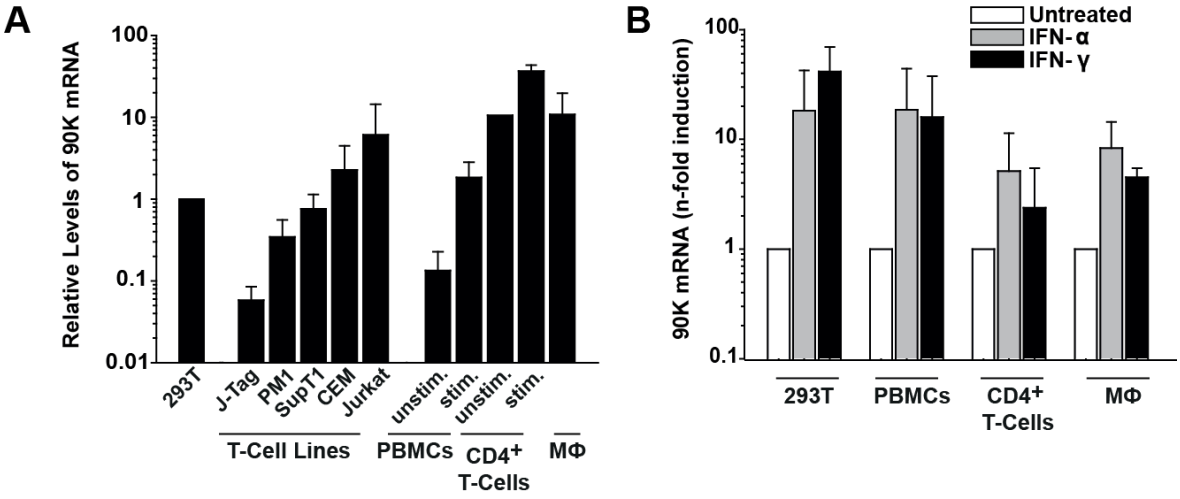


Fig. 16: 90K mRNA levels in HIV-1 target cells and interferon susceptibility thereof. (A) Total RNA was isolated from the indicated cell types and mRNA was reverse transcribed into cDNA. 90K mRNA expression was quantified by TaqMan qPCR using a 90K specific primer/probe combination and normalized to the housekeeping gene RNAseP. Relative 90K mRNA levels were calculated with the value obtained for 293T cells arbitrarily set to 1. Diagrams show arithmetic means ± S.E.M. of three independent experiments/donors. The column for unstimulated CD4+ T-cells represents arithmetic mean of two independent donors. PBMCs and CD4+ T-cells were stimulated with IL-2/PHA for three days or immediately used without stimulation. (B) Indicated primary cells were treated with IFN-α (100 U/ml) or IFN-γ (100 U/ml) for 24-48 hours or left untreated. 90K mRNA levels were detected as described in (A). Shown is the fold increase of 90K mRNA levels from 2-3 experiments, each performed in duplicates. IFN= interferon. MΦ = macrophages. Figure adapted from [101], p.10-11.

90K has been shown by others to be upregulated by type I and type II interferons (IFNs) [16, 76, 108]. Therefore 293T cells and primary cells were treated with Interferon-α or Interferon-γ and the induction of mRNA was calculated compared to respective untreated cells (Fig. 16 B). After IFN-α treatment, 90K mRNA increased by the factor of 11 in 293T cells as well as in PBMCs. To a lesser degree, 90K mRNA levels increased in CD4+ T-cells and macrophages by the factor of five and

eight, respectively. IFN-γ treatment upregulated 90K mRNA levels in 293T cells by a factor of 13 and in PBMCs by a factor of 10.5. Again, 90K mRNA levels in CD4+ T-cells and macrophages were upregulated to a lower degree, namely 2.5-fold and 4.5-fold. The mRNA analysis indicates that *90K* is expressed in all tested HIV-1 relevant target cells and responsive to IFN treatment to a different degree depending on the cell type.

3.12 Cell-type specific expression of 90K protein

90K mRNA was detectable in all tested HIV-1 target cells (Fig. 16). Levels of mRNA, however, are not predictive for the protein expression. The extent of endogenous 90K protein expression within HIV-1 relevant cells was thus analyzed by immunoblotting (Fig. 17 A). In 293T cells, 90K protein was strongly induced by IFN-α, but just marginally by IFN-γ. Untreated macrophages contained detectable levels of 90K protein. Nevertheless, after IFN-α but not –γ treatment, 90K protein expression increased in macrophages from two different donors as seen for the 293T cells. Because the fold induction of 90K expression by IFN treatment in 293T cells and macrophages was much lower than expected from the mRNA quantification (Fig. 16 B), the IFN- induced transmembrane proteins 2 and 3 (IFITM 2/3) were used as positive control since IFITM 2/3 is highly inducible by type I and II IFNs (Fig. 17 B) [48]. Macrophages showed more than five- and two-fold increases in IFITM 2/3 protein expression following IFN-α or IFN–γ treatment, confirming that the used IFN batches were active. Immunoblotting of the very same samples and staining for 90K revealed a two-fold induction by IFN-α and again no marked effect after IFN–γ stimulation.

Neither in any T-cell line nor in primary CD4+ T-cells from two different donors, 90K protein was observed by immunoblotting (Fig. 17 A). In order to exclude a minor 90K protein amount, which may not be detectable by Western Blot, cell-associated 90K protein expression was analyzed using a sensitive commercial anti-90K ELISA. This technique allows detection of 90K protein in the ng/ml range. With the anti-90K ELISA the detection of very low 90K protein levels in Jurkat cells and primary CD4+ T-cells was possible, however IFN treatment did not further increase the 90K protein amount (Fig. 17 C). As expected, 90K protein levels in untreated macrophages were easily detectable and further induced by IFN-α but not IFN-γ.

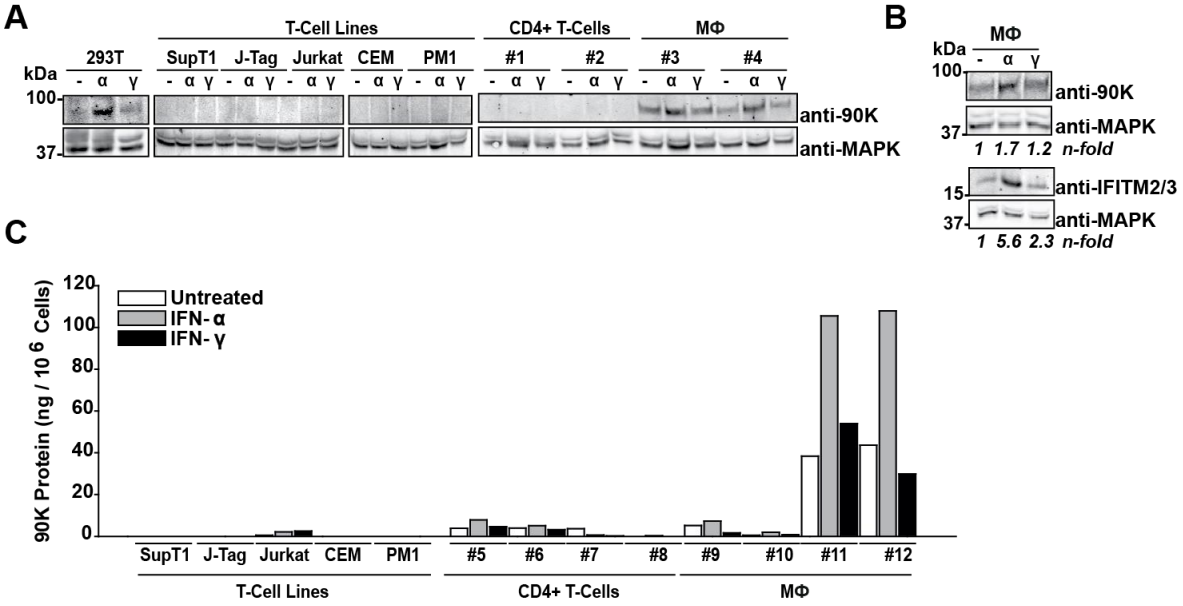


Fig. 17: Endogenous 90K protein expression in HIV-1 target cells and interferon susceptibility thereof. (A-B) Indicated cells were stimulated with IFN-α (100 U/ml) or IFN-γ (100 U/ml) for 48 hours or left untreated. Cell lysates were analyzed by immunoblotting using the indicated antibodies. (B) Numbers indicate relative 90K and IFITM 2/3 expression levels, respectively, defined as signal intensity normalized to MAPK housekeeping gene signal intensity. The ratio obtained for untreated cells was set to 1. (C) Indicated cells were stimulated with IFN-α (100 U/ml) or IFN-γ (100 U/ml) for 48 hours or left untreated and cell lysates thereof were subjected to an anti-90K ELISA. MAPK = MAP kinase, MΦ = macrophages, #number = different donors. Figure adapted from [101], p.10-11.

Taken together, 90K is endogenously expressed in all relevant HIV-1 target cells, although to different extents. Primary CD4+ T-cells contain very low 90K protein levels that are not altered by interferon treatment. Macrophages, though, bear higher basal 90K protein levels, which increase upon IFN-α treatment.

3.13 Depletion of 90K expression in primary HIV-1 target cells improves Env incorporation into HIV-1 progeny and accelerates HIV-1 spread

Compared to the effective antiviral amounts of 90K after heterologous expression in 293T cells (1.3 µg - 0.15 µg), the endogenously expressed 90K protein levels in macrophages are nine-fold to 19-fold lower (Fig. 18 A). The antiviral potency of endogenous 90K was probed in an infection assay in macrophages from one donor, which expressed normal or reduced amounts of 90K. Specifically, macrophages were transduced with VSV-G (Vesicular stomatitis virus glycoprotein) pseudotyped, *env* intact NL4.3 HIV-1, followed by siRNA-mediated reduction of 90K expression.

Because 90K seems to act in the late phase of the HIV-1 replication cycle, macrophages were transfected with a 90K specific siRNA or a non-targeting control siRNA after transduction. Seven days post transduction, the particle infectivity of released HIV-1 progeny was determined (Fig. 18 B). Taking into account that reinfection of macrophages with T-cell-tropic HIV-1 progeny, like NL4.3, rarely occurs [123], this experimental set should largely reflect a single round infection. In virus originating from the 90K siRNA depleted macrophage culture, the HIV-1 particle infectivity was three-fold higher than that obtained from control siRNA treated macrophages, suggesting that endogenous 90K protein levels in macrophages are able to inhibit HIV-1. Reduction of 90K expression in the 90K-siRNA treated culture was confirmed by immunoblotting (Fig. 18 C). Newly synthesized virus particles in the supernatant were purified and also subjected to immunoblotting. Viral p24 release was not affected, but mature gp120 was more efficiently incorporated into the virus when 90K expression was depleted, confirming the observations in transfected 293T cells (Fig. 5 B-C). In striking contrast, no improved processing of the gp160 precursor to gp120 was observed within the cell lysates after 90K expression knockdown.

Endogenously expressed 90K in macrophages was proven to exert an antiviral function in a single round infection assay, but this is not well reflecting a naturally occurring infection. To better analyze 90K´s impact, it was important to test 90K´s effect on a spreading infection. For this purpose, macrophages obtained from two different donors were first transfected with 90K specific or control siRNA followed by infection with the macrophage-tropic HIV-1 strain Ba-L (Fig. 19 A). Virus release, measured at different time points post infection by p24 ELISA, revealed a significant spreading advantage of HIV-1 Ba-L in the 90K siRNA depleted macrophage cultures. Immunoblotting of cell lysates at day 13 post infection demonstrated a stable depletion of 90K expression after siRNA transfection.

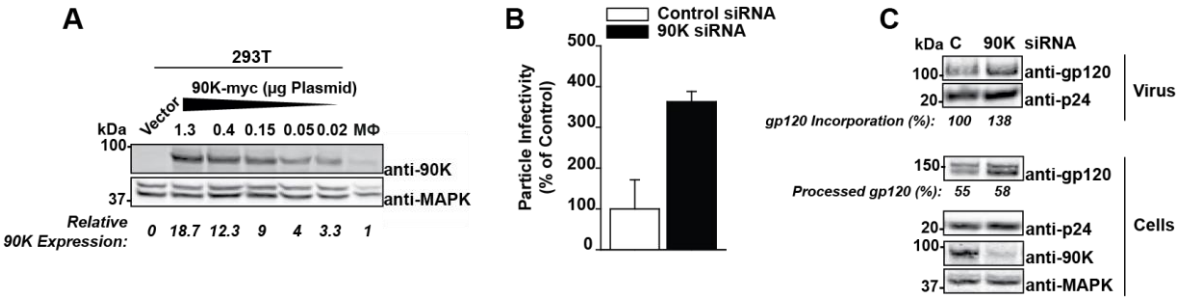


Fig. 18: Depletion of 90K expression in primary macrophages increases HIV-1 particle infectivity and Env incorporation. (A) 293T cells were transfected with decreasing amounts (1.3, 0.4, 0.15, 0.05, 0.02 µg) of 90K-myc expression plasmid. DNA content was kept constant by filling up with empty vector. Immunoblot of the 293T cell lysates and untreated macrophages was analyzed with indicated antibodies. Band intensities were quantified by Infrared-based imaging with the LICOR system. Numbers indicate relative 90K expression levels defined as signal intensity normalized to MAPK signal intensity. The ratio obtained for untreated macrophages was set to 1. (B) Primary macrophages were transduced with VSV-G pseudotyped HIV-1 NL4.3 and transfected on the following day with a non-targeting control siRNA or a 90K specific siRNA. At day 7 post infection, particle infectivity of newly produced virus was calculated as infectivity per released p24 capsid antigen. (C) Cell lysates and virus purified by ultracentrifugation through a sucrose cushion were subjected to immunoblotting using the indicated antibodies. Numbers indicate the Env processing efficiency as percentage of gp120 from total Env and the relative gp120 incorporation as amount of gp120 per p24. C= control. MAPK = MAP kinase. Figure adapted from [101], p.12-13.

Finally, it was investigated, if the very low 90K protein levels in PBMCs can also exert an antiviral function during spreading infection. PBMCs were nucleofected with 90K specific or control siRNA and subsequently infected with the T-cell-tropic HIV-1 strain NL4.3 (Fig. 19 B). A two-fold 90K knock down was achieved and proven with a sensitive anti-90K-ELISA. In PBMC cultures, obtained from two different donors, p24 release over time was significantly improved when 90K expression was depleted from the cultures indicating that already low 90K protein amounts have respectable antiviral potential.

Taken together, even the low amounts of endogenously expressed 90K in selected HIV-1 target cells constitute a hurdle to an efficient HIV-1 spread underlining 90K´s relevance as antiviral factor *in vivo*.

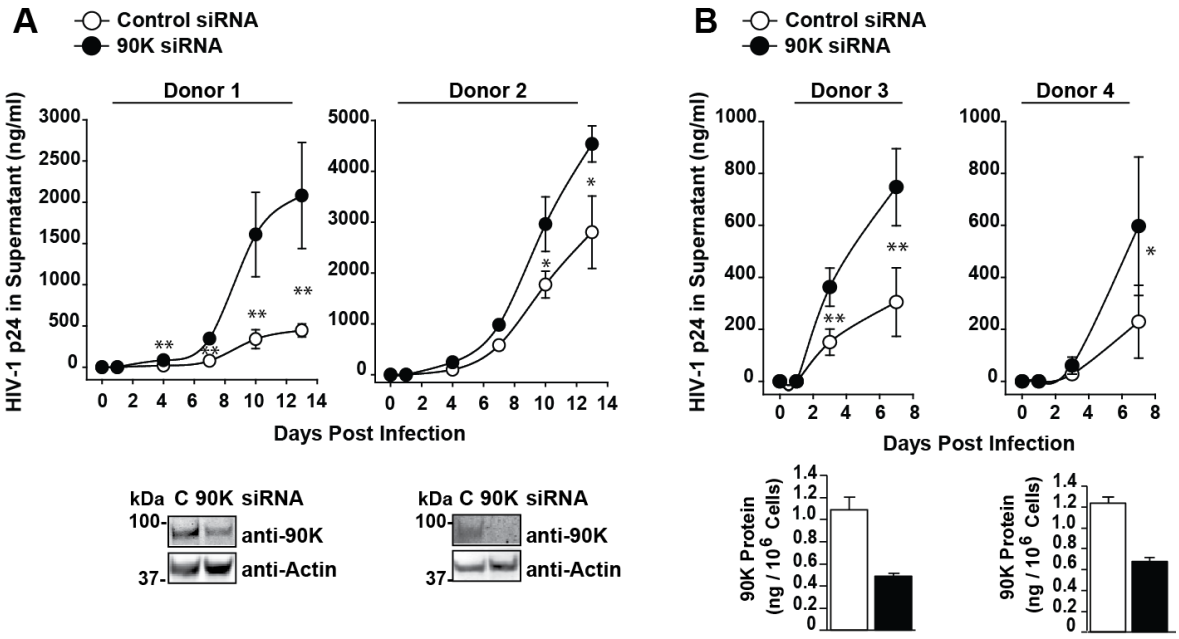


Fig. 19: Depletion of 90K in primary cells improves HIV-1 spread. (A) Macrophages obtained from two different donors were transfected twice with control or 90K specific siRNA followed by infection with HIV-1 Ba-L. Inoculum virus was removed by thorough washing. p24 content in supernatant at indicated time points was quantified by p24 capsid antigen ELISA. Aliquots of cells were taken for 90K knock down validation over time by immunoblotting. Shown is 90K expression at day 13 post infection. (B) IL-2/PHA stimulated PBMCs obtained from two donors were nucleofected twice with control or 90K specific siRNA followed by infection with HIV-1 NL4.3 over night. Inoculum virus was removed by thorough washing. P24 content in supernatant at indicated time points was quantified by p24 capsid antigen ELISA. 90K knock down at the time point of infection was verified by anti-90K ELISA. C=control. *: <0.05; **: <0.02 (Student´s T-Test). Figure adapted from [101], p.12-13

4 Discussion

Several hundred genes are upregulated by type I and II interferons, which are accordingly designated as ISGs (interferon-stimulated genes) [33, 35]. Interferons have been discovered in 1957 as substance that inhibits the growth of influenza virus [77] and nowadays IFNs are well known to initiate an antiviral state against multiple viruses [128]. Among the ISGs, restriction factors constitute a first line of defence against different viruses [11]. Recently it has been shown, that restriction factor mRNA expression *in vivo* increases during HIV-1 infection [129]. 90K belongs to the ISGs and 90K mRNA is upregulated in CD4+ T-cells from HIV-1 infected patients [136] making it a promising candidate for a novel antiviral protein. In the present study was shown that 90K exerts anti-HIV-1 activity. 90K interferes with the incorporation of Env into HIV-1 progeny and thereby lowers the particle infectivity of newly synthesized virions.

Noteworthy, 293T cells lack endogenous expression of 90K making them suitable for studying the effects of 90K in transfection experiments (Fig. 4). When HIV-1 proviral DNA was co-transfected with 90K, the infectivity of newly produced HIV-1 was dose-dependently reduced by 90K without affecting virus release. Hence, intracellular 90K impaired the quality of HIV-1 progeny which was defined herein as particle infectivity. In contrast, the secreted 90K did not display anti-HIV-1 activity in the experimental set-ups employed so far [101]. Quantitative immunoblot analysis revealed, that the decrease in particle infectivity was accompanied by a reduced processing of the Env precursor gp160 to gp120 and gp41 and a paucity of these mature Env proteins in the virus particles (Fig. 5). Confirming the assumption of a 90K induced Env incorporation defect into nascent virions, 90K reduced Env levels at the cell surface, where the trimeric Env spikes usually are incorporated into the budding virus (Fig. 7).

Importantly, 90K specifically diminished particle infectivity. Reduction of Env processing efficiency and virus incorporation were observed for the X4-tropic HIV-1 strain NL4.3, but also for the R5-tropic strains YU-2 and LAI (Fig. 6). With this, 90K´s antiviral function can overcome the tropism bias of HIV-1 entry inhibitors like the CCR5 antagonist Maraviroc, the CCR5 agonist CCL14(9-74) or the CXCR4 antagonist AMD3100 that solely target one of the HIV-1 co-receptors [31, 37, 114, 174]. 90K acts at a later step in virus replication compared to the entry inhibitors,

but its tropism independent mode of action still makes it a potential candidate for HIV-1 therapy development. Moreover, not only the laboratory adapted strains NL4.3, YU-2 and LAI were potently blocked by 90K but also three tested transmitted founder viruses, two of them even stronger than the laboratory adapted strains (Fig. 6). In 60-80 % of mucosal infections, the main route of HIV transmission, one single virus variant accounts for infection. This single variant is termed TFV and was extracted by single genome amplification of plasma virion RNA followed by sequencing and was identified by *env* sequence phylogenetic trees [81, 140]. One characteristic of TFVs is a 1.9 fold higher Env protein content compared to chronic viruses [119]. On the one hand, high Env levels make these viruses probably more successful in initiating an infection, on the other hand, this could render them more susceptible to 90K induced restriction. Considering this, 90K could constitute a hurdle for viral burst especially early during infection.

Mechanistically, there are several possibilities how 90K could reduce gp120 at the cell surface leading to less efficient Env incorporation into HIV-1 progeny. Since total Env protein levels within cell lysates were not markedly altered, 90K induced degradation of Env seems unlikely (Fig. 5). More plausible would be miss-localization and/or intracellular trapping of Env. During its transport, the gp120 and gp41 precursor gp160 is cleaved by cellular furin or furin like proteases for which the processing efficiency lies between 38 % and 58 % [12]. Confirming the data from *Binley et al.* the Env processing efficiencies in absence of 90K detected herein were about 46 % to 70 % (Fig. 5 and 8). A reduction in the gp160 cleavage was always observed in presence of 90K. Hence it was possible that 90K perturbs furin cleavage followed by improper trafficking or trapping of the immature gp160. Like HIV-1 Env, the furin dependent envelope protein from Ebola was cleaved to a lower degree when 90K was expressed. In contrast, no processing defect was observed for the furin dependent Influenza HA precursor HA0 and the cellular receptor Glypican 3, arguing against a general 90K induced furin inhibition (Fig. 8). Of note, the HA0 used for this study was derived from the H7 Influenza virus, which is processed with high efficiency, whereas HIV-1 gp160 is a poorly cleaved substrate of furin [12]. Therefore, HA0 may be less sensitive to small changes in furin potency in contrast to HIV-1 Env. Furin mediated cleavage, however, is not crucial for proper Env trafficking, since uncleaved gp160 can also be detected at the cell surface [112].

Taking this into account, 90K could induce Env trapping independent of the impeded Env processing.

For the surface receptor NTB-A it was formerly shown that its cell surface expression is reduced by the HIV-1 protein Vpu which altered the glycosylation pattern of NTB-A. The NTB-A associated glycans remained sensitive to the glycosidase EndoH in presence of Vpu indicating that it is trapped in the ER [14]. In contrast to this, the Env glycosylation pattern was not altered by 90K and did not become EndoH sensitive arguing against 90K induced trapping of Env in the ER (Fig. 10). With this, however, cannot be excluded, that 90K leads to Env sequestration in other cellular compartments as is has been shown for Vpu and tetherin [40, 70, 144].

For Vpu´s effect on tetherin, binding is required [89, 111] as it is often observed for restriction factors and their targets [13]. Association of 90K and Env could be possible since they are both trafficked through the secretory pathway. In the immunofluorescence pictures it is clearly visible that both proteins co-localize to a high degree in the same cellular compartments (Fig. 9). The slightly higher co-localization of 90K with Env than the co-localization of Env with 90K could be due to an additional portion of Env expressed at the cell surface. In co-immunoprecipitation assays, however, no direct interaction between 90K and Env was observed (Fig. 9). A negative result in Co-IP cannot totally rule out an interaction between 90K and Env. This method is rather harsh and strongly depends on buffer conditions making it difficult to especially detect weak interactions. An additional scenario could also involve an adaptor protein that links 90K and Env. Noteworthy, preliminary data gave evidence that Env binds to a 90K construct only consisting of the two intermediate domains (data not shown). This observation could point toward a weak interaction of Env also with full-length 90K.

Taken together, 90K neither seems to induce degradation or ER trapping of Env nor could any direct interaction with Env be shown. Therefore, the exact mechanism how 90K leads to a less efficient viral Env incorporation remains elusive and requires further investigation.

Although 90K´s antiviral mechanism was not solved in detail, yet, the domains within 90K important for its anti-HIV-1 activity were successfully mapped (Fig. 11). The 90K protein can be divided into four domains, a SRCR-domain, a BTB/POZ domain followed by an IVR and a C-terminally region without any homology to known protein motifs [113]. Truncation mutants revealed, that the two central protein binding

domains BTB/POZ and IVR are required and sufficient for the restriction of HIV-1. Robinson and Cooley discussed for the *Drosophila* Kelch protein that its BTB domain mediates dimerization as a low affinity association which is further promoted by the IVR [134]. Possibly, 90K has to dimerize *via* its BTB domain and this conformation has to be stabilized by the IVR to act in an antiviral manner. Notably, the mutant consisting of domain two and three only, was even more potent in reducing particle infectivity and Env incorporation than wild-type 90K. A C-terminal 90K truncation mutant consisting of amino acid 1-383 was shown to be not secreted and retained in the ER [92]. The highly active 90K-BTB/POZ-IVR-myc lacks a major part of its C-terminus and thus might be also retained in the ER. An intracellular retention of the 90K truncation mutant bearing solely domain two and three would underline the importance of intracellular 90K in restricting HIV-1 [101] and gives a hint that the antiviral mechanism, at least in part, takes place in the ER.

Human 90K is able to restrict HIV-1 and restriction factors commonly function in a species specific mode [67]. There are highly homologous 90K orthologs existing within non-human primates as well as a 69 % homologous 90K protein in mice which is called CypCAP due to its association to cyclophilin C [27, 47]. Human 90K does not interact with cyclophilin C in affinity precipitation [79]. For the 90K orthologs from non-human primates, interaction with cyclophilin C was not investigated, yet. The 90K orthologs from six non-human primates were able to reduce particle infectivity and viral Env incorporation, whereas CypCAP as well as rhesus derived 90K were inactive against HIV-1 (Fig. 12). Owl monkey derived 90K that shows lower homology to human 90K on the protein level than rhesus derived 90K, was fully active in inhibiting HIV-1. Possibly, there exist further determinants for 90K´s antiviral potential, like the property to oligomerize or to build secondary structures, rather than single motifs within the primary amino acid sequence. Intriguingly, besides the antiviral active 90K orthologs, also rhesus 90K and mouse CypCAP slightly reduced gp160 processing to mature gp120. This could indicate that the Env processing defect and the reduction in Env incorporation into newly produced virus are uncoupled effects.

Knowing that the two central protein binding domains are required and sufficient for 90K´s antiviral function and that mouse CypCAP as well as rhesus derived 90K are antivirally inactive, 90K chimeras were constructed carrying reciprocal exchanges of the two intermediate domains (Fig. 14). Introduction of domains two and three

from rhesus and mouse into human 90K destroyed the antiviral activities of human 90K, probably explaining the failure of rhesus 90K and mouse CypCAP to inhibit HIV-1. However *vice versa* introduction of active human domains did not rescue the antiviral potential of rhesus 90K and mouse CypCAP, indicating that their domains one and four additionally exert some inhibitory effect (Fig. 15). Since the human 90K-(2-3)-myc mutant was more successful in reducing particle infectivity and gp120 incorporation than full-length 90K, it is likely, that also human domain one and four bear some minor inhibitory function. Considering the structure of 90K dimers (Fig. 3 A), one could speculate, that domains one and four sterically impede 90K-(2-3)-myc to exert its antiviral function. Taking into account that human domain two and three are required for 90K´s antiviral potential, it was surprising that human 90K stayed active after replacing one of them with the inactive rhesus 90K or mouse CypCAP counterparts (Fig. 15). Possibly, formation of a specific structure of BTB/POZ and IVR is needed which can still be formed in presence of at least one of the human domains. A role of protein motifs within human 90K mutated in rhesus derived 90K and mouse CypCAP still cannot be excluded and remains elusive. However, the structure rather than the primary amino acid sequence might account for 90K´s antiviral function, since human and rhesus 90K as well as mouse CypCAP share high sequence homologies on the protein level. Similarly, creation of a completely artificial tetherin showed that its special structure, not the primary amino acid sequence, is required for tethering budding virions to the cell membrane [121]. Confirming the observation that Env processing and incorporation defect are uncoupled effects, all chimeras induced an Env processing defect.

The antiviral potential of human 90K, the 90K orthologs and mouse CypCAP was highly conserved between HIV-1, SIVmac239 and HIV-2 (Fig. 13). SIVmac239 was inhibited to a similar degree as HIV-1 even by CypCAP but not rhesus 90K, and all tested 90K orthologs as well as the mouse homolog were active in reducing particle infectivity of HIV-2. Notably, the inhibition of HIV-2 was less pronounced than for HIV-1 and SIVmac239. The slight differences in susceptibility of HIV-1, SIVmac239 and HIV-2 to 90K, its orthologs and the mouse homolog could be due to a natural variation in the amount of virally incorporated Env spikes. Two from three tested transmitted founder viruses, which have been reported to incorporate more Env, were better inhibited by 90K than the laboratory adapted strains (Fig. 6). If inter-virus differences in Env incorporation into HIV-1, HIV-2 and SIVmac239 account for

the different susceptibility to 90K-mediated restriction remains speculative. There is no report available, which directly and quantitatively compares natural incorporation of Env spikes into these viruses. The finding that 90K´s antiviral activity is highly conserved between different retroviruses provides a small first hint to a broader antiviral spectrum.

In contrary to the here presented study, it has previously been reported, that the extracellular 90K but not the cell associated form, binds to recombinant adeno-associated viruses (rAAVs) and thereby reduces transduction efficiencies [34]. This, though, could imply that intracellular as well as extracellular 90K exerts an antiviral function and inhibits various viruses with different modes of actions.

To be an antiviral innate immunity factor of relevance *in vivo*, 90K has to be expressed in primary HIV-1 target cells. Herein was shown that primary human monocyte derived macrophages, PBMCs and CD4+ T-cells bear 90K protein to a different degree. Macrophages express high amounts of 90K protein, CD4+ T-cells and PBMCs only very low to undetectable levels (Fig. 17). The IFN responsiveness of 90K mRNA expression was confirmed for all cell types tested (Fig.16). Surprisingly, increased 90K protein expression after IFN-α treatment was only seen in macrophages within primary cells. This discrepancy between mRNA levels and protein amount in T-cells could point toward a tight regulation of mRNA stability and/or protein translation as it is frequently observed for genes of the innate immunity [21]. Since 90K expression is linked to tumor growth [58], preventing 90K protein accumulation within CD4+ T-cells might be necessary to prevent tumor development. In contrast to non-replicating, fully differentiated macrophages, lymphoma represent a severe problem in T-cells. This, however, remains speculative and the exact reason for the translational repression of 90K in CD4+ T-cells needs further investigation. For an additional restriction factor, *samhd1*, it has been reported that its expression is inducible in dendritic cells and monocytes [9, 98], but not in primary macrophages and CD4+ T-cells [56]. In contrast to primary CD4+ T-cells, induction of *trim5α* in T-cell-lines is weak, again showing the cell type dependent differences in protein upregulation after IFN treatment [55]. Nevertheless, all those genes are classified as ISGs.

Most importantly, the relevance of 90K in impeding virus replication was confirmed in primary HIV-1 target cells. Infection of primary monocyte-derived macrophages and PBMCs from various donors performed herein, confirmed the antiviral potential

of endogenously expressed 90K during HIV-1 infection (Fig. 19). Depletion of 90K expression in primary macrophage cultures from two different donors led to a significant increase in the release of macrophage tropic HIV-1 Ba-L. Improved release was also observed for the T-cell tropic NL4.3 after *90K* silencing in PBMCs showing that already very low amounts of 90K in these cells are sufficient to inhibit HIV-1 replication.

Particle infectivity of HIV-1 progeny from infected primary macrophages was boosted when 90K expression was depleted and the virus released from these cells displayed higher amounts of virus-incorporated gp120 (Fig. 18). Improved Env incorporation into viral particles, however, was not preceded by a more efficient processing of the gp160 precursor to gp120. This indicates again that the 90K induced Env processing defect and the reduction of Env incorporation could be uncoupled effects corroborating the observations with the chimeric 90K proteins (Fig. 15). Interestingly, lowered particle infectivity and a paucity in virus incorporated Env has been reported in virus progeny from IFN-α treated, HIV-1 infected H9 T-cells and the chronically infected myeloid U937 cells [38, 65]. It is tempting to speculate that in these studies the IFN-induced 90K at least in part elicited the observed Env incorporation defect.

90K belongs to the ISGs and acts in an antiviral and species specific manner, therefore fulfilling important criteria of restriction factors. Two additional hallmarks of most restriction factors are, that they have evolved under positive selection and are counteracted by viral proteins. 90K shows no signs of positive selection (unpublished observation of Amalio Telenti) and no viral antagonist has been identified so far. In the future, a possible viral antagonist or evasion strategy could be identified by long-term passaging of the virus on 90K-postive cells. Notably, the recently characterized restriction factors SAMHD1 and Mx2 are, according to current knowledge, also not directly counteracted by HIV-1 encoded proteins. However, HIV-1 can subvert Mx2 induced restriction by capsid mutations implying that the virus has evolved other strategies to circumvent this antiviral protein. By counteracting SAMHD1 the virus might even have a disadvantage, because besides its restricting activity, SAMHD1 acts as negative regulator of ISGs [132]. Likewise, 90K expression could provide an advantage for HIV-1 replication that is more pronounced than the viral inhibition. *90K* seems to have essential physiological functions for cell-growth. It has been reported, that *90K* microRNA depleted human

oral keratinocytes (RT7 cells) and oral squamous cell carcinoma cells are inhibited in their cell growth [42]. Importantly, HIV-1 contains only few Env proteins [26, 177] and it is hypothesized that this contributes to escape from antibody-mediated immune response [87]. Whether 90K´s effect in reducing viral Env yield is even an advantage for better HIV-1 immune escape *in vivo*, requires further investigation.

Taken together, 90K constitutes a relevant new antiviral factor against HIV-1, which reduces particle infectivity of newly produced virus by impairing incorporation of Env protein into the budding virion. The antiviral active domains were mapped to the two central protein-binding domains BTB/POZ and IVR, and probably the structure plays a key role for 90K´s antiviral potential. The results presented herein may pave the way for further studies to develop a 90K based small molecule with implication for anti- HIV-1 treatment. An elegant way for therapies based on ISGs could be the development of small molecules mimicking the effects of antiviral factors like it was observed for PF74 mimicking the inhibition of HIV-1 by simian TRIM5α [150]. Conceivable would be the designing of a peptide or small molecule consisting of an optimized protein sequence of 90K´s two intermediate domains or even a shortened form thereof. Sequence optimization to raise 90K´s antiviral function in reducing virus incorporated Env to nearly 100 % would help to minimize the risk of advantages in antibody-mediated immune escape of low-Env virus variants. For this intention, further studies are required to map the minimally needed antivirally active determinants within 90K and to reveal its exact antiviral mode of action. Since there are only few Env molecules incorporated into the virus [26, 177], it should be possible to prevent Env incorporation to a high degree by a potent 90K variant or equivalent. Nevertheless, one should keep in mind that 90K is a tumor associated antigen. For its cell-adhesive and thereby malignant properties, however, all four domains seem to be required [71]. A 90K-like small molecule lacking at least domain one and four might not have malignant features and act in a potent antiviral manner. Interestingly, no viral 90K antagonist has been identified so far. However, if the lacking antiviral counteraction holds true, needs to be confirmed. Finally, 90K inhibits a step in the viral replication cycle, which is not targeted by any other therapeutic molecule. A 90K-based peptide or small molecule with cell penetrating properties could therefore contribute to combination therapy of HIV-1 infected patients.

5 Summary

Cellular restriction factors inhibit HIV-1 at different stages of its replication cycle. One hallmark of these antiviral proteins is their interferon-inducible expression. Probably, further natural HIV-1 inhibitors among the hundreds of interferon inducible genes await discovery. The secreted glycoprotein 90K is also upregulated by interferon and induced in HIV-1 infected people. Herein, 90K was in-depth characterized as novel antiviral factor against HIV-1. Cellular 90K reduced the particle infectivity of HIV-1 progeny. Flow cytometry analysis revealed reduced levels of gp120 at the cell surface in presence of 90K expression leading to a lack in viral envelope incorporation. Additionally, a 90K induced processing defect of the gp160 precursor to mature gp120 and gp41 was observed, but seems to be uncoupled from the envelope incorporation defect. Moreover, 90K did not act as a general inhibitor of furin cleavage nor did it trap Envelope in the endoplasmic reticulum. Envelope and 90K are both trafficked through the secretory pathway and therefore highly co-localize within cellular compartments, but direct interaction was not observed by co-immunoprecipitation. Although 90K´s exact antiviral mechanism remains elusive, the antiviral activity of 90K was mapped to the two central protein binding domains BTB/POZ and IVR. 90K´s antiviral potential was conserved between 90K orthologs from six non-human primates. In contrast, 90K derived from rhesus macaques and the mouse homolog CypCAP failed to inhibit HIV-1, indicating 90K´s species specificity. Importantly, 90K is expressed in HIV-1 relevant CD4+ T-cells, PBMCs and primary macrophages. In the latter, 90K expression is further stimulated by type I interferons. siRNA mediated knockdown of 90K in primary macrophage and PBMC cultures led to improved virus production. Silencing of 90K expression in primary macrophages boosted particle infectivity and enhanced Envelope incorporation into HIV-1 progeny virions. 90K also inhibited HIV-2 and SIVmac239, pointing toward a broader antiviral spectrum. Conclusively, 90K constitutes a relevant novel antiviral factor against HIV-1. Considering the broad antiviral spectrum of restriction factors, it will be interesting for future studies to investigate 90K´s potential to inhibit further viruses. This would underline the importance of 90K as antiviral factor.

6 References

[1] Abacioglu, Y. H., Fouts, T. R., Laman, J. D., Claassen, E., Pincus, S. H., Moore, J. P., Roby, C. A., Kamin-Lewis, R., and Lewis, G. K. 1994. Epitope mapping and topology of baculovirus-expressed HIV-1 gp160 determined with a panel of murine monoclonal antibodies. *AIDS Res. Hum. Retroviruses* 10, 371–381.

[2] Adachi, A., Gendelman, H. E., Koenig, S., Folks, T., Willes, R., Rabson, A., and Martin, M. A. 1986. Production of acquired immunodeficiency syndrome-associated retrovirus in human and nonhuman cells transfected with an infectious molecular clone. *J. Virol.* 59, 284–291.

[3] Ahmad, K. F., Engel, C. K., and Privé, G. G. 1998. Crystal structure of the BTB domain from PLZF. *Proc. Natl. Acad. Sci. U.S.A.* 95, 12123–12128.

[4] Allan, J. S., Coligan, J. E., Barin, F., McLane, M. F., Sodroski, J. G., Rosen, C. A., Haseltine, W. A., Lee, T. H., and Essex, M. 1985. Major glycoprotein antigens that induce antibodies in AIDS patients are encoded by HTLV-III. *Science* 228, 1091–1094.

[5] Aravind, L. and Koonin, E. V. 1999. Fold prediction and evolutionary analysis of the POZ domain: structural and evolutionary relationship with the potassium channel tetramerization domain. *J. Mol. Biol.* 285, 1353–1361.

[6] Artini, M., Natoli, C., Tinari, N., Costanzo, A., Marinelli, R., Balsano, C., Porcari, P., Angelucci, D., D'Egidio, M., Levrero, M., and Iacobelli, S. 1996. Elevated serum levels of 90K/MAC-2 BP predict unresponsiveness to alpha-interferon therapy in chronic HCV hepatitis patients. *J. Hepatol.* 25, 212–217.

[7] Aydin, H., Taylor, M. W., and Lee, J. E. 2014. Structure-guided analysis of the human APOBEC3-HIV restrictome. *Structure* 22, 668–684.

[8] Baldauf, H.-M., Pan, X., Erikson, E., Schmidt, S., Daddacha, W., Burggraf, M., Schenkova, K., Ambiel, I., Wabnitz, G., Gramberg, T., Panitz, S., Flory, E., Landau, N. R., Sertel, S., Rutsch, F., Lasitschka, F., Kim, B., König, R., Fackler, O. T., and Keppler, O. T. 2012. SAMHD1 restricts HIV-1 infection in resting CD4(+) T cells. *Nat. Med.* 18, 1682–1687.

[9] Berger, A., Sommer, Andreas F R, Zwarg, J., Hamdorf, M., Welzel, K., Esly, N., Panitz, S., Reuter, A., Ramos, I., Jatiani, A., Mulder, L. C. F., Fernandez-Sesma, A., Rutsch, F., Simon, V., König, R., and Flory, E. 2011. SAMHD1-deficient CD14+ cells from individuals with Aicardi-Goutières syndrome are highly susceptible to HIV-1 infection. *PLoS Pathog.* 7, e1002425.

[10] Bernstein, H. B., Tucker, S. P., Hunter, E., Schutzbach, J. S., and Compans, R. W. 1994. Human immunodeficiency virus type 1 envelope glycoprotein is modified by O-linked oligosaccharides. *J. Virol.* 68, 463–468.

[11] Bieniasz, P. D. 2004. Intrinsic immunity: a front-line defense against viral attack. *Nat. Immunol.* 5, 1109–1115.

[12] Binley, J. M., Sanders, R. W., Master, A., Cayanan, C. S., Wiley, C. L., Schiffner, L., Travis, B., Kuhmann, S., Burton, D. R., Hu, S.-L., Olson, W. C., and Moore, J. P. 2002. Enhancing the Proteolytic Maturation of Human Immunodeficiency Virus Type 1 Envelope Glycoproteins. *Journal of Virology* 76, 2606–2616.

[13] Blanco-Melo, D., Venkatesh, S., and Bieniasz, P. D. 2012. Intrinsic cellular defenses against human immunodeficiency viruses. *Immunity* 37, 399–411.

[14] Bolduan, S., Hubel, P., Reif, T., Lodermeyer, V., Höhne, K., Fritz, J. V., Sauter, D., Kirchhoff, F., Fackler, O. T., Schindler, M., and Schubert, U. 2013. HIV-1 Vpu affects

the anterograde transport and the glycosylation pattern of NTB-A. *Virology* 440, 190–203.

[15] Bour, S., Boulerice, F., and Wainberg, M. A. 1991. Inhibition of gp160 and CD4 maturation in U937 cells after both defective and productive infections by human immunodeficiency virus type 1. *J. Virol.* 65, 6387–6396.

[16] Brakebusch, C., Sures, I., Jallal, B., Mossie, K., Fusco, O., Iacobelli, S., and Ullrich, A. 1999. Isolation and functional characterization of the human 90K promoter. *Genomics* 57, 268–278.

[17] Brandt, S. M., Mariani, R., Holland, A. U., Hope, T. J., and Landau, N. R. 2002. Association of chemokine-mediated block to HIV entry with coreceptor internalization. *J. Biol. Chem.* 277, 17291–17299.

[18] Briggs, N. C., Natoli, C., Tinari, N., D'Egidio, M., Goedert, J. J., and Iacobelli, S. 1993. A 90-kDa protein serum marker for the prediction of progression to AIDS in a cohort of HIV-1+ homosexual men. *AIDS Res. Hum. Retroviruses* 9, 811–816.

[19] Bryant, M. L., Yamamoto, J., Luciw, P., Munn, R., Marx, P., Higgins, J., Pedersen, N., Levine, A., and Gardner, M. B. 1985. Molecular comparison of retroviruses associated with human and simian AIDS. *Hematol Oncol.* 3 (1985), 187–197.

[20] Bullock, W. O., Fernandez, J. M., and Short, J. M. 1987. XL1-Blue: A high efficiency plasmid transforming recA Escherichia coli strain with beta-galactosidase selection. *Bio Techniques* 5, 376–378.

[21] Carpenter, S., Ricci, E. P., Mercier, B. C., Moore, M. J., and Fitzgerald, K. A. 2014. Post-transcriptional regulation of gene expression in innate immunity. *Nat. Rev. Immunol.* 14, 361–376.

[22] Chan, D. C., Fass, D., Berger, J. M., and Kim, P. S. 1997. Core structure of gp41 from the HIV envelope glycoprotein. *Cell* 89, 263–273.

[23] Chan, S. Y., Speck, R. F., Ma, M. C., and Goldsmith, M. A. 2000. Distinct mechanisms of entry by envelope glycoproteins of Marburg and Ebola (Zaire) viruses. *J. Virol.* 74, 4933–4937.

[24] Checkley, M. A., Luttge, B. G., and Freed, E. O. 2011. HIV-1 envelope glycoprotein biosynthesis, trafficking, and incorporation. *J. Mol. Biol.* 410, 582–608.

[25] Chen, Y., Hojo, S., Matsumoto, N., and Yamamoto, K. 2013. Regulation of Mac-2BP secretion is mediated by its N-glycan binding to ERGIC-53. *Glycobiology* 23, 904–916.

[26] Chertova, E., Bess, J. W., Crise, B. J., Sowder II, R. C., Schaden, T. M., Hilburn, J. M., Hoxie, J. A., Benveniste, R. E., Lifson, J. D., Henderson, L. E., and Arthur, L. O. 2002. Envelope Glycoprotein Incorporation, Not Shedding of Surface Envelope Glycoprotein (gp120/SU), Is the Primary Determinant of SU Content of Purified Human Immunodeficiency Virus Type 1 and Simian Immunodeficiency Virus. *Journal of Virology* 76, 5315–5325.

[27] Chicheportiche, Y. and Vassalli, P. 1994. Cloning and expression of a mouse macrophage cDNA coding for a membrane glycoprotein of the scavenger receptor cysteine-rich domain family. *J. Biol. Chem.* 269, 5512–5517.

[28] Choe, H., Farzan, M., Sun, Y., Sullivan, N., Rollins, B., Ponath, P. D., Wu, L., Mackay, C. R., LaRosa, G., Newman, W., Gerard, N., Gerard, C., and Sodroski, J. 1996. The beta-chemokine receptors CCR3 and CCR5 facilitate infection by primary HIV-1 isolates. *Cell.* 85, 1135–1148.

[29] Chojnacki, J., Staudt, T., Glass, B., Bingen, P., Engelhardt, J., Anders, M., Schneider, J., Müller, B., Hell, S. W., and Kräusslich, H.-G. 2012. Maturation-dependent HIV-1

surface protein redistribution revealed by fluorescence nanoscopy. *Science* 338, 524–528.

[30] Clavel, F., Guétard, D., Brun-Vézinet, F., Chamaret, S., Rey M., Santos-Ferreira M. O., Laurent, A. G., Dauguet, C., Katlama, C., Rouzioux, C., Klatzmann D., Champalimaud J. L., and Montagnier, L. 1986. Isolation of a New Human Retrovirus from West African Patients with AIDS. *Science* 233, 343–346.

[31] Clercq, E. de, Yamamoto, N., Pauwels, R., Balzarini, J., Witvrouw, M., Vreese, K. de, Debyser, Z., Rosenwirth, B., Peichl, P., and Datema, R. 1994. Highly potent and selective inhibition of human immunodeficiency virus by the bicyclam derivative JM3100. *Antimicrobial Agents and Chemotherapy* 38, 668–674.

[32] Crise, B., Buonocore, L., and Rose, J. K. 1990. CD4 is retained in the endoplasmic reticulum by the human immunodeficiency virus type 1 glycoprotein precursor. *J. Virol.* 64, 5585–5593.

[33] de Veer, M. J., Holko, M., Frevel, M., Walker, E., Der, S., Paranjape, J. M., Silverman, R. H., and Williams, B. R. 2001. Functional classification of interferon-stimulated genes identified using microarrays. *J. Leukoc. Biol.* 69, 912–920.

[34] Denard, J., Beley, C., Kotin, R., Lai-Kuen, R., Blot, S., Leh, H., Asokan, A., Samulski, R. J., Moullier, P., Voit, T., Garcia, L., and Svinartchouk, F. 2012. Human galectin 3 binding protein interacts with recombinant adeno-associated virus type 6. *J. Virol.* 86, 6620–6631.

[35] Der, S. D., Zhou, A., Williams, B. R., and Silverman, R. H. 1998. Identification of genes differentially regulated by interferon alpha, beta, or gamma using oligonucleotide arrays. *Proc. Natl. Acad. Sci. U.S.A.* 95, 15623–15628.

[36] Descours, B., Cribier, A., Chable-Bessia, C., Ayinde, D., Rice, G., Crow, Y., Yatim, A., Schwartz, O., Laguette, N., and Benkirane, M. 2012. SAMHD1 restricts HIV-1 reverse transcription in quiescent CD4(+) T-cells. *Retrovirology* 9, 87.

[37] Detheux, M., Ständker, L., Vakili, J., Münch, J., Forssmann, U., Adermann, K., Pöhlmann, S., Vassart, G., Kirchhoff, F., Parmentier, M., and Forssmann, W. G. 2000. Natural proteolytic processing of hemofiltrate CC chemokine 1 generates a potent CC chemokine receptor (CCR)1 and CCR5 agonist with anti-HIV properties. *J. Exp. Med.* 192, 1501–1508.

[38] Dianzani, F., Castilletti, C., Gentile, M., Gelderblom, H. R., Frezza, F., and Capobianchi, M. R. 1998. Effects of IFNα on late stages of HIV-1 replication cycle. *Biochimie* 80, 745–754.

[39] Doranz, B. J., Rucker, J., Yi, Y., Smyth, R. J., Samson, M., Peiper, S. C., Parmentier, M., Collman, R. G., and Doms, R. W. 1996. A dual-tropic primary HIV-1 isolate that uses fusin and the beta-chemokine receptors CKR-5, CKR-3, and CKR-2b as fusion cofactors. *Cell.* 85, 1149–1158.

[40] Dubé, M., Roy, B. B., Guiot-Guillain, P., Mercier, J., Binette, J., Leung, G., and Cohen, E. A. 2009. Suppression of Tetherin-restricting activity upon human immunodeficiency virus type 1 particle release correlates with localization of Vpu in the trans-Golgi network. *J. Virol.* 83, 4574–4590.

[41] Earl, P. L., Moss, B., and Doms, R. W. 1991. Folding, interaction with GRP78-BiP, assembly, and transport of the human immunodeficiency virus type 1 envelope protein. *J. Virol.* 65, 2047–2055.

[42] Endo, H., Muramatsu, T., Furuta, M., Uzawa, N., Pimkhaokham, A., Amagasa, T., Inazawa, J., and Kozaki, K.-i. 2013. Potential of tumor-suppressive miR-596 targeting LGALS3BP as a therapeutic agent in oral cancer. *Carcinogenesis* 34, 560–569.

[43] Faria, N. R., Rambaut, A., Suchard, M. A., Baele, G., Bedford, T., Ward, M. J., Tatem, A. J., Sousa, J. D., Arinaminpathy, N., Pépin, J., Posada, D., Peeters, M., Pybus, O. G., and Lemey, P. 2014. HIV epidemiology. The early spread and epidemic ignition of HIV-1 in human populations. *Science* 346, 56–61.

[44] Feng, Y., Broder, C. C., Kennedy, P. E., and Berger, E. A. 1996. HIV-1 entry cofactor: functional cDNA cloning of a seven-transmembrane, G protein-coupled receptor. *Science* 272, 872–877.

[45] Fornarini, B., D'Ambrosio, C., Natoli, C., Tinari, N., Silingardi, V., and Iacobelli, S. 2000. Adhesion to 90K (Mac-2 BP) as a mechanism for lymphoma drug resistance in vivo. *Blood* 96, 3282–3285.

[46] Fricke, T., White, T. E., Schulte, B., de Souza Aranha Vieira, Daniel A, Dharan, A., Campbell, E. M., Brandariz-Nuñez, A., and Diaz-Griffero, F. 2014. MxB binds to the HIV-1 core and prevents the uncoating process of HIV-1. *Retrovirology* 11, 68.

[47] Friedman, J., Trahey, M., and Weissman, I. 1993. Cloning and characterization of cyclophilin C-associated protein: a candidate natural cellular ligand for cyclophilin C. *Proc. Natl. Acad. Sci. U.S.A.* 90, 6815–6819.

[48] Friedman, R. L., Manly, S. P., McMahon, M., Kerr, I. M., and Stark, G. R. 1984. Transcriptional and posttranscriptional regulation of interferon-induced gene expression in human cells. *Cell* 38, 745–755.

[49] Galão, R. P., Le Tortorec, A., Pickering, S., Kueck, T., and Neil, S. J. D. 2012. Innate sensing of HIV-1 assembly by Tetherin induces NFκB-dependent proinflammatory responses. *Cell Host Microbe* 12, 633–644.

[50] Gao, F., Yue, L., Robertson, D. L., Hill, S. C., Hui, H., Biggar, R. J., Neequaye, A. E., Whelan, T. M., Ho, D. D., and Shaw, G. M. 1994. Genetic diversity of human immunodeficiency virus type 2: evidence for distinct sequence subtypes with differences in virus biology. *J. Virol.* 68, 7433–7447.

[51] Gao, F., Yue, L., White, A. T., Pappas, P. G., Barchue, J., Hanson, A. P., Greene, B. M., Sharp, P. M., Shaw, G. M., and Hahn, B. H. 1992. Human infection by genetically diverse SIVSM-related HIV-2 in West Africa. *Nature* 358, 495–499.

[52] Garten, W., Vey, M., Ohuchi, R., Ohuchi, M., and Klenk, H. D. 1991. Modification of the cleavage activation of the influenza virus hemagglutinin by site-specific mutagenesis. *Behring Inst. Mitt.*, 12–22.

[53] Goldstone, D. C., Ennis-Adeniran, V., Hedden, J. J., Groom, H. C. T., Rice, G. I., Christodoulou, E., Walker, P. A., Kelly, G., Haire, L. F., Yap, M. W., de Carvalho, L. P. S., Stoye, J. P., Crow, Y. J., Taylor, I. A., and Webb, M. 2011. HIV-1 restriction factor SAMHD1 is a deoxynucleoside triphosphate triphosphohydrolase. *Nature* 480, 379–382.

[54] Götz, N., Sauter, D., Usmani, S. M., Fritz, J. V., Goffinet, C., Heigele, A., Geyer, M., Bibollet-Ruche, F., Learn, G. H., Fackler, O. T., Hahn, B. H., and Kirchhoff, F. 2012. Reacquisition of Nef-mediated tetherin antagonism in a single in vivo passage of HIV-1 through its original chimpanzee host. *Cell Host Microbe* 12, 373–380.

[55] Goujon, C. and Malim, M. H. 2010. Characterization of the alpha interferon-induced postentry block to HIV-1 infection in primary human macrophages and T cells. *J. Virol.* 84, 9254–9266.

[56] Goujon, C., Moncorgé, O., Bauby, H., Doyle, T., Ward, C. C., Schaller, T., Hué, S., Barclay, W. S., Schulz, R., and Malim, M. H. 2013. Human MX2 is an interferon-induced post-entry inhibitor of HIV-1 infection. *Nature* 502, 559–562.

[57] Graham, F. L., Smiley, J., Russell, W. C., and Nairn, R. 1977. Characteristics of a Human Cell Line Transformed by DNA from Human Adenovirus Type 5. *Journal of General Virology* 36, 59–72.

[58] Grassadonia, A., Tinari, N., Iurisci, I., Piccolo, E., Cumashi, A., Innominato, P., D'Egidio, M., Natoli, C., Piantelli, M., and Iacobelli, S. 2004. 90K (Mac-2 BP) and galectins in tumor progression and metastasis. *Glycoconj. J.* 19, 551–556.

[59] Gray, E. S., Madiga, M. C., Hermanus, T., Moore, P. L., Wibmer, C. K., Tumba, N. L., Werner, L., Mlisana, K., Sibeko, S., Williamson, C., Abdool, K. S. S., and Morris, L. 2011. The neutralization breadth of HIV-1 develops incrementally over four years and is associated with CD4+ T cell decline and high viral load during acute infection. *J. Virol.* 85, 4828–4840.

[60] Greco, C., Vona, R., Cosimelli, M., Matarrese, P., Straface, E., Scordati, P., Giannarelli, D., Casale, V., Assisi, D., Mottolese, M., Moles, A., and Malorni, W. 2004. Cell surface overexpression of galectin-3 and the presence of its ligand 90k in the blood plasma as determinants in colon neoplastic lesions. *Glycobiology* 14, 783–792.

[61] Gröschel, B., Braner, J. J., Funk, M., Linde, R., Doerr, H. W., Cinatl, J., and Iacobelli, S. 2000. Elevated plasma levels of 90K (Mac-2 BP) immunostimulatory glycoprotein in HIV-1-infected children. *J. Clin. Immunol.* 20, 117–122.

[62] Haffar, O. K., Dowbenko, D. J., and Berman, P. W. 1988. Topogenic analysis of the human immunodeficiency virus type 1 envelope glycoprotein, gp160, in microsomal membranes. *J. Cell Biol.* 107, 1677–1687.

[63] Hahn, B. H., Shaw, G. M., De Cock, K. M., and Sharp, P. M. 2000. AIDS as a Zoonosis: Scientific and Public Health Implications. *Science* 287, 607–614.

[64] Hallenberger, S., Bosch, V., Angliker, H., Shaw, E., Klenk, H. D., and Garten, W. 1992. Inhibition of furin-mediated cleavage activation of HIV-1 glycoprotein gp160. *Nature* 360, 358–361.

[65] Hansen, B. D., Nara, P. L., Maheshwari, R. K., Sidhu, G. S., Bernbaum, J. G., Hoekzema, D., Meltzer, M. S., and Gendelman, H. E. 1992. Loss of infectivity by progeny virus from alpha interferon-treated human immunodeficiency virus type 1-infected T cells is associated with defective assembly of envelope gp120. *J. Virol.* 66, 7543–7548.

[66] Harris, R. S., Bishop, K. N., Sheehy, A. M., Craig, H. M., Petersen-Mahrt, S. K., Watt, I. N., Neuberger, M. S., and Malim, M. H. 2003. DNA Deamination Mediates Innate Immunity to Retroviral Infection. *Cell* 113, 803–809.

[67] Harris, R. S., Hultquist, J. F., and Evans, D. T. 2012. The restriction factors of human immunodeficiency virus. *J. Biol. Chem.* 287, 40875–40883.

[68] Hatziioannou, T., Del Prete, G. Q., Keele, B. F., Estes, J. D., McNatt, M. W., Bitzegeio, J., Raymond, A., Rodriguez, A., Schmidt, F., Mac Trubey, C., Smedley, J., Piatak, M., KewalRamani, V. N., Lifson, J. D., and Bieniasz, P. D. 2014. HIV-1-induced AIDS in monkeys. *Science* 344, 1401–1405.

[69] Hatziioannou, T., Princiotta, M., Piatak, M., Yuan, F., Zhang, F., Lifson, J. D., and Bieniasz, P. D. 2006. Generation of simian-tropic HIV-1 by restriction factor evasion. *Science* 314, 95.

[70] Hauser, H., Lopez, L. A., Yang, S. J., Oldenburg, J. E., Exline, C. M., Guatelli, J. C., and Cannon, P. M. 2010. HIV-1 Vpu and HIV-2 Env counteract BST-2/tetherin by sequestration in a perinuclear compartment. *Retrovirology* 7, 51.

[71] Hellstern, S., Sasaki, T., Fauser, C., Lustig, A., Timpl, R., and Engel, J. 2002. Functional studies on recombinant domains of Mac-2-binding protein. *J. Biol. Chem.* 277, 15690–15696.

[72] Hepojoki, J., Strandin, T. M., Hetzel, U., Sironen, T., Klingström, J., Sane, J., Mäkelä, S., Mustonen, J., Meri, S., Lundkvist, A., Vapalahti, O., Lankinen, H. M., and Vaheri, A. 2014. Acute Hantavirus Infection Induces Galectin-3 Binding Protein. *J. Gen. Virol.* 95, 2356–2364.

[73] Hrecka, K., Hao, C., Gierszewska, M., Swanson, S. K., Kesik-Brodacka, M., Srivastava, S., Florens, L., Washburn, M. P., and Skowronski, J. 2011. Vpx relieves inhibition of HIV-1 infection of macrophages mediated by the SAMHD1 protein. *Nature* 474, 658–661.

[74] Hultquist, J. F., Lengyel, J. A., Refsland, E. W., LaRue, R. S., Lackey, L., Brown, W. L., and Harris, R. S. 2011. Human and rhesus APOBEC3D, APOBEC3F, APOBEC3G, and APOBEC3H demonstrate a conserved capacity to restrict Vif-deficient HIV-1. *J. Virol.* 85, 11220–11234.

[75] Iacobelli, S., Arnò, E., D'Orazio, A., and Coletti, G. 1986. Detection of antigens recognized by a novel monoclonal antibody in tissue and serum from patients with breast cancer. *Cancer Res.* 46, 3005–3010.

[76] Iacobelli, S., Scambia, G., Natoli, C., Panici, P. B., Baiocchi, G., Perrone, L., and Mancuso, S. 1988. Recombinant human leukocyte interferon-alpha 2b stimulates the synthesis and release of a 90K tumor-associated antigen in human breast cancer cells. *Int. J. Cancer* 42, 182–184.

[77] Isaacs, A. and Lindenmann, J. 1957. Virus interference. I. The interferon. *Proc. R. Soc. Lond., B, Biol. Sci.* 147, 258–267.

[78] Jabbar, M. A. and Nayak, D. P. 1990. Intracellular interaction of human immunodeficiency virus type 1 (ARV-2) envelope glycoprotein gp160 with CD4 blocks the movement and maturation of CD4 to the plasma membrane. *J. Virol.* 64, 6297–6304.

[79] Jalkanen, K., Leu, T., Bono, P., Salmi, M., Jalkanen, S., and Smith, D. J. 2001. Distinct ligand binding properties of Mac-2-binding protein and mouse cyclophilin [correction of mousephilin] C-associated protein. *Eur. J. Immunol.* 31, 3075–3084.

[80] Kane, M., Yadav, S. S., Bitzegeio, J., Kutluay, S. B., Zang, T., Wilson, S. J., Schoggins, J. W., Rice, C. M., Yamashita, M., Hatziioannou, T., and Bieniasz, P. D. 2013. MX2 is an interferon-induced inhibitor of HIV-1 infection. *Nature* 502, 563–566.

[81] Keele, B. F., Giorgi, E. E., Salazar-Gonzalez, J. F., Decker, J. M., Pham, K. T., Salazar, M. G., Sun, C., Grayson, T., Wang, S., Li, H., Wei, X., Jiang, C., Kirchherr, J. L., Gao, F., Anderson, J. A., Ping, L.-H., Swanstrom, R., Tomaras, G. D., Blattner, W. A., Goepfert, P. A., Kilby, J. M., Saag, M. S., Delwart, E. L., Busch, M. P., Cohen, M. S., Montefiori, D. C., Haynes, B. F., Gaschen, B., Athreya, G. S., Lee, H. Y., Wood, N., Seoighe, C., Perelson, A. S., Bhattacharya, T., Korber, B. T., Hahn, B. H., and Shaw, G. M. 2008. Identification and characterization of transmitted and early founder virus envelopes in primary HIV-1 infection. *Proc. Natl. Acad. Sci. U.S.A.* 105, 7552–7557.

[82] Keele, B. F., Jones, J. H., Terio, K. A., Estes, J. D., Rudicell, R. S., Wilson, M. L., Li, Y., Learn, G. H., Beasley, T. M., Schumacher-Stankey, J., Wroblewski, E., Mosser, A., Raphael, J., Kamenya, S., Lonsdorf, E. V., Travis, D. A., Mlengeya, T., Kinsel, M. J., Else, J. G., Silvestri, G., Goodall, J., Sharp, P. M., Shaw, G. M., Pusey, A. E., and Hahn, B. H. 2009. Increased mortality and AIDS-like immunopathology in wild chimpanzees infected with SIVcpz. *Nature* 460, 515–519.

[83] Keele, B. F., van Heuverswyn, F., Li, Y., Bailes, E., Takehisa, J., Santiago, M. L., Bibollet-Ruche, F., Chen, Y., Wain, L. V., Liegeois, F., Loul, S., Ngole, E. M., Bienvenue, Y., Delaporte, E., Brookfield, J. F. Y., Sharp, P. M., Shaw, G. M., Peeters, M., and Hahn, B. H. 2006. Chimpanzee reservoirs of pandemic and nonpandemic HIV-1. *Science* 313, 523–526.

[84] Khalid, M., Yu, H., Sauter, D., Usmani, S. M., Schmokel, J., Feldman, J., Gruters, R. A., van der Ende, M. E., Geyer, M., Rowland-Jones, S., Osterhaus, A. D., and Kirchhoff, F. 2012. Efficient Nef-mediated downmodulation of TCR-CD3 and CD28 is associated with high CD4+ T cell counts in viremic HIV-2 infection. *J. Virol.* 86, 4906–4920.

[85] Klatzmann, D., Champagne, E., Chamaret, S., Gruest, J., Guetard, D., Hercend, T., Gluckman, J. C., and Montagnier, L. 1984. T-lymphocyte T4 molecule behaves as the receptor for human retrovirus LAV. *Nature* 312, 767–768.

[86] Klein, F., Gaebler, C., Mouquet, H., Sather, D. N., Lehmann, C., Scheid, J. F., Kraft, Z., Liu, Y., Pietzsch, J., Hurley, A., Poignard, P., Feizi, T., Morris, L., Walker, B. D., Fätkenheuer, G., Seaman, M. S., Stamatatos, L., and Nussenzweig, M. C. 2012. Broad neutralization by a combination of antibodies recognizing the CD4 binding site and a new conformational epitope on the HIV-1 envelope protein. *J. Exp. Med.* 209, 1469–1479.

[87] Klein, J. S. and Bjorkman, P. J. 2010. Few and far between: how HIV may be evading antibody avidity. *PLoS Pathog.* 6, e1000908.

[88] Kluge, S. F., Mack, K., Iyer, S. S., Pujol, F. M., Heigele, A., Learn, G. H., Usmani, S. M., Sauter, D., Joas, S., Hotter, D., Bibollet-Ruche, F., Plenderleith, L. J., Peeters, M., Geyer, M., Sharp, P. M., Fackler, O. T., Hahn, B. H., and Kirchhoff, F. 2014. Nef proteins of epidemic HIV-1 group O strains antagonize human tetherin. *Cell Host Microbe* in press (2014).

[89] Kobayashi, T., Ode, H., Yoshida, T., Sato, K., Gee, P., Yamamoto, S. P., Ebina, H., Strebel, K., Sato, H., and Koyanagi, Y. 2011. Identification of amino acids in the human tetherin transmembrane domain responsible for HIV-1 Vpu interaction and susceptibility. *J. Virol.* 85, 932–945.

[90] Koths, K., Taylor, E., Halenbeck, R., Casipit, C., and Wang, A. 1993. Cloning and characterization of a human Mac-2-binding protein, a new member of the superfamily defined by the macrophage scavenger receptor cysteine-rich domain. *J. Biol. Chem.* 268, 14245–14249.

[91] Kwong, P. D., Wyatt, R., Robinson, J., Sweet, R. W., Sodroski, J., and Hendrickson, W. A. 1998. Structure of an HIV gp120 envelope glycoprotein in complex with the CD4 receptor and a neutralizing human antibody. *Nature* 393, 648–659.

[92] Laferté, S., Loh, L. C., and Keeler, V. 2000. Monoclonal antibodies specific for human tumor-associated antigen 90K/Mac-2 binding protein: tools to examine protein conformation and function. *J. Cell. Biochem.* 77, 540–559.

[93] Laguette, N., Sobhian, B., Casartelli, N., Ringeard, M., Chable-Bessia, C., Ségéral, E., Yatim, A., Emiliani, S., Schwartz, O., and Benkirane, M. 2011. SAMHD1 is the dendritic- and myeloid-cell-specific HIV-1 restriction factor counteracted by Vpx. *Nature* 474, 654–657.

[94] Lahouassa, H., Daddacha, W., Hofmann, H., Ayinde, D., Logue, E. C., Dragin, L., Bloch, N., Maudet, C., Bertrand, M., Gramberg, T., Pancino, G., Priet, S., Canard, B., Laguette, N., Benkirane, M., Transy, C., Landau, N. R., Kim, B., and Margottin-Goguet, F. 2012. SAMHD1 restricts the replication of human immunodeficiency virus type 1 by

depleting the intracellular pool of deoxynucleoside triphosphates. *Nat. Immunol.* 13, 223–228.

[95] Lee, J. H., Bae, J. A., Lee, J. H., Seo, Y.-W., Kho, D. H., Sun, E. G., Lee, S. E., Cho, S. H., Joo, Y. E., Ahn, K. Y., Chung, I. J., and Kim, K. K. 2010. Glycoprotein 90K, downregulated in advanced colorectal cancer tissues, interacts with CD9/CD82 and suppresses the Wnt/beta-catenin signal via ISGylation of beta-catenin. *Gut* 59, 907–917.

[96] Leonard, C. K., Spellman, M. W., Riddle, L., Harris, R. J., Thomas, J. N., and Gregory, T. J. 1990. Assignment of intrachain disulfide bonds and characterization of potential glycosylation sites of the type 1 recombinant human immunodeficiency virus envelope glycoprotein (gp120) expressed in Chinese hamster ovary cells. *J. Biol. Chem.* 265, 10373–10382.

[97] Li, M., Kao, E., Gao, X., Sandig, H., Limmer, K., Pavon-Eternod, M., Jones, T. E., Landry, S., Pan, T., Weitzman, M. D., and David, M. 2012. Codon-usage-based inhibition of HIV protein synthesis by human schlafen 11. *Nature* 491, 125–128.

[98] Li, N., Zhang, W., and Cao, X. 2000. Identification of human homologue of mouse IFN-γ induced protein from human dendritic cells. *Immunology Letters* 74, 221–224.

[99] Linsley, P. S., Horn, D., Marquardt, H., Brown, J. P., Hellström, I., Hellström, K. E., Ochs, V., and Tolentino, E. 1986. Identification of a novel serum protein secreted by lung carcinoma cells. *Biochemistry* 25, 2978–2986.

[100] Liu, Z., Pan, Q., Ding, S., Qian, J., Xu, F., Zhou, J., Cen, S., Guo, F., and Liang, C. 2013. The interferon-inducible MxB protein inhibits HIV-1 infection. *Cell Host Microbe* 14, 398–410.

[101] Lodermeyer, V., Suhr, K., Schrott, N., Kolbe, C., Stürzel, C. M., Krnavek, D., Münch, J., Dietz, C., Waldmann, T., Kirchhoff, F., and Goffinet, C. 2013. 90K, an interferon-stimulated gene product, reduces the infectivity of HIV-1. *Retrovirology* 10, 111.

[102] Longo, G., Natoli, C., Rafanelli, D., Tinari, N., Morfini, M., Rossi-Ferrini, P., D'Ostilio, N., and Iacobelli, S. 1993. Prognostic value of a novel circulating serum 90K antigen in HIV-infected haemophilia patients. *Br. J. Haematol.* 85, 207–209.

[103] Lusso, P., Cocchi, F., Balotta, C., Markham, P. D., Louie, A., Farci, P., Pal, R., Gallo, R. C., and Reitz, M. S. JR. 1995. Growth of Macrophage-Tropic and Primary Human Immunodeficiency Virus Type 1 (HIV-1) Isolates in a Unique CD4+ T-Cell Clone (PM1): Failure to Downregulate CD4 and to Interfere with Cell-line-Tropic HIV-1. *J.Virol* 69, 3712–3720.

[104] Lynch, R. M., Tran, L., Louder, M. K., Schmidt, S. D., Cohen, M., Dersimonian, R., Euler, Z., Gray, E. S., Abdool, K. S., Kirchherr, J., Montefiori, D. C., Sibeko, S., Soderberg, K., Tomaras, G., Yang, Z.-Y., Nabel, G. J., Schuitemaker, H., Morris, L., Haynes, B. F., and Mascola, J. R. 2012. The development of CD4 binding site antibodies during HIV-1 infection. *J. Virol.* 86, 7588–7595.

[105] Mangeat, B., Turelli, P., Caron, G., Friedli, M., Perrin, L., and Trono, D. 2003. Broad antiretroviral defence by human APOBEC3G through lethal editing of nascent reverse transcripts. *Nature* 424, 99–103.

[106] Marchetti, A., Tinari, N., Buttitta, F., Chella, A., Angeletti, C. A., Sacco, R., Mucilli, F., Ullrich, A., and Iacobelli, S. 2002. Expression of 90K (Mac-2 BP) correlates with distant metastasis and predicts survival in stage I non-small cell lung cancer patients. *Cancer Res.* 62, 2535–2539.

[107]Marlink, R., Kanki, P., Thior, I., Travers, K., Eisen, G., Siby, T., Traore, I., Hsieh, C. C., Dia, M. C., and Gueye, E. H. 1994. Reduced rate of disease development after HIV-2 infection as compared to HIV-1. *Science* 265, 1587–1590.

[108]Marth, C., Dreps, A., Natoli, C., Zeimet, A. G., Lang, T., Widschwendter, M., Daxenbichler, G., Ullrich, A., and Iacobelli, S. 1994. Effects of type-I and -II interferons on 90K antigen expression in ovarian carcinoma cells. *Int. J. Cancer* 59, 808–813.

[109]McCune, J. M., Rabin, L. B., Feinberg, M. B., Lieberman, M., Kosek, J. C., Reyes, G. R., and Weissman, I. L. 1988. Endoproteolytic cleavage of gp160 is required for the activation of human immunodeficiency virus. *Cell* 53, 55–67.

[110]McDougal, J. S., Kennedy, M. S., Sligh, J. M., Cort, S. P., Mawle, A., and Nicholson, J. K. 1986. Binding of HTLV-III/LAV to T4+ T cells by a complex of the 110K viral protein and the T4 molecule. *Science* 231, 382–385.

[111]McNatt, M. W., Zang, T., and Bieniasz, P. D. 2013. Vpu binds directly to tetherin and displaces it from nascent virions. *PLoS Pathog.* 9, e1003299.

[112]Moulard, M., Hallenberger, S., Garten, W., and Klenk, H.-D. 1999. Processing and routage of HIV glycoproteins by furin to the cell surface. *Virus Research* 60, 55–65.

[113]Müller, S. A., Sasaki, T., Bork, P., Wolpensinger, B., Schulthess, T., Timpl, R., Engel, A., and Engel, J. 1999. Domain organization of Mac-2 binding protein and its oligomerization to linear and ring-like structures. *J. Mol. Biol.* 291, 801–813.

[114]Münch, J., Standker, L., Pöhlmann, S., Baribaud, F., Papkalla, A., Rosorius, O., Stauber, R., Sass, G., Heveker, N., Adermann, K., Escher, S., Kluver, E., Doms, R. W., Forssmann, W.-G., and Kirchhoff, F. 2002. Hemofiltrate CC Chemokine 1[9-74] Causes Effective Internalization of CCR5 and Is a Potent Inhibitor of R5-Tropic Human Immunodeficiency Virus Type 1 Strains in Primary T Cells and Macrophages. *Antimicrobial Agents and Chemotherapy* 46, 982–990.

[115]Natali, P. G., Wilson, B. S., Imai, K., Bigotti, A., and Ferrone, S. 1982. Tissue distribution, molecular profile, and shedding of a cytoplasmic antigen identified by the monoclonal antibody 465.12S to human melanoma cells. *Cancer Res.* 42, 583–589.

[116]Natoli, C., Dianzani, F., Mazzotta, F., Balocchini, E., Pierotti, P., Antonelli, G., and Iacobelli, S. 1993. 90K protein: a new predictor marker of disease progression in human immunodeficiency virus infection. *J. Acquir. Immune Defic. Syndr.* 6, 370–375.

[117]Neil, S. J. D., Zang, T., and Bieniasz, P. D. 2008. Tetherin inhibits retrovirus release and is antagonized by HIV-1 Vpu. *Nature* 451, 425–430.

[118]Ochsenbauer, C., Edmonds, T. G., Ding, H., Keele, B. F., Decker, J., Salazar, M. G., Salazar-Gonzalez, J. F., Shattock, R., Haynes, B. F., Shaw, G. M., Hahn, B. H., and Kappes, J. C. 2012. Generation of transmitted/founder HIV-1 infectious molecular clones and characterization of their replication capacity in CD4 T lymphocytes and monocyte-derived macrophages. *J. Virol.* 86, 2715–2728.

[119]Parrish, N. F., Gao, F., Li, H., Giorgi, E. E., Barbian, H. J., Parrish, E. H., Zajic, L., Iyer, S. S., Decker, J. M., Kumar, A., Hora, B., Berg, A., Cai, F., Hopper, J., Denny, T. N., Ding, H., Ochsenbauer, C., Kappes, J. C., Galimidi, R. P., West, A. P., Bjorkman, P. J., Wilen, C. B., Doms, R. W., O'Brien, M., Bhardwaj, N., Borrow, P., Haynes, B. F., Muldoon, M., Theiler, J. P., Korber, B., Shaw, G. M., and Hahn, B. H. 2013. Phenotypic properties of transmitted founder HIV-1. *Proc. Natl. Acad. Sci. U.S.A.* 110, 6626–6633.

[120]Pegu, A., Yang, Z.-Y., Boyington, J. C., Wu, L., Ko, S.-Y., Schmidt, S. D., McKee, K., Kong, W.-P., Shi, W., Chen, X., Todd, J.-P., Letvin, N. L., Huang, J., Nason, M. C., Hoxie, J. A., Kwong, P. D., Connors, M., Rao, S. S., Mascola, J. R., and Nabel, G. J.

2014. Neutralizing antibodies to HIV-1 envelope protect more effectively in vivo than those to the CD4 receptor. *Sci Transl Med* 6, 243ra88.

[121]Perez-Caballero, D., Zang, T., Ebrahimi, A., McNatt, M. W., Gregory, D. A., Johnson, M. C., and Bieniasz, P. D. 2009. Tetherin inhibits HIV-1 release by directly tethering virions to cells. *Cell* 139, 499–511.

[122]Pertel, T., Hausmann, S., Morger, D., Züger, S., Guerra, J., Lascano, J., Reinhard, C., Santoni, F. A., Uchil, P. D., Chatel, L., Bisiaux, A., Albert, M. L., Strambio-De-Castillia, C., Mothes, W., Pizzato, M., Grütter, M. G., and Luban, J. 2011. TRIM5 is an innate immune sensor for the retrovirus capsid lattice. *Nature* 472, 361–365.

[123]Peters, P. J., Sullivan, W. M., Duenas-Decamp, M. J., Bhattacharya, J., Ankghuambom, C., Brown, R., Luzuriaga, K., Bell, J., Simmonds, P., Ball, J., and Clapham, P. R. 2006. Non-macrophage-tropic human immunodeficiency virus type 1 R5 envelopes predominate in blood, lymph nodes, and semen: implications for transmission and pathogenesis. *J. Virol.* 80, 6324–6332.

[124]Pinter, A., Honnen, W. J., Tilley, S. A., Bona, C., Zaghouani, H., Gorny, M. K., and Zolla-Pazner, S. 1989. Oligomeric structure of gp41, the transmembrane protein of human immunodeficiency virus type 1. *J. Virol.* 63, 2674–2679.

[125]Plantier, J.-C., Leoz, M., Dickerson, J. E., Oliveira, F. de, Cordonnier, F., Lemée, V., Damond, F., Robertson, D. L., and Simon, F. 2009. A new human immunodeficiency virus derived from gorillas. *Nat. Med.* 15, 871–872.

[126]Powell, T. J., Schreck, R., McCall, M., Hui, T., Rice, A., App, H., Azam, M., Ullrich, A., and Shawver, L. K. 1995. A tumor-derived protein which provides T-cell costimulation through accessory cell activation. *J Immunother Emphasis Tumor Immunol* 17, 209–221.

[127]Rambaut, A., Posada, D., Crandall, K. A., and Holmes, E. C. 2004. The causes and consequences of HIV evolution. *Nat. Rev. Genet.* 5, 52–61.

[128]Randall, R. E. and Goodbourn, S. 2008. Interferons and viruses: an interplay between induction, signalling, antiviral responses and virus countermeasures. *J. Gen. Virol.* 89, 1–47.

[129]Raposo, R. A. S., Abdel-Mohsen, M., Deng, X., Hecht, F. M., Pilcher, C. D., Pillai, S. K., and Nixon, D. F. 2014. Dynamic Regulation of Host Restriction Factor Expression over the Course of HIV-1 Infection In Vivo. *J. Virol.* 88, 11624–11629.

[130]Reeves J. D. and Doms, R. W. 2002. Human immunodeficiency virus type 2. *J Gen Virol.* 83, 1253–1265.

[131]Refsland, E. W., Hultquist, J. F., and Harris, R. S. 2012. Endogenous origins of HIV-1 G-to-A hypermutation and restriction in the nonpermissive T cell line CEM2n. *PLoS Pathog.* 8, e1002800.

[132]Rice, G. I., Bond, J., Asipu, A., Brunette, R. L., Manfield, I. W., Carr, I. M., Fuller, J. C., Jackson, R. M., Lamb, T., Briggs, T. A., Ali, M., Gornall, H., Couthard, L. R., Aeby, A., Attard-Montalto, S. P., Bertini, E., Bodemer, C., Brockmann, K., Brueton, L. A., Corry, P. C., Desguerre, I., Fazzi, E., Cazorla, A. G., Gener, B., Hamel, B. C. J., Heiberg, A., Hunter, M., van der Knaap, M. S, Kumar, R., Lagae, L., Landrieu, P. G., Lourenco, C. M., Marom, D., McDermott, M. F., van der Merwe, W., Orcesi, S., Prendiville, J. S., Rasmussen, M., Shalev, S. A., Soler, D. M., Shinawi, M., Spiegel, R., Tan, T. Y., Vanderver, A., Wakeling, E. L., Wassmer, E., Whittaker, E., Lebon, P., Stetson, D. B., Bonthron, D. T., and Crow, Y. J. 2009. Mutations involved in Aicardi-Goutières syndrome implicate SAMHD1 as regulator of the innate immune response. *Nat. Genet.* 41, 829–832.

[133]Robey, W. G., Safai, B., Oroszlan, S., Arthur, L. O., Gonda, M. A., Gallo, R. C., and Fischinger, P. J. 1985. Characterization of envelope and core structural gene products of HTLV-III with sera from AIDS patients. *Science* 228, 593–595.

[134]Robinson, D. N. and Cooley, L. 1997. Drosophila kelch is an oligomeric ring canal actin organizer. *J. Cell Biol.* 138, 799–810.

[135]Rosenberg, I., Cherayil, B. J., Isselbacher, K. J., and Pillai, S. 1991. Mac-2-binding glycoproteins. Putative ligands for a cytosolic beta-galactoside lectin. *J. Biol. Chem.* 266, 18731–18736.

[136]Rotger, M., Dang, K. K., Fellay, J., Heinzen, E. L., Feng, S., Descombes, P., Shianna, K. V., Ge, D., Günthard, H. F., Goldstein, D. B., and Telenti, A. 2010. Genome-wide mRNA expression correlates of viral control in CD4+ T-cells from HIV-1-infected individuals. *PLoS Pathog.* 6, e1000781.

[137]Rowell, J. F., Stanhope, P. E., and Siliciano, R. F. 1995. Endocytosis of endogenously synthesized HIV-1 envelope protein. Mechanism and role in processing for association with class II MHC. *J. Immunol.* 155, 473–488.

[138]Russell, R. S., Liang, C., and Wainberg, M. A. 2004. Is HIV-1 RNA dimerization a prerequisite for packaging? Yes, no, probably? *Retrovirology* 1, 23.

[139]Ryoo, J., Choi, J., Oh, C., Kim, S., Seo, M., Kim, S.-Y., Seo, D., Kim, J., White, T. E., Brandariz-Nuñez, A., Diaz-Griffero, F., Yun, C.-H., Hollenbaugh, J. A., Kim, B., Baek, D., and Ahn, K. 2014. The ribonuclease activity of SAMHD1 is required for HIV-1 restriction. *Nat. Med.* 20, 936–941.

[140]Salazar-Gonzalez, J. F., Bailes, E., Pham, K. T., Salazar, M. G., Guffey, M. B., Keele, B. F., Derdeyn, C. A., Farmer, P., Hunter, E., Allen, S., Manigart, O., Mulenga, J., Anderson, J. A., Swanstrom, R., Haynes, B. F., Athreya, G. S., Korber, B. T. M., Sharp, P. M., Shaw, G. M., and Hahn, B. H. 2008. Deciphering human immunodeficiency virus type 1 transmission and early envelope diversification by single-genome amplification and sequencing. *J. Virol.* 82, 3952–3970.

[141]Sasaki, T., Brakebusch, C., Engel, J., and Timpl, R. 1998. Mac-2 binding protein is a cell-adhesive protein of the extracellular matrix which self-assembles into ring-like structures and binds beta1 integrins, collagens and fibronectin. *EMBO J.* 17, 1606–1613.

[142]Sauter, D. 2014. Counteraction of the multifunctional restriction factor tetherin. *Front Microbiol* 5, 163.

[143]Schindler, M., Wurfl, S., Benaroch, P., Greenough, T. C., Daniels, R., Easterbrook, P., Brenner, M., Münch, J., and Kirchhoff, F. 2003. Down-Modulation of Mature Major Histocompatibility Complex Class II and Up-Regulation of Invariant Chain Cell Surface Expression Are Well-Conserved Functions of Human and Simian Immunodeficiency Virus nef Alleles. *Journal of Virology* 77, 10548–10556.

[144]Schmidt, S., Fritz, J. V., Bitzegeio, J., Fackler, O. T., and Keppler, O. T. 2011. HIV-1 Vpu blocks recycling and biosynthetic transport of the intrinsic immunity factor CD317/tetherin to overcome the virion release restriction. *MBio* 2, e00036-11.

[145]Schmittgen, T. D. and Livak, K. J. 2008. Analyzing real-time PCR data by the comparative C(T) method. *Nat Protoc* 3, 1101–1108.

[146]Sharp, P. M. and Hahn, B. H. 2011. Origins of HIV and the AIDS pandemic. *Cold Spring Harb Perspect Med* 1, a006841.

[147]Sharp, P. M., Shaw, G. M., and Hahn, B. H. 2005. Simian immunodeficiency virus infection of chimpanzees. *J. Virol.* 79, 3891–3902.

[148]Sheehy, A. M., Gaddis, N. C., Choi, J. D., and Malim, M. H. 2002. Isolation of a human gene that inhibits HIV-1 infection and is suppressed by the viral Vif protein. *Nature* 418, 646–650.

[149]Sheehy, A. M., Gaddis, N. C., and Malim, M. H. 2003. The antiretroviral enzyme APOBEC3G is degraded by the proteasome in response to HIV-1 Vif. *Nat. Med.* 9, 1404–1407.

[150]Shi, J., Zhou, J., Shah, V. B., Aiken, C., and Whitby, K. 2011. Small-molecule inhibition of human immunodeficiency virus type 1 infection by virus capsid destabilization. *J. Virol.* 85, 542–549.

[151]Shingai, M., Nishimura, Y., Klein, F., Mouquet, H., Donau, O. K., Plishka, R., Buckler-White, A., Seaman, M., Piatak, M., Lifson, J. D., Dimitrov, D. S., Nussenzweig, M. C., and Martin, M. A. 2013. Antibody-mediated immunotherapy of macaques chronically infected with SHIV suppresses viraemia. *Nature* 503, 277–280.

[152]Smith, S. D., Shatsky, M., Cohen, P. S., Warnke, R., Link, M. P., and Glader, B. E. 1984. Monoclonal Antibody and EnzymaticProfiles of Human Malignant T-Lymphoid Cells and Derived Cell Lines. *Cancer Res.* 44, 5657–5660.

[153]Sougrat, R., Bartesaghi, A., Lifson, J. D., Bennett, A. E., Bess, J. W., Zabransky, D. J., and Subramaniam, S. 2007. Electron tomography of the contact between T cells and SIV/HIV-1: implications for viral entry. *PLoS Pathog.* 3, e63.

[154]Stremlau, M., Owens, C. M., Perron, M. J., Kiessling, M., Autissier, P., and Sodroski, J. 2004. The cytoplasmic body component TRIM5alpha restricts HIV-1 infection in Old World monkeys. *Nature* 427, 848–853.

[155]Stremlau, M., Perron, M., Lee, M., Li, Y., Song, B., Javanbakht, H., Diaz-Griffero, F., Anderson, D. J., Sundquist, W. I., and Sodroski, J. 2006. Specific recognition and accelerated uncoating of retroviral capsids by the TRIM5alpha restriction factor. *Proc. Natl. Acad. Sci. U.S.A.* 103, 5514–5519.

[156]Takehisa, J., Kraus, M. H., Ayouba, A., Bailes, E., van Heuverswyn, F., Decker, J. M., Li, Y., Rudicell, R. S., Learn, G. H., Neel, C., Ngole, E. M., Shaw, G. M., Peeters, M., Sharp, P. M., and Hahn, B. H. 2009. Origin and biology of simian immunodeficiency virus in wild-living western gorillas. *J. Virol.* 83, 1635–1648.

[157]Tanaka, M. and Herr, W. 1990. Differential transcriptional activation by Oct-1 and Oct-2: Interdependent activation domains induce Oct-2 phosphorylation. *Cell* 60, 375–386.

[158]Timár, J., Nagy, K., and Lapis, K. 1986. Morphologic and immunoelectronmicroscopic identification of human T-cell lymphotropic virus type III (HTLV-III). *Histol. Histopathol.* 1, 43–47.

[159]Tinari, N., Lattanzio, R., Querzoli, P., Natoli, C., Grassadonia, A., Alberti, S., Hubalek, M., Reimer, D., Nenci, I., Bruzzi, P., Piantelli, M., and Iacobelli, S. 2009. High expression of 90K (Mac-2 BP) is associated with poor survival in node-negative breast cancer patients not receiving adjuvant systemic therapies. *Int. J. Cancer* 124, 333–338.

[160]Tokarev, A., Suarez, M., Kwan, W., Fitzpatrick, K., Singh, R., and Guatelli, J. 2013. Stimulation of NF-κB activity by the HIV restriction factor BST2. *J. Virol.* 87, 2046–2057.

[161]Trkola, A., Purtscher, M., Muster, T., Ballaun, C., Buchacher, A., Sullivan, N., Srinivasan, K., Sodroski, J., Moore, J. P., and Katinger, H. 1996. Human monoclonal antibody 2G12 defines a distinctive neutralization epitope on the gp120 glycoprotein of human immunodeficiency virus type 1. *J. Virol.* 70, 1100–1108.

[162]Ullrich, A., Sures, I., D'Egidio, M., Jallal, B., Powell, T. J., Herbst, R., Dreps, A., Azam, M., Rubinstein, M., and Natoli, C. 1994. The secreted tumor-associated antigen 90K is a potent immune stimulator. *J. Biol. Chem.* 269, 18401–18407.

[163]Ulmer, T. A., Keeler, V., Loh, L., Chibbar, R., Torlakovic, E., André, S., Gabius, H.-J., and Laferté, S. 2006. Tumor-associated antigen 90K/Mac-2-binding protein: possible role in colon cancer. *J. Cell. Biochem.* 98, 1351–1366.

[164]UNAIDS. 2014. The Gap Report.http://www.unaids.org/en/resources/campaigns/2014/2014gapreport/ (16.10.2014).

[165]Vallari, A., Holzmayer, V., Harris, B., Yamaguchi, J., Ngansop, C., Makamche, F., Mbanya, D., Kaptué, L., Ndembi, N., Gürtler, L., Devare, S., and Brennan, C. A. 2011. Confirmation of putative HIV-1 group P in Cameroon. *J. Virol.* 85, 1403–1407.

[166]van Damme, N., Goff, D., Katsura, C., Jorgenson, R. L., Mitchell, R., Johnson, M. C., Stephens, E. B., and Guatelli, J. 2008. The interferon-induced protein BST-2 restricts HIV-1 release and is downregulated from the cell surface by the viral Vpu protein. *Cell Host Microbe* 3, 245–252.

[167]Veronese, F. D., DeVico, A. L., Copeland, T. D., Oroszlan, S., Gallo, R. C., and Sarngadharan, M. G. 1985. Characterization of gp41 as the transmembrane protein coded by the HTLV-III/LAV envelope gene. *Science* 229, 1402–1405.

[168]Veugelers, M., Cat, B. D., Muyldermans, S. Y., Reekmans, G., Delande, N., Frints, S., Legius, E., Fryns, J. P., Schrander-Stumpel, C., Weidle, B., Magdalena, N., and David, G. 2000. Mutational analysis of the GPC3/GPC4 glypican gene cluster on Xq26 in patients with Simpson-Golabi-Behmel syndrome: identification of loss-of-function mutations in the GPC3 gene. *Hum. Mol. Genet.* 9, 1321–1328.

[169]Walker, L. M., Huber, M., Doores, K. J., Falkowska, E., Pejchal, R., Julien, J.-P., Wang, S.-K., Ramos, A., Chan-Hui, P.-Y., Moyle, M., Mitcham, J. L., Hammond, P. W., Olsen, O. A., Phung, P., Fling, S., Wong, C.-H., Phogat, S., Wrin, T., Simek, M. D., Koff, W. C., Wilson, I. A., Burton, D. R., and Poignard, P. 2011. Broad neutralization coverage of HIV by multiple highly potent antibodies. *Nature* 477, 466–470.

[170]Wei, X., Decker, J. M., Liu, H., Zhang, Z., Arani, R. B., Kilby, J. M., Saag, M. S., Wu, X., Shaw, G. M., and Kappes, J. C. 2002. Emergence of Resistant Human Immunodeficiency Virus Type 1 in Patients Receiving Fusion Inhibitor (T-20) Monotherapy. *Antimicrobial Agents and Chemotherapy* 46, 1896–1905.

[171]Weiss, A., Wiskocil, R. L., and Stobo, J. D. 1984. The role of T3 surface molecules in the activation of human T cells: a two-stimulus requirement for IL 2 production reflects events occuring at a pre-translational level. *J Immunol.* 133, 123–128.

[172]Wilen, C. B., Tilton, J. C., and Doms, R. W. 2012. HIV: cell binding and entry. *Cold Spring Harb Perspect Med* 2, a006866.

[173]Wilson, S. J., Schoggins, J. W., Zang, T., Kutluay, S. B., Jouvenet, N., Alim, M. A., Bitzegeio, J., Rice, C. M., and Bieniasz, P. D. 2012. Inhibition of HIV-1 particle assembly by 2',3'-cyclic-nucleotide 3'-phosphodiesterase. *Cell Host Microbe* 12, 585–597.

[174]Wood, A. and Armour, D. 2005. The discovery of the CCR5 receptor antagonist, UK-427,857, a new agent for the treatment of HIV infection and AIDS. *Prog Med Chem* 43, 239–271.

[175]Wyatt, R., Kwong, P. D., Desjardins, E., Sweet, R. W., Robinson, J., Hendrickson, W. A., and Sodroski, J. G. 1998. The antigenic structure of the HIV gp120 envelope glycoprotein. *Nature* 393, 705–711.

[176]Zeev-Ben-Mordehai, T., Vasishtan, D., Siebert, C. A., and Grünewald, K. 2014. The full-length cell-cell fusogen EFF-1 is monomeric and upright on the membrane. *Nat Commun* 5, 3912.

[177]Zhu, P., Chertova, E., Bess, J., Lifson, J. D., Arthur, L. O., Liu, J., Taylor, K. A., and Roux, K. H. 2003. Electron tomography analysis of envelope glycoprotein trimers on HIV and simian immunodeficiency virus virions. *Proc. Natl. Acad. Sci. U.S.A.* 100, 15812–15817.

[178]Zolla-Pazner, S. and Cardozo, T. 2010. Structure-function relationships of HIV-1 envelope sequence-variable regions refocus vaccine design. *Nature reviews. Immunology* 10, 527–535.

Acknowledgements

First I would like to thank my supervisors Prof. Christine Goffinet and Prof. Frank Kirchhoff for the opportunity to work on this exciting project. Foremost, I want to thank Prof. Goffinet for her excellent support and advice in any situation. I thank Prof. Kirchhoff for the unique chance to finish my work in Ulm in one of the leading HIV research groups worldwide.

Thanks to all lab members for the nice time I had. In particular I would like to thank Prof. Daniel Sauter and his group for welcoming me in their meetings, Dr. Christina Stürzel for always giving advice and having a helping hand and Kristina Suhr for the fruitful contribution to the paper. Furthermore I have to thank Regina Linsenmeyer, Nicola Schrott, Daniela Krnavek, Susanne Engelhart and Martha Mayer for their technical support.

I would like to thank our collaborator Prof. Amalio Telenti for providing the 90K ortholog constructs. Additionally, I thank Prof. Valerie Bosch, Prof. Guido David, Dr. Giada Frascaroli, Prof. Wolfgang Garten, Prof. Beatrice Hahn, Prof. Stefano Iacobelli, Prof. Oliver Keppler, Prof. Ji Hee Lee, PD Dr. Barbara Müller, Dr. Jens von Einem and Prof. Ulrich Schubert for the kind gift of reagents.

Many thanks to Dr. Andrea Blötz, Dominik Hotter and Dr. David Palesch for their critical and helpful comments on this thesis.

Finally, I am heartily thankful to my mother and Ferdinand for their patience, support and love.

Curriculum Vitae

Date of Birth: June 27th 1987

Education

11/2011 - 01/2015	PhD student, Institute of Molecular Virology, Ulm Research Fellowship (LGFG) Doctoral Thesis: *Characterization of 90K/LGALS3BP as antiviral factor.*
10/2009 - 09/2011	Master in Cell and Molecular Biology, Friedrich-Alexander-University Erlangen, Major Subject: Virology Master Thesis: *Interaction of the HIV-1 accessory protein Vpu with the immuno-receptors NTB-A and CD1d.* Degree: Master of Science
10/2006 - 08/2009	Bachelor in Biology, Friedrich-Alexander-University Erlangen Bachelor Thesis: *Analysis of the repertoire of κ-light chains in B-cells of the μH hypomorphic mouse mutant DD7.* Degree: Bachelor of Science
09/1997 - 06/2006	Gabrieli-Gymnasium, Eichstätt Degree: Abitur

---

Work Experience

06/2009 - 02/2011	Scientific Assistant, Institute of Virology, Erlangen
11/2008 - 02/2009	Tutor, Friedrich-Alexander-University Erlangen, Department Biology

Publications

Lodermeyer V., K. Suhr, N. Schrott, C. Kolbe, C.M. Stürzel, D. Krnavek, J. Münch, C. Dietz, T. Waldmann, F. Kirchhoff, C. Goffinet: *90K, an interferon stimulated gene product, reduces the infectivity of HIV-1.* **Retrovirology, 2013**

Bolduan, S., P. Hubel, T. Reif, **V. Lodermeyer**, K. Höhne, J.V. Fritz, D. Sauter, F. Kirchhoff, O.T. Fackler, M. Schindler, U. Schubert: *HIV-1 Vpu affects the anterograde transport and the glycosylation pattern of NTB-A.* **Virology, 2013**

Bolduan, S., J. Votteler, **V. Lodermeyer**, T. Greiner, H. Koppensteiner, M. Schindler, G. Thiel, U. Schubert*: Ion channel activity of HIV-1 Vpu is dispensable for counteraction of CD317.* **Virology, 2011**